1-1-2008

Rheology, fresh and hardened properties of self-consolidating concrete utilizing metal and PVA polymer fibers

Moustafa M. Sammour
Ryerson University

RHEOLOGY, FRESH AND HARDENED PROPERTIES OF SELF-CONSOLIDATING CONCRETE UTILIZING METAL AND PVA POLYMER FIBERS

by

Moustafa M. Sammour

BSc in Civil Engineering, Garyounis University, 1984

A thesis
presented to
Ryerson University
in partial fulfillment of the
requirements for the degree of
Master of Applied Science
in the Program of
Civil Engineering

Toronto, Ontario, Canada, 2008

Author's Declaration

I hereby declare that I am the sole author of this thesis.

I authorize Ryerson University to lend this thesis or dissertation to other institutions or individuals for the purpose of scholarly research.

Author's signature _____ _____ Date _

I further authorize Ryerson University to reproduce this thesis or dissertation or by photocopying or by other means, in total or in part, at the request of other institutions or individuals for the purpose of scholarly research.

Author's signature _____ _____ Date _

Borrowers

Ryerson University requires the signatures of all persons using or photocopying this thesis. Please sign below, and give address and date.

Name	Signature of Borrower	Address	Date

Abstract

Rheology, Fresh and Hardened Properties of Self Consolidating Concrete Utilising Metal and PVA Polymer Fibers

Moustafa Sammour
Department of Civil Engineering, Ryerson University

Fiber reinforced self-consolidating concrete (FRSCC) has a tremendous potential to be used in construction industry as it combines the advantages of both self-consolidating concrete (SCC) and fiber reinforced concrete (FRC). 18 concrete mixtures were developed by incorporating different volumes (0 to 0.3%) of polyvinyl alcohol (PVA) and metallic fibers. Fresh, rheological, mechanical and durability (in terms of chloride penetration resistance) properties of all FRSCC mixtures were evaluated. The influences of fiber types/size/dosages and fiber combination (used in hybrid mixes) on fresh (slump flow, L-box passing ability, V-funnel flow time and segregation index), rheological (plastic viscosity and yield stress) and hardened (fracture energy and compressive/flexural/splitting tensile strength) properties were critically analyzed to examine the relationships among various properties as well as to suggest suitable FRSCC mixtures. The fibers (especially metallic ones) were more effective in increasing the fracture energy of FRSCC than compressive/splitting tensile/flexural strength. A fracture energy gain of about 730% was observed (which is substantial) compared to 10% of compressive strength, 39% of splitting tensile strength and 124% of flexural strength. The improved strength and fracture energy of FRSCC mixtures can significantly reduce the amount of tensile reinforcement and substantially increase the energy absorbing capacity of concrete structures.

Acknowledgements

I would like to express my deepest gratitude to my supervisors, Dr. Mohamed Lachemi, and Dr. Anwar Hossain, for their guidance, support and patience during the development of this thesis. During my years at Ryerson they have been there for me without hesitation.

Many thanks to Dr. Mohamed Lachemi for his encouragement and continual support throughout my time at Ryerson.

I would like to thank Dr. Anwar Hossain for willingness to always help with patience, kind words and belief in me, which pulled me through this thesis. His countless proof readings, corrections and support made this document possible.

I would also like to thank Ryerson's Civil Engineering technicians who provided technical assistance during the experimental program of this thesis. I would also like to thank my colleagues and friends, for there help and assistance over the years.

Finally, special gratitude goes to my family. Without their constant love, support and sacrifices my successes would not be possible.

Dedications

To My Wife

And

My Daughter

NOOR

And

To those who support me towards success

Table of Contents

List of Tables

List of Figures

NOTATIONS

A_{lig}	area of ligament
a_o	depth of the notch
b	width of the beam specimen
D	diameter of the cylinder
d	depth of the beam specimen
d_o	maximum deformation at failure of the beam
F	shear force
g	flow resistance factor
G_f	fracture energy
h	viscosity factor
l	length of the cylinder
L	span of the beam specimen
m	self weight of the beam
P	maximum applied load
R	modulus of rupture of concrete
T	splitting tensile strength of concrete
V	velocity/speed
W_o	area under the load-deflection curve
μ	viscosity of concrete
τ	shear stress
γ	shear rate
τ_o	yield stress of concrete

1. Introduction

1.1 Background

Self-consolidating concrete (SCC) is a new generation of high performance concrete that can be placed and compacted under its self weight with little or no vibration effort. These characteristics translate into a substantial reduction in labour cost and construction time, and a better working environment by eliminating the impact of vibration. SCC was developed in Japan in the late 1980s to be mainly used for highly congested steel bar reinforced concrete structures in high activity seismic regions [Ozawa et al. 1989].

The use of SCC technology is on the increase in various parts of the world including Canada and the SCC technology has been continuously improved due to extensive research studies conducted over the last decade [Ozawa et al. 1989, Rols et al. 1999, Bui et al. 2002, Lachemi et al. 2004, Hossain and Lachemi 2004]. Moreover, this technology can be improved by further developments of material science, construction methods and field applications.

Since its invention in the early 1960s, fiber reinforced concrete (FRC) has been used in various construction applications [Vondran 1991, ACI 1984]. The addition of fibers improves durability and mechanical properties of hardened concrete such as flexural strength, toughness, impact strength, resistance to fatigue and vulnerability to cracking and spalling [Williamson 1965, ACI Committee 544 1990, Nehdi and Khan 2001, Tlemat et al. 2003]. Different types of fibers made of steel, glass, carbon, plastic, polymer or shredded rubber can be used for the manufacture of FRC [Beaudoin 1982].

Research has been conducted on the development of hybrid fiber reinforced SCC (FRSCC) which combines better mechanical, durability and ductility characteristics of FRC with the workability of conventional SCC [Khayat and Roussel 2000, Miao

et al. 2003, Sahmaran et al. 2005, Ding et al. 2008]. A proper design and control of fibers and matrix in FRSCC will improve workability; provide sufficient consolidation and improve fiber dispersion. A FRSCC should freshly spread into formworks without vibration and gain high design strength plus high durability at hardened state.

FRSCC has a tremendous potential to be used in construction industry as it combines the advantages of both SCC and FRC. To combine the technologies of both SCC and FRC, FRSCC should be developed and tailored depending on the required construction applications. Selection of appropriate types of fibers and determination of their dosages are essential in mix design processes of FRSCC to control both fresh and hardened properties. The mix design depends on the type and geometry of structure, the selected method of concrete placement and the degree of congestion due to reinforcing bars as well as fiber properties and their behaviours - not only in the hardened state but also in the fresh state. When fiber parameters are adjusted and optimized, FRSCC mixtures can provide better crack resistance as well as better strength, fracture and toughness characteristics compared to normal SCC [Grünewald and Walraven 2001, Corinaldesi and Moriconi, 2004].

Though the properties of FRSCC have been studied by few researchers in recent years, there is a great deal of work that remains to be completed in the field. Again most of these researches were concentrated mainly on the use of steel fibers in FRSCC. The limited published studies dealing with FRSCC strongly recommend further research.

1.2 Research Objectives

As infrastructure ages, cost of repairs and maintenance magnifies. Conventional structural concrete can significantly deteriorate with time requiring regular and often costly maintenance. The use of FRSCC with excellent mechanical and durability properties can reduce deterioration of structures and hence minimize maintenance

cost. Improved understanding of the characteristics of FRSCC will speed their implementation into Canadian construction practices.

This research is intended to develop FRSCC by incorporating different types of fibers and their combinations (hybrid). The objectives of this research include:

1. The review of previous research studies conducted on SCC, FRC and FRSCC technologies covering fresh and mechanical properties as well as durability characteristics.
2. Development of FRSCC mixtures with polyvinyl alcohol (PVA) and FibraFlex metallic fibers based on a control SCC.
3. Investigation on the performance of FRSCC mixtures based on the test results of workability/rheology/mechanical properties and durability characteristics.
4. Study of the influence of fiber types and dosages on the fresh, mechanical and durability properties of FRSCC
5. Establishment of relations among fresh properties, among mechanical properties and between fresh and rheological properties of FRSCC.
6. Making recommendations for suitable FRSCC mixtures for construction applications.

1.3 Scope of the Research

The scope of this research includes a comprehensive experimental investigation covering fresh, rheological, mechanical and durability tests in order to develop FRSCC mixtures using fibers of different types and their combinations. Fresh property tests include the determination of slump flow (spread), V-funnel flow time and filling/passing ability while mechanical property tests include fracture energy and compressive/splitting tensile/flexural strength. Rhelogical tests are conducted to evaluate plastic viscosity and shear yield stress of concrete mixtures. Resistance to chloride ion penetration is also evaluated by rapid chloride penetration test (RCPT).

Analysis of test results and recommendations on FRSCC mixture design and properties are also included in the scope of this research. Various aspects of the research conducted on FRSCC will be described in various chapters of this thesis.

Chapter 2 provides a literature review of previous research studies and information relevant to SCC and FRSCC technologies including materials, design concepts, properties and applications.

Chapter 3 presents the experimental program highlighting materials used and their properties/specifications. It also describes the methodology that applied on mix proportioning of FRSCC as well as methods of testing fresh/workability, rheological, mechanical and durability properties. The mixing, casting and curing methods are also described in addition to plastic viscosity and shear yield stress determination using a coaxial ConTec BML viscometer.

Chapter 4 presents the results and discussions on fresh, rheological, mechanical and durability properties of FRSCC mixtures.

Chapter 5 is structured to give the summary and conclusion of this research. Furthermore, it also outlines possible recommendations for further research on FRSCC.

2. Literature Review

2.1 Introduction

Concrete is a material that literally forms the basis of our society [Mindess et al. 2002]. Actually concrete is brittle under tensile loading and its mechanical properties could be improved by adding fibers which prevent or control propagation of cracks. The incorporation of fibers enhances the structural performance of concrete, including the reduction of spalling of the cover over reinforcement in column elements, the increase in shear strength of beams, as well as the enhancement of ductility of beam-column connections [Khayat and Roussel 2000].

Fiber reinforced self-consolidating concrete (FRSCC) has a great potential to be used as high performance materials in the 21st century as it combines the advantages of both self-consolidating concrete (SCC) and fiber reinforced concrete (FRC). This chapter provides a literature review on the current state of the art technologies of SCC and FRSCC by summarizing design methodology and fresh/rheological/hardened/durability properties as well as structural performance.

2.2 Self-Consolidating Concrete

Self consolidating concrete, initially, was developed in Japan in the late 1980s to be mainly used for highly congested steel bar reinforced structures in high activity seismic regions [Ozawa et al. 1989]. SCC generated great interest worldwide due to certain cost-effective advantages over normal concrete. However, gaining acceptance of SCC in the cast-in-place market is a matter of education than promotion and the benefits of SCC do not always come easily or immediately. Like with all new products, there is a learning curve for using SCC [Joe 2003].

SCC isn't a new idea, although the SCC technology is different from what it was in the past. Marketing of "flowing concrete" started in the early 1980s in the United States after the introduction of super plasticizers. In 1989, Master Builders,

Cleveland, developed and marketed a high strength concrete with a slump flow of 580 mm to 660 mm in a high-rise application. This concrete, however, still required some minimal vibration for consolidation [Joe 2003].

SCC has provided many benefits to the construction industry today. The fluidity and high segregation resistance of SCC help to attain a high degree of mix homogeneity, minimal concrete voids and uniform strength, as well as provides the potential for a superior level of finish and durability to the structure. The benefits of SCC also include fast construction, absence of vibration, reduced man power, enhanced flow around congested reinforcement and economy [Ouchi et al. 2003].

Although SCC is not expected to ever completely replace conventionally vibrated concrete, the use of the material in both the precast and ready-mix markets in the UK, Europe and the rest of the world is expected to continue to increase as the experience and technology improves, the clients demand a higher-quality finished product while the availability of skilled labour continues to decrease [Goodier 2003].

2.2.1 SCC Technology

Several different approaches have been used to develop SCC. One method to achieve self-consolidating property is to increase significantly the amount of fine materials or mineral admixtures, for example fly ash (FA), ground granulated blast furnace slag (GGBFS), silica fume, limestone (LS) filler, volcanic ash (VA) or cement kiln dust (CKD) without changing the water content compared to common concrete [Khayat et al. 1997, Bui et al. 2002, Lachemi et al. 2003, Patel et al. 2004, Hossain and Lachemi 2004, European SCC Guidelines 2005]. The use of such mineral admixtures can improve the slump flow and cohesiveness, reduce the segregation, lower the cost by replacing relatively costlier cement, lower the heat of hydration, lower the permeability and lower the shrinkage and creep of SCC. Mineral admixtures can also exert beneficial effect on concrete for the improvement of interfacial transition zone [Gue et al. 2007]. GGBFS provides

reactive fines with a low heat of hydration. A high proportion (more than 30% of binder) of GGBFS may affect stability of SCC while slower setting can also increase the risk of segregation [European SCC Guidelines, 2005]. The high level of fineness and spherical shape of silica fume results in good cohesion and improved resistance to segregation when used in SCC. However, silica fume is also very effective in reducing or eliminating bleed and this can give rise to problems of rapid surface crusting. This can result in cold joints or surface defects if there are any breaks in concrete delivery and also to difficulty in finishing the top surface [European SCC Guidelines 2005].

One alternative approach to produce SCC consists of incorporating a viscosity modifying admixture (VMA) to enhance stability [Rols et al. 1999, Lachemi et al. 2004]. The use of VMA along with adequate concentration of superplasticizer (SP) can ensure high deformability and adequate workability leading to a good resistance to segregation.

To avoid segregation, SCC utilizes a limited aggregate content and super plasticizer as well as low water-to-powder ratio [Okamura and Ouchi 2003]. SCC performance is highly affected by the characteristics of the ingredient materials such as size, shape, surface area and grain size distribution of aggregates [Saak et al. 2002]. SCC may be classified into three types: the powder type, viscosity agent type and the combination type [EFNARC 2006]:

- In the powder type, SCC is characterized by the large amounts of powder (all material < 0.15 mm), usually in the range of 550 to 650 kg/m^3. The powder provides the plastic viscosity and hence, the segregation resistance of the mix. The other rheological property (yield stress) is controlled by the addition of SP.
- In the viscosity type SCC, the powder content is lower (350 to 450 kg/m^3). The segregation resistance is mainly controlled by a VMA and the yield stress by the addition of SP.
- In the combination type SCC, the powder content varies from 450 to 550 kg/m^3 but in addition the rheology is also controlled by a VMA as well as an

appropriate dosage of SP. The purpose of the addition of a VMA is to replace or limit the addition of fines, thus making a fresh concrete more cohesive [EFNARC 2006].

All types of cements can be used in the SCC production, but should develop a satisfactory interaction and compatibility with chemical additives, viscosity modifying admixtures and super plasticizers.

Super plasticizers improve workability and strength of concrete with reduced water-cement (w/c) ratio. SPs are also often used when pozzolanic materials are added to concrete to improve strength. SPs have been manufactured from sulfonated naphthalene formaldehyde or sulfonated melamine formaldehyde. New products based on polycarboxylic ethers (PCE) are also developed. PCEs are not only chemically different from the older sulphonated melamine and naphthalene based products, but their action mechanism is also different, giving cement dispersion by steric stabilizations, instead of electrostatic repulsion. This form of dispersion is more powerful in its effect and gives improved workability retention to the cementitious mix. Furthermore, the chemical structure of PCE allows for a greater degree of chemical modification than the older products, offering a range of performance that can be tailored to meet specific needs [Zhong et al. 2006]. Naphthalene and melamine superplasticizers are organic polymers. The long molecules wrap themselves around the cement particles, giving them a highly negative charge so that they repel each other [Khayat 1998]. The workability of SCC and performance of the hardened concrete depend on the type of SP [Khayat and Hwang 2006].

There is no standard method for SCC mix design and many academic institutions and contracting companies have developed their own mix proportioning methods. Mix designs often use volume as a key parameter because of the importance of the need to over fill the voids between the aggregate particles. Some methods try to fit available constituents to an optimised grading envelope. Another method is to

evaluate and optimise the flow and stability of the paste and then the mortar fractions before the coarse aggregate is added and the whole SCC mix tested. Table 2.1 gives a restrictive indication of the typical range of constituents in SCC by weight and by volume [European SCC Guidelines 2005].

Table 2.1 Typical range of SCC composition

Constituent	Typical range by mass (kg/m^3)	Typical range by volume ($litres/m^3$)
Powder	380 - 600	-
Paste	-	300 - 380
Water	150 - 210	150 - 210
Coarse aggregate	750 - 1000	270 - 360
Fine aggregate (sand)	Content balances the volume of the other constituents, typically 48 – 55% of total aggregate weight.	
Water/Powder ratio	-	0.85 – 1.10

Sixty eight case studies on applications of SCC (from 1993 to 2003 in different countries) have been analysed with details [Domone 2006]. A clear majority (70%) of cases used aggregate with a maximum size between 16 and 20 mm. The use of crushed rock or gravel aggregates seemed to depend on local availability. Approximately half the cases used a VMA in addition to superplasticizer and could therefore be considered as a combined type of SCC. Limestone was the most common addition (41% of the cases). Median values of the key mix proportions were coarse aggregate content of 31.2% by volume, paste content of 34.8% by volume, powder content of 500 kg/m^3, water/powder ratio of 0.34 by weight and fine aggregate/mortar of 47.5% by volume. In ninety percent of the cases, SCC with slump flow in the range 600–750 mm was used while 80% had compressive strengths in excess of 40 MPa [Domone 2006].

2.2.2 Fresh Properties of SCC

SCC fresh properties are characterized by its deformability and stability as well as its bleeding and segregation resistance. SCC remarks its capacity to flow homogeneously without segregation between ingredients or bleeding. The method

for achieving self-compactability involves not only high deformability of paste or mortar, but also resistance to segregation between coarse aggregate and mortar when the concrete flows through the confined zone of reinforcing bars [Okamura and Ouchi 2003]. SCC should have static and dynamic stability without bleeding or surface settlement prior to stiffening [Bui et al. 2002, Khayat et al. 2004]. The lack of static stability can cause surface defects, including the presence of bleed channels. Bleeding and settlement can decline the quality of the interface between aggregate and cement paste with direct bearing on impermeability and hardened mechanical properties [Khayat and Guizani 1997]. SCC fresh properties are described in the following sections.

2.2.2.1 Deformability

Deformability can be defined as the ability of a SCC to flow in a heavily reinforced section and other restricted areas. Highly flowable SCC should have relatively low yield stress to ensure good deformability. Inter-particle friction between coarse aggregate, sand, and binder increases the internal resistance of flow, limiting the deformability and speed of flow of SCC [Khayat et al. 1999]. Such friction can be high when concrete flows through restricted spacing because of greater chances of collision between the various solids. The deformability of SCC can be increased by increasing the water to binder ratio (W/B), increasing the dosage of SP, and by incorporating very fine supplementary cementing materials (SCM) [Nanayakkara et al. 1998, Khayat et al. 1999]. Increase in the W/B can secure high deformability but it may affect the mechanical and durability properties of SCC in the long run. Increasing W/B can also reduce cohesiveness and can cause segregation that may leads to blockage during flow. Inter particle friction between binder grains can be reduced by using SP to disperse the cement grains. A high dosage of SP can however lead to the segregation and blockage of the SCC flow [Bui et al. 2002, Khayat et al 1999]. Very fine and glossy textured particle of SCM can reduce the inter-particles friction and lead to higher deformability.

2.2.2.2 Stability and Segregation

The stability of fresh concrete is characterized by its resistance to segregation, and bleeding and is affected by the mixture proportioning, aggregate shape and gradation, and the placement conditions. When a mixture does not possess an adequate level of stability, the cement paste may not be cohesive enough to retain individual aggregate particles in a homogeneous suspension. This causes the concrete constituents to separate, thus resulting in a significant reduction in mechanical properties and durability [Khayat et al. 1999, Bui et al. 2002].

There are two kinds of segregation. The first is the separation of mortar from coarse aggregates and second is bleeding. Bleeding is defined as a phenomenon whose external manifestation is the appearance of water on the top surface after concrete has been placed but before it has set. Bleeding is the form of segregation where solids in suspension tend to move downward under the force of gravity. Bleeding occurs due to the inability of the constituent materials to hold all the mixing water in a dispersed state. Some bleeding water reaches to the surface; large amount of it gets trapped under large pieces of aggregates, and horizontal reinforcing bars, which affect the mechanical performance of concrete such as strength and bond [Bui et al. 2002].

Improper consistency, excessive amount of large particles in coarse aggregates with either too high or too low density, presence of less fines (due to low cement and sand contents or the use of poorly graded sand) can cause segregation and bleeding in SCC. The concrete without mineral admixtures may suffer segregation and bleeding in concrete. Some of the measures that can be used to enhance the stability of fresh SCC are:

- The reduction in water-to- binder ratio (W/B);
- The increase of cementing material content such as fly ash, GGBFS and other fines;
- The incorporation of viscosity modifying admixture (VMA).

A large decrease in aggregate volume or an increase in water content can reduce the cohesiveness and lead to segregation. A relative high sand-to-total aggregate content of 42 to 52 % is often used to enhance cohesiveness and reduce the risk of segregation and water dilution [Bui et al. 2002].

2.2.3 Test Procedures for Fresh Properties of SCC

Several tests to evaluate deformability, stability, bleeding and segregation for SCC are available in the literature. Some of the important tests are discussed briefly.

Slump flow (SF): The deformability and flowability of fresh SCC in absence of obstructions can be evaluated by using slump flow test [EFNARC 2006]. The slump flow value represents the mean diameter (measured in two perpendicular direction) of SCC spread after lifting the standard slump cone and concrete stopped flowing. According to Nagataki and Fujiwara et al. [1995], the slump flow value of concrete should be ranged between 550 and 700 mm to qualify for the SCC. Tang et al. [2001] suggested a slump value of 500 mm or more for SCC under conditions that no aggregate segregation. Xie et al. [2002] suggested limit of 650 to 750 mm for SCC. The SCC may segregate at slump flow higher than 750 mm and less than 550 mm slump flow may be insufficient to pass through highly congested reinforcement. Slump flow time to reach 500 mm of spread (T_{500}) is also considered as a measure of flowability

V-funnel and L-box tests: The deformability of SCC through restricted areas can be evaluated by using V-funnel test [EFNARC 2006; Ozawa et al. 1995]. In this test, a V-shaped funnel is filled completely with fresh SCC without any consolidation and the bottom outlet is opened, allowing concrete to fall out under gravity. The time of flow from the opening of bottom outlet to the complete seizure of flow is considered as a V-funnel flow time. The V-funnel flow time could be high if paste viscosity and inter-particle friction are high. The L-box test is used to

determine the ability of SCC to flow through the gaps between reinforcing bars [PCI, TR6-03, 2003]. A V-funnel flow time of up to 6s and L-box index (passing ability) of above 0.8 are recommended for SCC.

Static Segregation Visual Stability Index of Hardened SCC: Static segregation is mainly controlled by gravity. Visually, segregation and stability could be inspected and evaluated for fresh mixes by investigating hardened cylindrical specimens. At the Illinois Department of Transportation (IDOT), SCC stability is assessed visually, using protocols described in the Illinois Test Procedure SCC- 6, Test Method for Static Segregation of Hardened Self-Consolidating Concrete Cylinders. This test, which has been used since 2003, involves casting or coring concrete, cutting the core lengthwise in two, visually examining the extent of segregation, and expressing such stability in terms of a Hardened Visual Stability Index (HVSI). HVSI ratings have four levels that are based on the length of top concrete mortar layer and variance in size and coverage of coarse aggregate distribution from top to bottom of concrete sample. Traditionally, HVSI assessment is based on visual judgment and is therefore, severely limited by human error, low efficiency, and work tedium [Fang and Labi 2007].

A methodology for automatically measuring the static segregation resistance (stability) of SCC has been developed [Fang and Labi 2007]. The automated system can replace the traditional (visual) assessment method as it overcomes the limitations of the latter such as human error, low efficiency, and work tedium. The automated process involves: digital processing of a concrete sample image, and then generate a binary image of light colors (aggregates) and dark colors (concrete cement), see Figure 2.1. Also, this system identifies aggregate sizes and positions, and detects the mortar layer position and thickness, and assessing the concrete sample stability in terms of HVSI. The developed algorithms were implemented using standard coding languages. The accuracy of the automated system was checked using control observations and it is found that this new system is capable

of reliably and consistently assessing concrete stability in terms of static segregation resistance.

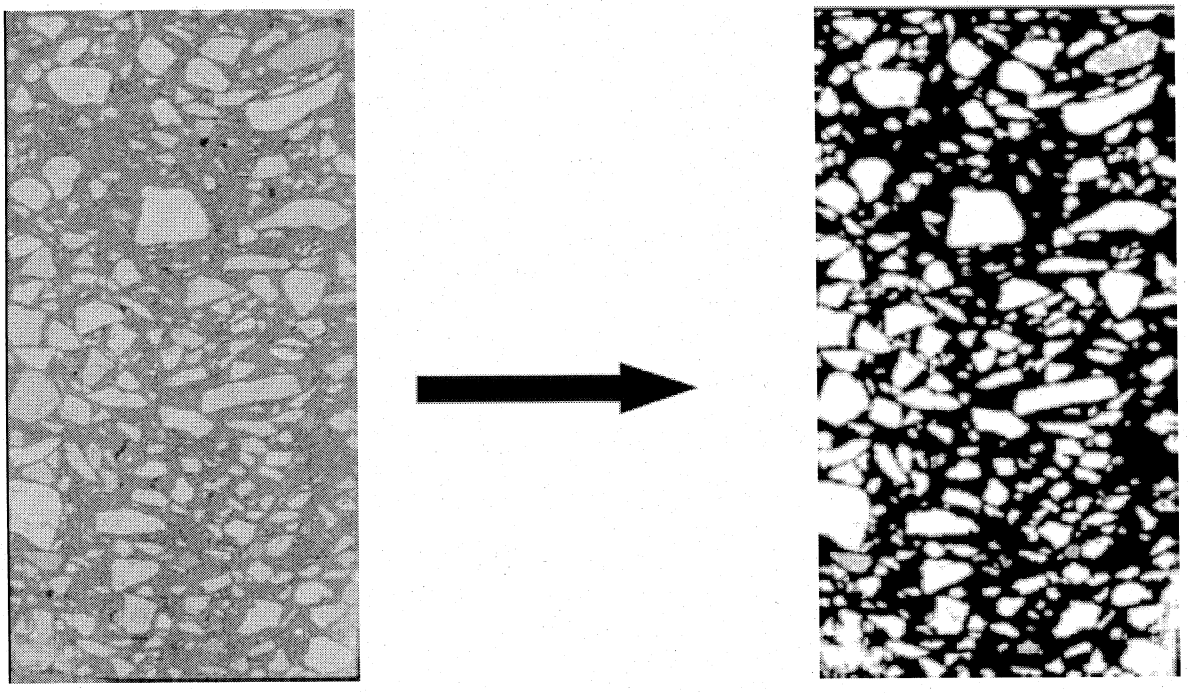

Figure 2.1 Original and grey image binary segmentation

This technology involved the use of an imaging device (camera) and a set of algorithms to assess aggregate and binder distributions by viewing a cut concrete surface thereby evaluating the quality of SCC material from the perspective of aggregate stability in the binder. Also, this technology can easily be adapted to carry out particle size distribution of aggregates in finished asphalt and Portland-cement concrete of all kinds, and to determine the percentage of the binder or air voids in concrete. This would greatly reduce the resources and time used (and would also decrease inherent uncertainties) in post-construction quality assurance [Purdue 2008].

Stability index of SCC provides a visual evaluation of the SCC patty resulting from observation of the SCC just prior to placement and after the performance of the slump flow test [PCI, TR-6-30 2003]. It is used to evaluate the relative stability and

segregation of batches of the same or similar SCC mixes. This visual test is related to dynamic segregation of SCC flow and it is rating from 0 to 3 in increments of 0.5.

2.2.4 SCC Classification Based on Fresh Properties

SCC has been used for many different applications, including bridge decks, precast bridge members, and pavement repairs. Depending on the type of application; classification for specifications in the fresh state is required. The main concern is confinement conditions related to the concrete element geometry, quantity, type and location of reinforcement, delivery (e.g. pump, direct from truck-mixer, or tremie), and placing methods.

Table 2.2 Fresh Properties of SCC for applications based on [Walraven 2003]

Viscosity				**Segregation resistance/ Passing ability**
VS2 VF2	Ramps			Specify passing ability for SF1 & SF2
VS1 or 2 VF1 or 2 or a target value	Walls And Piles	Tall and Slender		Specify SR for SF3
VS1 VF1	Floors and slabs			Specify SR for SF2 & SF3
	SF1	SF2	SF3	
	Slump Flow (SF)			

The classified systems are detailed in Tables 2.2, 2.3, 2.4, 2.5 and 2.6. They describe the appropriate classifications and the required specifications of SCC to cover these application requirements. Here, the segregation ratio is calculated as the weight percentage of a sample passing through a sieve with 5 mm square apertures. Table 2.2 highlights the initial parameters and classes to be considered

for specifying SCC in different applications. It does not take account of specific confinement conditions, element geometry, placing method or characteristics of the materials to be used in the concrete mix. Discussions should normally be held with the concrete producer before a final specification decision is made [European SCC Guidelines 2005].

Table 2.3 Consistent by Slump-flow diameter of SCC

SF1, 550-650 mm, un-reinforced or slightly reinforced concrete structures that are cast from the top with free displacement from the delivery point (e.g. housing slabs), or casting by a pump injection system (e.g. tunnel linings), or sections that are small enough to prevent long horizontal flow (e.g. piles and some deep foundations).
SF2, 660-750 mm, suitable for many normal applications (e.g. walls, columns)
SF3, 760-850 mm, typically produced with a small maximum size of aggregates (less than 16 mm) and is used for vertical applications in very congested structures, structures with complex shapes, or for filling under formwork. SF3 will often give better surface finish than SF 2 for normal vertical applications but segregation resistance is more difficult to control.

Table 2.4 Viscosity by Slump flow time T_{500} or V-funnel time of SCC

VS1 ≤ 2 or VF1≤ 8 has good filling ability even with congested reinforcement. It is capable of self-levelling and generally has the best surface finish. However, it is more likely to suffer from bleeding and segregation.
VS2 > 2 or VF2 = 9 to 25 has no upper class limit but with increasing flow time it is more likely to exhibit thixotropic effects, which may be helpful in limiting the formwork pressure or improving segregation resistance. Negative effects may be experienced regarding surface finish (blow holes) and sensitivity to stoppages or delays between successive lifts.

Table 2.5 Passing ability, PA (%) of SCC

PA1 ≥ 0.8 with two rebars, structures with a gap of 80 mm to 100 mm, (e.g. housing, vertical structures)
PA2 ≥ 0.8 with three rebars, structures with a gap of 60 mm to 80 mm, (e.g. civil engineering structures)

Table 2.6 Segregation resistance (SR) of SCC

SR1 ≤ 20 %, generally applicable for thin slabs and for vertical applications with a flow distance of less than 5 metres and a confinement gap greater than 80 mm.
SR2 ≤ 15 %, preferred in vertical applications if the flow distance is more than 5 meters with a confinement gap greater than 80 mm in order to take care of segregation during flow. It may also be used for tall vertical applications with a confinement gap of less than 80 mm if the flow distance is less than 5 meters but if the flow is more than 5 meters a target SR value of less than 10% is recommended.

Table 2.7 Guidance for using SCC in PCI [Lanier et al., 2003]

			Slump flow (mm)			**T_{500} time (sec)**			**L-Box (%)**			**V-Funnel (sec)**		
			< 558	558-660	> 660	< 3	3 - 5	> 5	< 75	75 - 90	> 90	< 6	6 - 10	> 10
Member Characteristics	Reinforcement Level	Low												
		Med	■			■			■			■		
		High	■			■			■			■		
	Element Shape Intricacy	Low												
		Med	■					■						■
		High	■	■				■						■
	Element Depth	Low												
		Med												
		High				■						■		
	Surface Finish Importance	Low												
		Med	■					■						■
		High	■	■				■						■
	Element Length	Low												
		Med	■						■					
		High	■	■		■			■	■		■		
	Wall Thickness	Low	■	■				■	■					■
		Med	■											
		High												
	Coarse Aggregate Content	Low												
		Med												
		High									■			■
	Placement Energy	Low	■	■					■					■
		Med	■											
		High				■						■		

Dark blocks represent potential problem areas.

Precast/Prestressed Concrete Institute (PCI), from Chicago, had provided a manual as guidance for using SCC with best available information on SCC, see Table 2.7, as it applies to current North American practice [Lanier et al., 2003].

Recent developments in SCC technology show that SCC material selection and mix design can be tailored for many applications. An example is the development of a new type of SCC for slip-form paving (SFSCC) with sufficient green strength right after paving extrusion while the concrete is still in plastic state [Wang et al. 2005].

The SFSCC is not as fluid as the conventional SCC. However, it is workable enough for machine placement, self-compacting with minimum segregation and holding shape after extrusion from a paver. It also has performance properties (strength and durability) compatible to current pavement concrete [Wang et al. 2005].

2.3 Rheology of Concrete with Reference to SCC

Rheology is the science dealing with deformation and flow of material under stress [Mindess et al. 2002]. Fluid rheology is applicable to fresh concrete, as it can be considered a fluid. The concrete is a very complex material due to several reasons. Concrete involves a very wide range of particle size. Concrete is a suspension of fine and coarse aggregates in cement paste which is, in turn, a concentrated suspension of cement particles in water. Concrete is a time-dependent material because its flow properties change with time due to hydration reactions. The rheology of concrete is a topic which has been widely studied and can be very useful in scientifically defining concrete workability [Erdoğan 2005].

If a shear force (F) is applied, a velocity (V) gradient is induced in a liquid as shown in Figure 2.2. The velocity gradient is equal to the shear rate. The proportionality between the force and shear rate is the viscosity. The stress needed to initiate flow is known as the yield stress [Ozyildirim and Lane 2003].

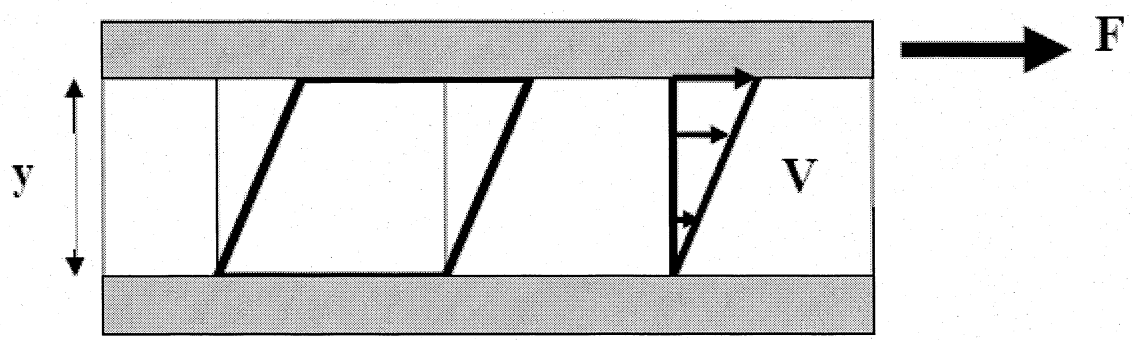

Figure 2.2 Two dimensional representation of viscous flow [Koehler 2004].

The relationship between the shear stress and shear rate of a fluid is often represented by a flow curve. The flow behaviour of fluids can be distinguished by comparing their flow curves. Figure 2.3 shows idealized flow curves based on some of the most common models [Erdoğan 2005].

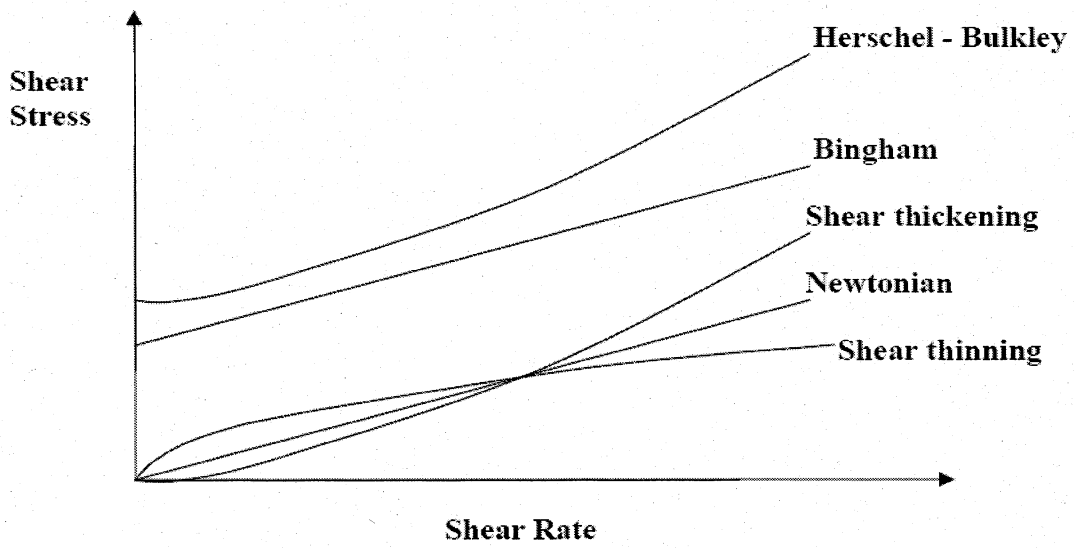

Figure 2.3 Idealized flow curves based on some common models [Erdoğan 2005].

Normally there are two types of flow behavior: Newtonian fluid and non-Newtonian fluid. In the Newtonian fluid, the shear stress is proportional to the shear rate (shear strain rate) and at a given temperature; the viscosity remains constant at any shear rate. While in the non-Newtonian fluid, when the shear rate is varied, the shear stress doesn't vary in the same proportion and same direction. The viscosity of this fluid changes as the shear rate varies [Ferraris 1999].

The most basic constitutive equation that describes fluid flow is for Newtonian fluids, such as water and oil at a given temperature. The flow of paste, mortar, and concrete is assumed to follow the non-Newtonian equation of viscous flow, where viscosity of the fluid is the ratio of shear stress to shear rate (shear strain rate). The most commonly used model for paste, mortar, and concrete is the Bingham model.

The Bingham Model, which is the most commonly used model for defining the flow of concrete mixtures, assumes a linear relationship between shear stress and shear rate and accounts for a yield stress, more correctly defining the flow behaviour of concrete mixtures. Concrete typically behaves like a liquid modeled by the Bingham equation 2.1 [Ozyildirim and Lane 2003]:

$$\tau = \tau_o + \mu\gamma \qquad (2.1)$$

Where, τ = Shear stress; μ= Viscosity; τ_o = Yield stress and γ = Shear rate

This model requires two parameters, ie. yield stress and plastic viscosity. The yield stress is the stress above which the material becomes fluid. In other words, the yield stress corresponds to the intercept on the shear stress axis. The plastic viscosity is the measure of how easily the material will flow, once the yield stress is overcome. The plastic viscosity is the slope of shear stress-shear rate plot as shown in Fig. 2.4 [Ferraris 1999].

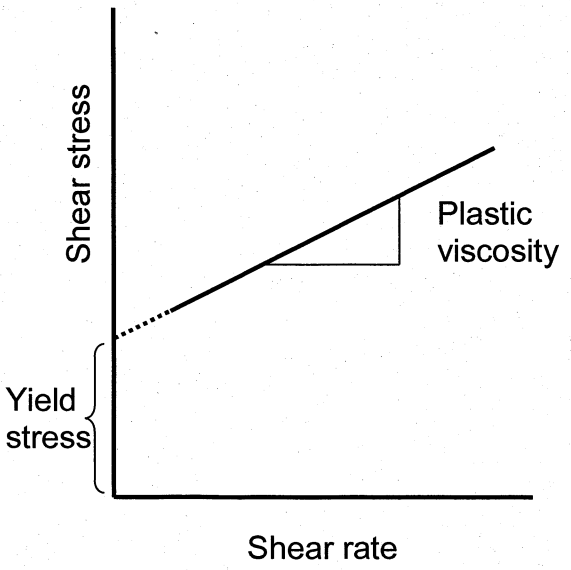

Figure 2.4 Bingham model showing plastic viscosity and yield stress

In concentrated suspensions, solid particles interact to form a flocculated (clumps or fluffy masses) structure that resists flow at sufficiently low stresses. Yield stress is related to the force required to break down this flocculated structure and to initiate flow. Yield stress is determined from a flow curve by extrapolating back the measured data points to intercept the shear stress axis (Fig. 2.4).

Some recent studies have shown that some types of concrete containing high amount of binder and super plasticizers had shown non-linear behaviour [De Larrard et al. 1998], but the simpler Bingham model is appropriate and sufficient for most cement paste, mortar and concrete [Newman and Choo 2003].

The Herschel-Bulkley model, another model which is commonly used for defining concrete flow, assumes a non-zero yield stress and a non-linear relationship between the applied shear stress and the shear rate as shown in Eq. 2.2 [Erdoğan 2005].

$$\tau = \tau_o + k\gamma^n \qquad (2.2)$$

where k is a constant, n = 1 for Newtonian flow, n > 1 for shear thickening and n < 1 for shear thinning (Fig. 2.3).

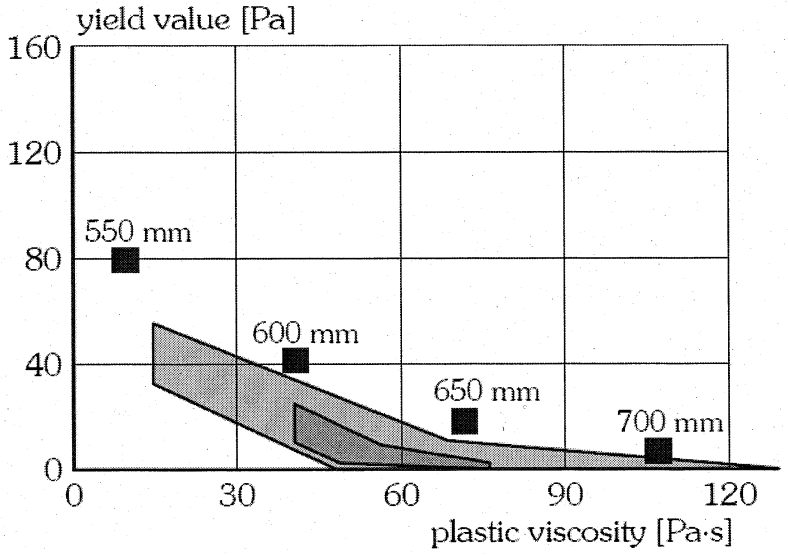

Figure 2.5 Range for SCC and recommended slump flow (grey areas).

SCC has been developed in a wide range of compositions [Grünewald 2004]. The dark grey region in Figure 2.5 marks the target area of SCC concerning the yield value and the plastic viscosity, which is the result of measurements executed with the BML-Viscometer [Nielsson and Wallevik 2003].

It is reported that the Bingham model describes the flow behavior of SCC best [Wallevik 2003]. However, flow curves of SCC using the BTRHEOM viscometer were described best by the Herschel-Bulkley model, which indicated SCC to be shear thickening [De Larrard et al. 1998].

2.3.1 Factors Affecting the Rheology of Concrete

Workability and other flow properties are related to the rheology of concrete which requires at least two parameters, such as the Bingham parameters, for adequate description. Principal factors influencing the rheological parameters of concrete

are: the composition of the concrete, including the chemical and mineral admixture dosage/type, the gradation/shape/type of aggregates, the water content and the cement characteristics. Also, pumping, spreading, moulding and compaction of concrete depend on rheology [Banfill 2003].

The same mixture design can result in different flow properties if secondary factors are not taken into account. These are: mixer type - pan, truck (these may induce various levels of deflocculation and air entrainment); mixing sequence i.e., sequence of introduction of the materials into the mixer; mixing duration and temperature [Ferraris et al. 2001].

SCC varies in materials, applications, methods of design and properties. Table 2.8 shows an estimation of typical SCC powder, water, and rheological parameters [Nielsson and Wallevik 2003].

Table 2.8 Estimate of typical SCC in developed countries

Country	**Powder** (Kg/m^3)	**Water** (Kg/m^3)	**Yield value** (Pa)	**Plastic viscosity** (Pa s)
Sweden	>550	180	0-30	50-100
The Netherlands	>550	190	0-10	60-120
Japan	>550	170	0-30	50-120
France	-	-	0-10	>60
Switzerland	<450	200	0-50	10-20
Norway	<450	170	10-50	30-45
Iceland	<450	180	10-50	20-40
Denmark	<400	160	30-60	<40
UK	>500	210	10-50	50-80
Germany	>500	180	0-10	60-90
US	>500	190	0-20	40-120

2.4 Fiber Reinforced Concrete (FRC)

The fiber reinforced concrete (FRC) is a concrete containing dispersed randomly oriented short discrete fibers. Since its invention in the early 1960s, fiber reinforced concrete (FRC) has been successfully used in various types of construction: airport and highway pavements, slabs and floors, bridge decks, tunnel linings, shotcrete coverings, seismic-resistant and explosion-resistant structures, etc. (Vondran, 1991; Shah and Skarendahl 1986, ACI 1984). Such a success is essentially due to the fact that adding fibers improves the durability and mechanical properties of hardened concrete, notably flexural strength, toughness, impact strength, resistance to fatigue, vulnerability to cracking and spalling (Williamson 1965, Bentur et al. 1989, Chanvillard and Aitcin 1990, Nakagawa et al. 1989, Beaudoin1990, ACI Committee 544 1990, Al-Tayyib and Al-Zahrani 1990, Mufti et al. 1993, Malhotra et al. 1994, Tlemat et al. 2003].

A high performance material called SIFCON (slurry infiltrated fiber concrete), which combines simultaneously a number of outstanding properties such as strength (compression, tension, bending, and shear), ductility, toughness, durability, stiffness, and energy absorption capacity under monotonic and cyclic loads was developed [Naaman 1991]. The properties of SIFCON are achieved through an optimized combination of matrix properties, fiber reinforcing parameters, fiber content, and interface characteristics between fiber and matrix.

High performance fiber reinforced engineered cementitious composites (ECCs) have been developed with superior ductility (about 1,000 times of the ductility of normal concrete in tension) [Li 1994, Li and Kanda 1998, Fischer and Li 2002a,b, Wang and Li 2006]. ECC is composed of cement, sand, water, a small amount of admixtures, and an optimal amount of fibers either polyethylene (PE) or Hydrophilic poly vinyl alcohol (PVA) based. ECC has a tensile strain capacity of up to 6% and exhibits pseudo-strain hardening behavior, while other FRCs require much larger amount of fibers for comparable mechanical properties [Li et al. 1998, Kong et al. 2003a,b].

Unlike some high performance FRCs, SIFCON (slurry infiltrated 5 - 20% of steel fibers - Naaman 1991), SIMCON (slurry infiltrated 6% steel fiber mat -Hackman et al. 1994, slurry infiltrated steel wool – Bentur and Cree, 1987), and CRC matrix (using 5 - 10% fine steel fibers - Bache 1987), which generally adopt very high fiber contents, ECC utilizes only a limited amount of fibers. In general, only 2% or less by volume of discontinuous fibers is used in ECC. ECC also has high ultimate tensile strength (5 -10 MPa) and modulus of rupture (8-25 MPa), high fracture toughness (25-30 kJ/m^2) and isotropic properties (Li, 1994). The ultra-high ductility is achieved by optimizing the microstructure of the composite employing micromechanical models that serves to establish the link between material constituents, such as matrix, fiber, and interface, and composite properties [Fischer and Li 2002]. PVA-ECC is favored for practical applications, since it is more cost-effective than PE-ECC. PVA-ECC also possesses higher durability characteristics that can increase its life cycle of a structure [Li 1993, Li et al. 1998].

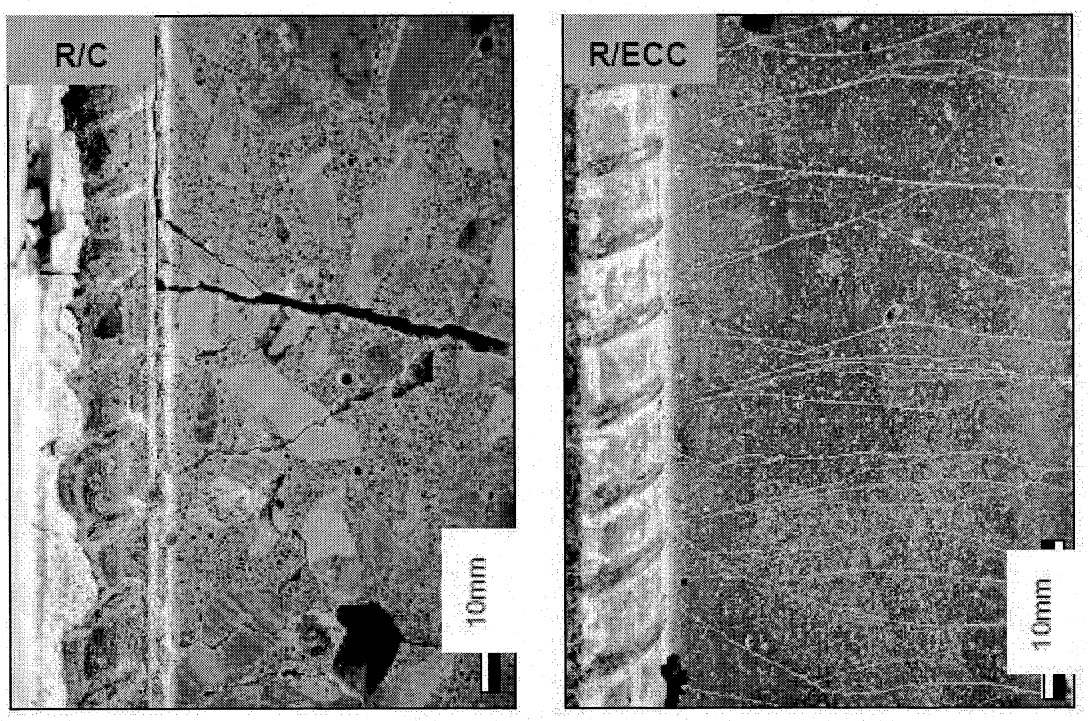

Figure 2.6 Performance of ECC and reinforced concrete

Figure 2.6 shows the improved performance of steel reinforced ECC (R/ECC) compared with reinforced concrete (R/C) near the interface (revealed in a cross-sectional cut of tension-stiffening specimens). Development of micro cracking in ECC is an indication that the load being transmitted via bridging fibers producing compatible deformation between ECC and steel reinforcement (right). In contrast, the brittle fracture of concrete in normal R/C (left) causes unloading of concrete, resulting in high interfacial shear and bond breakage [Li 2003].

2.5 Fiber Reinforced Self-consolidating Concrete (FRSCC)

A fiber reinforced SCC (FRSCC) can combine better mechanical, durability and ductility characteristics of FRC with the workability of conventional SCC. Development of FRSCC for higher performance has been studied and experimental tests have been conducted (Miao et al. 2003, Grünewald and Walraven 2001, Khayat and Roussel 2000, Sahmaran et al. 2005, Corinaldesi and Moriconi 2004). A FRSCC should freshly spread into formworks without vibration and gain high design strength plus high durability at hardened stages.

FRSCC offers several economic and technical benefits as its combines the advantages of SCC and FRC. The use of steel fiber as reinforcement in the concrete provides the control of micro and macro-cracking, increase the resistance to compression, fatigue, impact and abrasion. These improvements depend on the type of fiber, diameter, length, shape, volume fraction and spatial arrangement [Grünewald and Walraven 2001, Sahmaran et al. 2005, Corinaldesi and Moriconi, 2004].

2.5.1 FRSCC Mix Design and Methodology

No standard proportioning method is presently available for steel fiber reinforced self-compacting concrete. A FRSCC should be a fluid concrete without bleeding or segregation. The slump loss should also be well controlled. To satisfy those requirements, materials had to be carefully selected and their proportion optimized [Miao et al. 2003]. A proper design and control of fibers and matrix in SCC will

improve workability, provide sufficient consolidation and improve fiber dispersion. A FRSCC should freshly spread into formwork without vibration and gain high design strength plus high durability at hardened stage.

A method was proposed for the design of FRSCC based on an experimental investigation consisting of two references and 20 FRSCC mixtures [Grünewald and Walraven 2001].

A study of cost competitive FRSCC for pre-casting industrial applications was conducted [Pereira et al. 2005]. The mix design was developed based on three steps: 1) the proportions of the constituent materials of the binder paste plus the optimum percentage of limestone filler (LF) addition in the final composition are defined; 2) the proportions of each aggregate on the final solid skeleton are determined where the optimum aggregate mix was assumed to be the heaviest one and 3) binder paste and solid skeleton are mixed in different proportions until self-compacting requirements in terms of spread ability, correct flow velocity, filling ability, blockage and segregation resistance are assured.

FRSCC mixtures were developed by using a mix design that follows a simple methodology (previously applied to high-strength SCC) based on optimizing separately the paste and the granular skeleton [Barragan et al. 2005]. The results showed that the self-compactability can be obtained even with the incorporation of 40 kg/m^3 of steel fibers. Furthermore, the developed FRSCC was successfully applied in the construction of slender walls [Barragan et al. 2005].

A simple method for mix design of self-consolidating fiber reinforced concretes has been presented and assessed [Ferrara et al. 2007]. A "rheology of paste model" is applied to the mix design of FRSCC. Fibers are included in the particle size distribution of the solid skeleton through the concept of an equivalent diameter, defined on the basis of the specific surface. The influence of fibers (type and quantity) on the grading of solid skeleton, minimum content and rheological

properties of the paste required to achieve the required self-compactability and rheological stability were studied. Tests were conducted on both plain and fiber-reinforced concrete made with a variety of mix compositions. In addition, rheological tests were made with corresponding cement pastes [Ferrara et al. 2007]. However, further developments and application of the model with reference to differently graded aggregates, types and volume ratios of fiber reinforcement (even non-metallic ones) are required.

2.5.2 Fresh Properties of FRSCC

The fresh/workability properties of FRSCC are affected by the use of fiber, and the reduction of workability is directly proportional to the volume fraction of fibers used A study conducted on 22 concrete mixtures confirmed that high deformability, segregation resistance and passing ability are the characteristics that define the quality of FRSCC [Grünewald and Walraven, 2001]. It was also found that the flow behavior of FRSCC mixtures differs from that of plain SCC. Qualitative observations indicated that a homogenous distribution was achieved up to a critical fiber content. Once that critical fiber content was surpassed, a stiff structure of the granular skeleton made flow under concretes' own weight impossible. The slump flow test detected the clustering of coarse particles. In addition, to avoid the risk of blocking a larger free bar spacing compared with plain SCC appears to be necessary if steel fibers are applied. Finally, it was found that a considerable amount of fibers allowed self-compacting behaviour and the mixture composition of the reference mixture influenced the maximum possible fiber content [Grünewald and Walraven 2001].

It is important to determine the optimum fiber content in order to achieve the best required concrete workability and or strength. Workability depends on many parameters such as maximum aggregate size, fiber volume, fiber type, fiber geometry, and fiber aspect ratio (Sahmaran et al. 2005). For the same fiber content, better workability was achieved at lower aspect ratios of fibers [Grünewald and Walraven 2001].

The effects of fibers on the workability of FRSCC with two different types of steel fibers were quantified based on the fiber volume, length, and aspect ratios of the fibers [Sahmaran et al. 2005]. It was concluded that in addition to the above-mentioned quantifiable three properties, other properties of fibers such as shape and surface roughness are also found to be important. Similar conclusions were also derived from another study on FRSCC using a combination of carbon and steel fibers (hybrid) [Aydin 2007].

The workability of FRSCC was investigated by producing mixtures made with steel fibers, polypropylene (PP) fibers and fiber cocktail (Steel + PP) of various dosages [Ding et al. 2008]. The mixtures were tested using various new methods for evaluating the flowability, filling ability and segregation risk of the fresh mortar/concrete. Based on the experimental results of the workability, the suitable fiber types (steel, PP and fiber cocktail) and fiber dosages for FRSCC were suggested. For FRSCC, the reduction of flowability was found to be common when adding a significant amount of fibers.

Fresh state properties (rheological and workability) of FRSCC were correlated to hardened state properties such as splitting tensile strength and compressive strength in some research studies [Ozyurt 2007, Sahmaran and Yaman 2007].

An investigation was conducted to study the homogeneity of plain and steel fiber reinforced SCC to be used in slender elements of considerable height, avoiding the use of conventional reinforcement [Torijos et al. 2007]. Tests in the fresh state included the measurement of the rheological properties and self-compactability through engineering tests. Based on the casting of slender columns with plain concrete and FRSCC, it was found that the physical (fiber/aggregate distribution) and mechanical properties (elasticity, compressive strength) did not vary significantly along the height of the columns, though the aggregate distribution was slightly more homogeneous in the case of FRSCC.

2.5.3 Mechanical Properties of FRSCC including Fracture Energy

Miao et al. [2003] concluded that adding steel fibers not only increased the entrapped air content and improved the compressive strength of FRSCC but also significantly improved the flexural strength.

An investigation was conducted to develop FRSCC mixtures to study the effects of various fiber combinations on the workability and ability of FRSCC to flow around obstructions, compressive/flexural strengths, and flexural toughness [Nehdi and Ladanchuk 2004]. A total of 31 SCC mixtures were made based on the same control mixture with combinations of fibers in varying proportions from 0.25 to 1.0%. Two types of steel macrofibers of two different sizes were incorporated individually at a fiber volume of 1.0%. Also, synthetic polymer macrofibers of two different sizes were used individually and in different combinations at different volumes from 0 to 1.0% were used to evaluate their potential synergistic effects. The study showed that FRSCC mixtures made with shorter fibers had slightly higher 28-day compressive strengths and the fiber volume had little influence on the compressive strength. Generally, flexural toughness of FRSCC mixtures containing combinations of fibers with a total fiber volume of 1.0% was higher compared to those with single type of fiber of same fiber volume. The results of this research indicated that fibers can have rheological and mechanical synergistic effects, and that optimized fiber combinations can better increase toughness and flexural strength while maintaining adequate flow properties for FRSCC [Nehdi and Ladanchuk 2004].

An investigation was conducted to develop cost effective FRSCC [Pereira et al. 2005]. Developed FRSCCs had attained all the requirements of self-compactibility and compression strength of 25 MPa at 12 hours and 62 MPa at 28 days, with a cement content of about 360 kg/m^3.

The strength and flexural toughness of FRSCC was investigated by poducing mixtures made with steel fibers, PP-fibers and fiber cocktail of various dosages

[Ding et al. 2008]. A series of experiments had been carried out to evaluate the influences of different fibers on the compressive strength, flexural toughness and failure patterns of beams and slabs. The fiber cocktail (a combination of steel fibers and PP fibers) produced better strength and flexural toughness of FRSCC.

A comparative study of the fracture properties of SCC, high strength concrete (HSC) and normal concrete (NC) was conducted [Niwa and Tangtermsirikul 1997). The fracture energy of the concrete mixes was determined by testing notched beams of dimensions 10 x 10 x 80-cm under three point loading recommended by RILEM [1983]. The study confirmed that fracture energy of SCC was significantly lower than HSC and NSC of same strength due to the large amount of cementitious material. Therefore, the mechanical behaviour of SCC subjected to tension is considered to be more brittle than that of HSC and NSC.

Impact tests were carried out on small concrete beams reinforced with different volumes of both polypropylene and steel fibers to assess fracture energy characteristics [Wang et al. 1996]. It was found that, at volume fractions less than 0.5%, polypropylene fibers gave only a modest increase in fracture energy. Steel fibers could bring about much greater increases in fracture energy, between steel fiber volumes of 0.5% and 0.75%. Below 0.5%, fiber breaking was the primary failure mechanism and the increase in fracture energy was also modest; above 0.75% fiber pull-out was the primary mechanism with a large increase in fracture energy.

The fracture properties of FRC with polypropylene fibers and steel fibers (fiber content ranges from 0% to 0.95% by volume) are evaluated based on four-point bending test on notched prisms with the size of 100 × 100 × 500 mm [Qian and Stroeven 2000]. The results show that there is a positive synergy effect between large steel fibers and polypropylene fibers on the load-bearing capacity and fracture toughness. The large and strong steel fiber is better than soft polypropylene fiber and the small steel fiber is better in the aspect of energy

absorption capacity in the large displacement range. Another study on FRC with carbon fiber also showed considerable beneficial effect interms of flexural toughness [Deng 2005].

2.5.4 Durability Properties of FRSCC

The steel fiber addition proved to be very effective in counteracting drying shrinkage of FRSCC, which is usually a great problem for this material, rich in powders and poor in the coarse aggregate fraction [Corinaldesi and Moriconi 2003].

As any other cement based composite, SCC shrinks at an early age and can crack when shrinkage is restrained. One possible solution to reduce the impact of early age shrinkage on concrete durability is to include low volumetric fractions of short fibers in order to control crack growth [Barluenga and Hernández-Olivares 2007]. An experimental program to evaluate the cracking control ability of Alkali Resistant (AR) glass fibers in FRC and FRSCC was conducted The experimental program included compression and flexural strength tests, free shrinkage tests and double restrained slab cracking tests. The results showed that the inclusion of low volumetric fractions of AR-glass fiber can control the cracking produced due to very early age shrinkage on both FRC and FRSCC in two different ways: reducing the total cracked area and the maximum length of the cracks. Although drying shrinkage in FRSCC was larger, it produced similar performance compared with FRC in the hardened state based on equivalent cracking area [Barluenga and Hernández-Olivares 2007].

With the increasing application of SCC in construction and infrastructure, the fire spalling behavior of SCC has been attracting due attention. In high performance concrete (HPC), addition of PP fibers is widely used as an effective method to prevent explosive spalling. It is shown that the melting of PP fiber at high temperature does not significantly increase the total pore volume and also increase the connectivity of isolated pores leading to an increase of gas permeability. With the increase of temperature, the addition of PP fibers reduces

the damage of cement pastes. From the investigation, it is concluded that the connectivity of pores as well as the creation of micro cracks are the major factors which determine the gas permeability after exposure to high temperatures [Liu et al. 2008]. Investigation has shown that 0.5 kg/m^3 of polypropylene fibers in the self-compacting cement paste can avoid the fire damage efficiently at elevated temperature [Ye et al. 2007].

A new fiber reinforced self-compacting repair mortars (FR-SCRM) is developed for the rehabilitation and repair of reinforced concrete structures using steel fibers [Felekoğlu et al. 2007]. The self-compactability of repair mortars brings considerable advantages at narrow mould systems. However, due to the high powder content and absence of coarse aggregate, FR-SCRMs are susceptible to surface abrasion, especially in case of repair of surfaces under high rates of abrasion (floors, slabs). It is concluded that steel fibers can have rheological and mechanical synergistic effects, and that optimised fiber-superplasticizer dosage combinations can improve the wear resistance while maintaining adequate flow properties for FR-SCRM.

2.5.5 Fibers and their Influence on Concrete

Fibers can be used in the production of SCC, but they may reduce flowability and passing ability. Trials are therefore needed to establish the optimum type, length and quantity to achieve all the required properties in the fresh and hardened concrete [European SCC Guidelines, 2005].

Fiber length and quantity are selected depending on the maximum size of aggregate and on structural requirements. If fibers are used as a substitute for normal reinforcement, the risk of blockage is no longer applicable but it should be emphasised that using SCC with fibers in structures with normal reinforcement significantly increases the risk of blockage [European SCC Guidelines, 2005].

2.5.5.1 Types, Usage and Properties of Fibers

Fibers can be found in varieties of shapes and sizes and produced from steel, glass, carbon, plastic and natural materials [Beaudoin1982]. The most known are nylon, polyester, polyethylene (PE), polypropylene (PP), polyvinyl alcohol (PVA), acrylic, armed, cellulose, glass, carbon, asbestos, metallic, natural and fibers from wastes (steel fibers or shredded rubber from tyers). Apart from the normal steel fibers, also other fibers can be used in concrete. Synthetic fibers are often used for the control of shrinkage cracks [Grünewald and Walraven 2001].

Polymer fibers can be used to improve the stability of SCC, as they help prevent settlement and cracking due to plastic shrinkage of the concrete. Steel or long polymer structural fibers are used to modify the ductility/toughness of the hardened concrete [European SCC Guidelines 2005].

Properties of fibers that usually of interest are fiber concentration, fiber geometry, fiber orientation and distribution. A higher percentage of fiber in concrete is more difficult to distribute and more lower workability. It is important to verify and design the optimum content in order to achieve the best required concrete workability and or strength. Depending on many parameters such as maximum aggregate size, fiber volume, fiber type, fiber geometry, and fiber aspect ratio, fiber inclusion to concrete reduces the workability of concrete [Sahmaran et al. 2005].

The aspect ratio is the length of fiber divided by its diameter. The higher the aspect ratio was, the fewer fibers could be added to surpass the critical fiber content [Grünewald and Walraven 2001]. For the same fiber content, better workability was achieved at lower aspect ratios. Also the higher the aspect ratio and the volume concentration of the fibers, the better is the performance in the hardened state [Grünewald and Walraven 2001].

Low volume fraction (<1%) - use of fibers at this level reduces shrinkage cracking when they are used in slabs and pavements that have large exposed

surface leading to high shrinkage cracks. Also, dispersed fibers offer various advantages compared to steel bars and wire mesh. The dispersed fibers reduce shrinkage cracks as they are uniformly distributed in three-dimensions making an efficient load distribution. The the fibers are less sensitive to corrosion than the reinforcing steel bars and the use of fibers can reduce the labour cost of placing the bars and wire mesh [Mehta and Monteiro 2006].

Moderate volume fraction (between 1 and 2%) - use of fiber at this level increases modulus of rupture, fracture toughness, and impact resistance of the composites. Their use in construction methods such as shotcrete and in structures that require energy absorption capability, improved capacity against delamination, spalling, and fatigue [Mehta and Monteiro 2006].

High volume fraction (greater than 2%) - use of fiber at this level leads to strain hardening of the composites. Because of this improved behavior, these composites are often referred as high performance fiber-reinforced composites (HPFRC). In the last decade, even better composites were developed and were referred as ultra-high-performance fiber reinforced concretes (UHPFRC) [Mehta and Monteiro 2006].

2.5.5.2 PVA Fibers

Poly Vinyl Alcohol (PVA), an organic fiber (made of carbon, hydrogen, and oxygen) was created 50 years ago as the first Japanese organic fiber. Since then, PVA fibers have been used for various industrial applications. PVA fibers have high tensile strength and a high modulus of elasticity as well as excellent UV, chemical and weather resistance. Since 1980, rising concerns about the dangers of asbestos inhalation brought PVA fibers into the limelight as an asbestos replacement [Kuraray-am 2006].

PVA fiber has high adhesion to cement and develop a strong molecular bond with the cement during hydration and curing. This high bond strength makes PVA fibers

very tough to pull out during bending or tension. Due to its affinity and tendency to form bonds with cement, the surface of PVA fiber peels when pulling out, that is a high influence of bonding in matrix, see Figure 2.7 [Kuraray-am, 2006]. PVA fibers can be used together with steel reinforcement, where PVA's micro-crack control helps to prevent water penetration and improves toughness and stiffness.

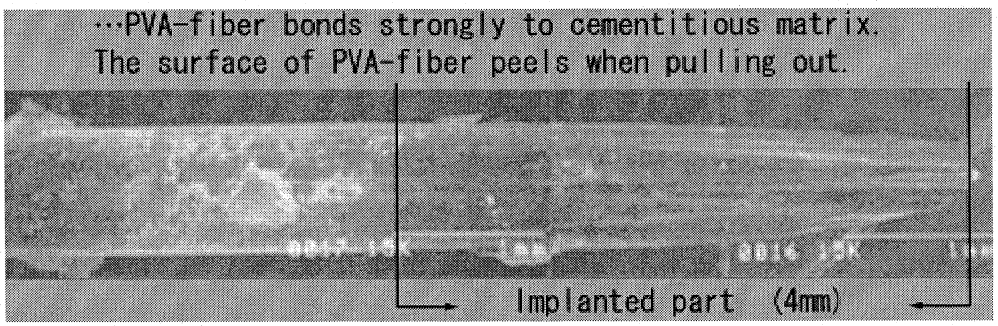

Figure 2.7 PVA fiber peels when pulling out

PVA fibers can be used alone as a truly structural fibers, whose modulus of elasticity is greater than that of regular concrete and two times stiffer than polypropylene (PP) fibers. Polypropylene, nylon and the other synthetic fibers used in concrete serve only to restrain plastic shrinkage. Even at much lower dosages, PVA fiber provides excellent control of all types of cracking including plastic, drying, autogenous, differential curing, settlement and structural. Steel fibers have greater tensile strength than PVA fibers, but this strength is rarely used. Steel fibers (act as passive reinforcement) have no reinforcing effect until the concrete cracks and tend to pull out rather than hold the concrete together. In contrast, molecular bond between PVA fibers and cement hold concrete together using full advantage of its tensile strength during a pullout. A coarser PVA fiber has been widely used in civil engineering applications, including tunnel lining, industrial floors, roadbed overlays and various kinds of shotcrete [Kuraray-am, 2006].

PVA fibers can be used in all types of mortar and concrete to enhance the strength and ductility. PVA can be used as replacement of glass fibers producing a less

expensive, lighter and more durable product. PVA fiber is about the same price as glass as and a little more expansive than polypropylene and nylon. PVA is extremely tough and durable compared to other fibers and has excellent UV radiation, chemical, weather and abrasion resistance. Even the best AR glass degrades in strength dramatically over time, up to 80%. Field studies have shown that PVA degrades about 1% over 20 years. Studies have demonstrated that PVA fibers suffer far less degradation in the harsh alkali environment than zirconia-coated fiberglass, nylon or poly-propylene fibers (Kuraray-am, 2006).

PVA improves concrete microstructure, increase the strength and decreases the porosity. The increase in strength is due to the interaction of PVA with cement, forming some new compounds that fill the pores or improve the bond with the cement [Singh and Sarita 2001].

PVA fibers are hydrophilic for water. They strongly bond to the surrounding cementitious matrix. This tends to limit the multiple cracking effect and leads to lower strain hardening profiles for the composite. Reducing the chemical debonding energy enhances the complementary energy by minimizing premature fibers breakage during the fiber/matrix interface debonding process, prior to fiber slippage [Li et al. 1997].

PVA fibers have a density greater than water (1.3), allowing them to stay in suspension during mixing and finishing which eliminates "hairy" concrete surfaces and jamming equipment (Kuraray-am 2006). PVA fiber is non-toxic for people and environment with long term reliability (U.S. Food and Drug Administration approved). PVA is safe in the event of fire as harmful substances such as dioxin and ammonia are not created [Kuraray-am, 2006].

2.5.5.3 Metallic FibraFlex Fibers

FibraFlex fibers are developed by the research center Saint-Gobain in France. Fibraflex is maufactured by quenching a molten alloy falling on a water cooled

wheel, rotating at high speed [Saint-Gobain 2008]. A specific molten alloy is placed in a crucible, the lower section of which is perforated and fitted with a capillary tube measuring just a few millimeters in diameter. Underneath the crucible, a water-cooled wheel with notches at regular intervals rotates at high speed. The alloy falls onto this wheel and undergoes hyper quenching. The jet of metal is cut in each notch to form the Fibraflix fibers (Figure 2.8).

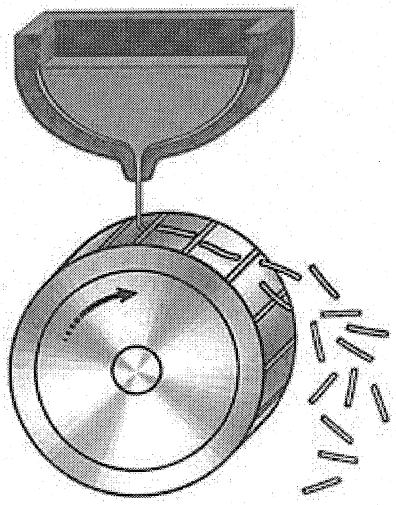

Figure 2.8 Technology of Fibraflex productions

This process solidifies the molten alloy in an amorphous structure, and gives the fiber a high mechanical strength, in addition to a great flexibility [Saint-Gobain, 2008].

As reported on site www.fibraflex.com, for Saint-Gobain SEVA, Fibraflex is very corrosion resistant, due to the chromium content of the alloy. In one kg of fibraflex, it contains 100 000 fibers at a minimum and may contain 1 100 000 - this is due to the thinness of each fiber. By reason of the very high specific area of each fiber, the obtained reinforcement is dense and homogeneous, very efficient to control and distribute cracking. Fibers are used to produce lightweight concrete for packaging and storage of low and medium radioactive wastes and have extreme resistant to impacts and explosions [Saint-Gobain 2008].

Influence of polypropylene and metallic fibers "Fibraflex" have been studied in different proportioning to reduce shrinkage and cracking. Fibraflex fibers contribute to the reduction of shrinkage and cracking under restrained conditions. Though Fibraflex fibers seem to be more efficient than polypropylene fibers, the reduction of shrinkage is not very significant [Mesbah and Buyle-Bodin 1999].

Fibraflex fibers are more effective in reducing restrained shrinkage cracking because of their higher stiffness, inducing better load transfer across the crack. When Fibraflex fibers are added, cracking decreases considerably. With a volume of 1%, the crack width after 50 days is only 0.14 mm compared to 1.1 mm for plain recycled aggregate mortar. The creation of the first crack is also delayed in time with an increase in fiber content [Mesbah and Buyle-Bodin 1999].

3. Experimental Program

3.1 Introduction

Experiments were conducted at concrete and structural laboratories of Ryerson University to develop fiber reinforced self-consolidating concrete (FRSCC) mixtures. In the first phase, tests were conducted to assess fresh/workability properties (such as slump flow, slump flow time T_{500}, L-box ratio, V-funnel time and segregation index) and rheology (plastic viscosity and yield stress) of a range of concrete mixtures with different types/volume percentages of fibers including a control SCC mix with zero fiber content. In the second phase, tests were conducted to determine hardened properties such as compressive/splitting tensile/flexural strengths, fracture energy and chloride penetration resistance of the concrete mixtures. Polymer polyvinyl alcohol (PVA) and metallic "FibraFlex" fibers were used in the concrete mixes. A total of twenty concrete mixtures including the control SCC mix (0% fiber) were evaluated.

3.2 Materials

3.2.1 Cement

Type GU (General Use), hydraulic cement in compliance with CSA A3001-03 (Type 10 normal Portland cement) was used. Chemical, physical and strength properties of the cement are shown in Table 3.1.

3.2.2 Slag

White slag type GranCem (Type S - ground granulated blast furnace slag as per CSA A25.3) was used. The chemical and physical properties of slag are presented in Table 3.1.

Table 3.1 Chemical and Physical properties of cement and GGBFS

Chemical Analysis (%)		**Cement**	**Slag**
Loss on ignition	LOI	2.02	0.30
Silicon dioxide	SiO_2	19.80	40.21
Aluminum Oxide	Al_2O_3	5.51	8.13
Ferric Oxide	Fe_2O_3	2.49	0.68
Calcium oxide	CaO	62.93	39.18
Magnesium oxide	MgO	2.43	11.20
Sulfur trioxide	SO_3	4.50	2.38
Potassium Oxide	K_2O		0.53
Sodium oxide	Na_2O		0.37
Tricalsium silicate	C_3S	52.26	
Dicalcium silicate	C_2S	17.37	
Tricalsium aluminates	C_3A	10.39	
Tetra calcium aluminoferritte	C_4AF	7.57	
Total Alkali		1.00	
Free Lime	CaO	0.79	
Insol.		0.59	
Physical Analysis		**Cement**	**Slag**
Residue 45 um (%)		10.02	8.04
Blaine (m2/kg)		410	415
Air Content (%)		7.79	
Initial Set (mins.)		113	
Auto. Exp. (%)		0.04	
Sulf. Exp. (%)		0.006	
Compressive Strength (MPA) 1 Day		19.41	
Compressive Strength (MPA) 3 Days		30.35	
Compressive Strength (MPA) 7 Days		35.23	
Compressive Strength (MPA) 28 Days		41.47	
Comp. Strength (MPA) (50:50 cement: slag) 7 Days		19.41	27.05
Comp. Strength (MPA) (50:50 cement: slag) 28 Days		30.35	42.71
Slag Activity Index (% of 28 day control)			102.6

3.2.3 Binder

Binder for all the concrete mixtures consists of 70% cement and 30% slag by weight. Total binder content for all 20 concrete mixtures was 450 kg/m^3 with 315 kg/m^3 of cement and 135 kg/m^3 of slag.

3.2.4 Water

Clean drinkable water with a temperature ranging between 22 and 24 ^{o}C was used.

Table 3.2 Grading of fine and coarse aggregate

Sieve Size	Percentage Retained	Cumulative Percentage Retained	Percentage Passing
Fine Aggregate			
9.5 mm (3/8-in)	0.0	0.0	100.0
4.75 mm (No. 4)	0.0	0.0	100.0
2.36 mm (No. 8)	15.2	15.2	84.8
1.18 mm (No. 16)	21.9	37.0	63.0
600 micron (No. 30)	20.6	57.6	42.4
300 micron (No. 50)	24.4	82.1	17.9
150 micron (No. 100)	14.5	96.5	3.5
PAN	3.5	100.0	
Fineness Modules = 2.92			
Coarse Aggregate			
40 mm (1 ½-in)	0	0	100
19 mm (3/8-in)	0	0	100
12.5 mm (1/2-in)	8.9	8.9	91.1
9.5 mm (3/8-in)	30.3	39.2	60.8
4.75 mm (No. 4)	53.7	92.9	7.2
PAN	5.1	100.0	
Nominal MSA = 12.5 mm			

3.2.5 Aggregate

The grading of coarse and crushed fine aggregates was according to ASTM C 136 [2005], and their grain size distributions are tabulated in Table 3.2 and shown in

Figures 3.1 and 3.2. Coarse aggregate was natural river gravel as shown in Figures 3.3 and 3.4.

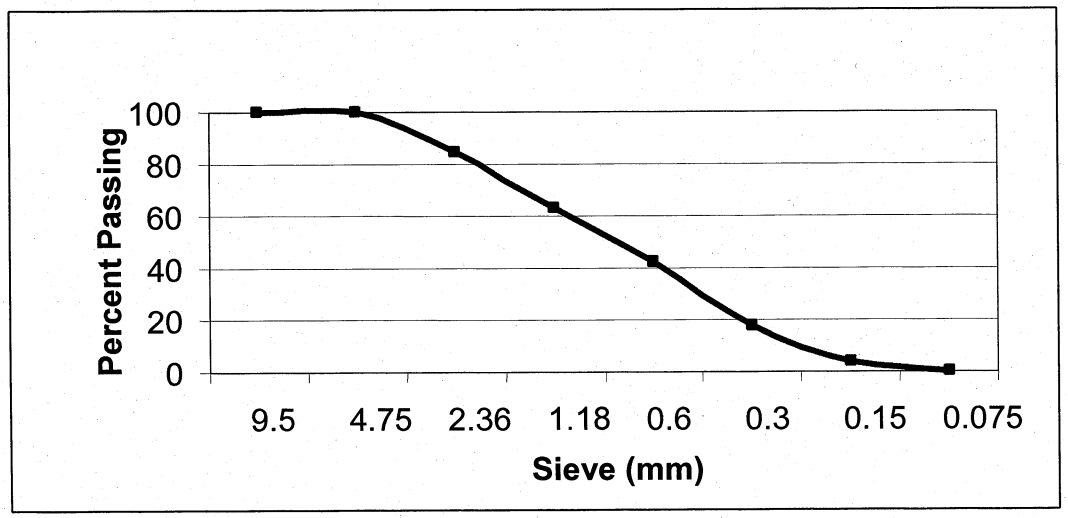

Figure 3.1 Grading of fine aggregate

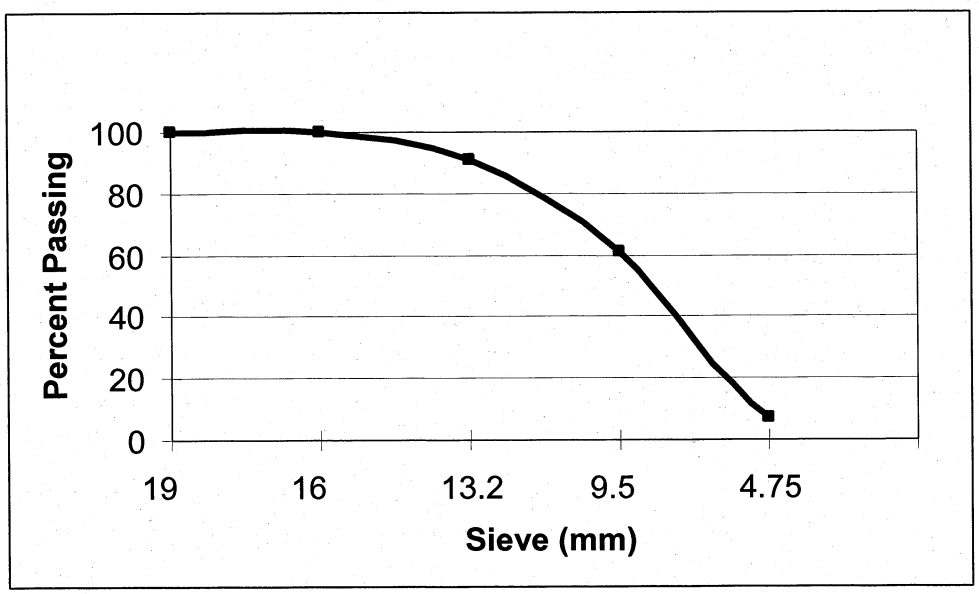

Figure 3.2 Grading of coarse aggregate

Figure 3.3 Used Aggregate AS IS

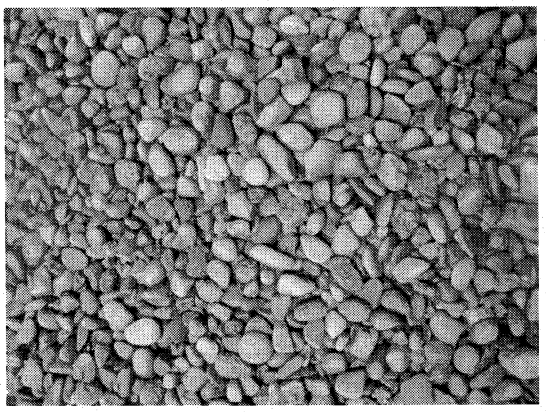

Figure 3.4 Aggregate if washed

Table 3.3 shows the specific gravity, bulk density, moisture absorption, and surface moisture content of coarse and fine aggregates calculated as per ASTM standards.

Table 3.3 Physical tests of coarse and fine aggregate

Test	Coarse Aggregate	Fine Aggregate
Dry loose bulk density. Kg/m^3	1684	1730
Specific gravity (SSD). Kg/m^3	2671	2714
Specific gravity (Bulk). Kg/m^3	2638	2670
Moisture absorption. %	1.2	2.1
Fineness Modules		2.92
Wash test pass 0.075 mm (% loss)	1.1	

3.2.6 Fibers

Two types of fibers were used which are Polyvinyl Alcohol (PVA), and FibraFlex metallic fibers (as shown in Figures 3.5 - 3.8). For FibraFlex, two sizes were used; long fiber FF20L6, and short fiber FF5E0. Table 3.4 shows characterisation from manufacturers. FibraFlex fibers are amorphous metal $(Fe, Cr)_{80}$ $(P, C, Si)_{20}$ with excellent corrosion resistance in salt (chlorides, sulphates) and acid environments. Corrosion tests in HCl (0.1 N) and $FeCl_3$ (0.4 N) showed no reaction after 24 hours [Saint-Gobain 2008].

Table 3.4 Characterisation of PVA & FibraFlex (FF20L6 and FF5E0) fibers

Type	PVA	FF20L6	FF5E0
Diameter (mm)	0.04	-	-
Width (mm)	-	1.6	1
Thickness (mm)	-	0.029	0.024
Length (mm)	8	20	5
Tensile Strength (N/mm^2)	1400	≥1400	≥1400
Elongation (%)	7	-	-
Young's Modulus (KN/mm^2)	32	-	-
Density (kg/m^3)	1300	7200	7200
Quantity of fibers/kg	76 500 000	150 000	1 100 000
Specific Area (m^2/kg)	76.9	9.6	11.6
Absorption	minimal	-	-
Chemical stability	stable	-	-
Color	white	silver shiny	silver shiny

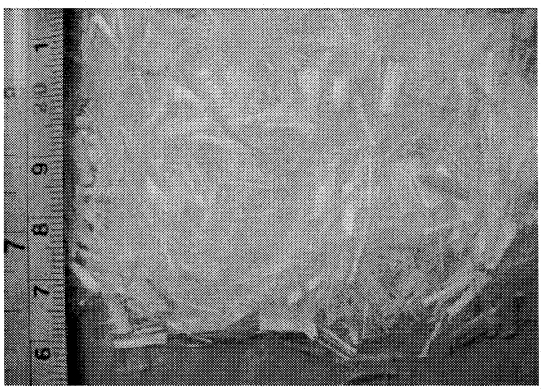

Figure 3.5 PVA fibers

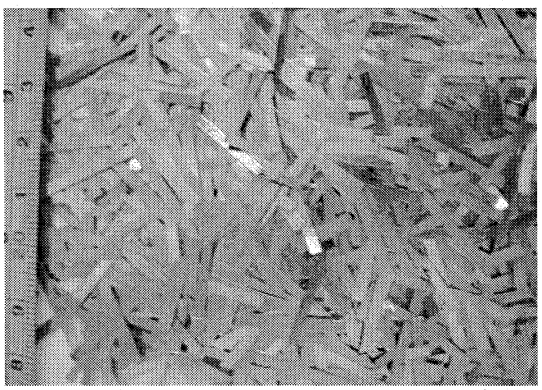

Figure 3.6 Coarse FF20L5 FibraFlex

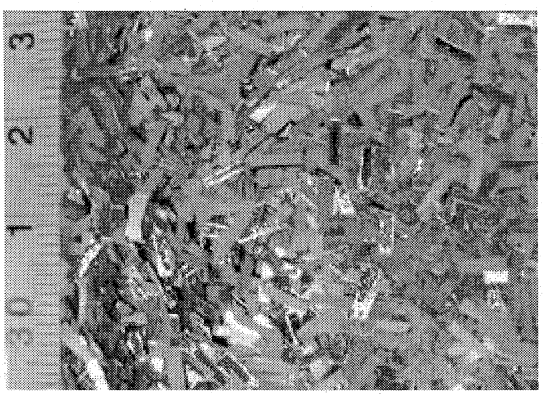

Figure 3.7 Fine FF5E0 FibraFlex fibers

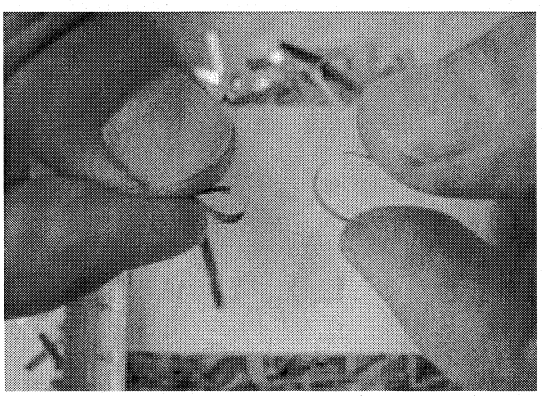

Figure 3.8 FibraFlex flexibility

3.2.7 Superplasticizer (SP)

PS-1466 from BASF Construction Chemicals (Master Builders) was used as SP. PS-1466 is based on polycarboxylate base and meets ASTM C 494/C 494M requirements for Type A, water-reducing; and Type F, high-range water reducing, admixtures. Table 3.5 shows characteristics of PS-1466 as per the producer.

Table 3.5 Super plasticizer PS-1466

Color	Brown
State	Liquid
Odour	No data
pH	5.7 – 6.5
Boiling point	100 C.
Freeze Point	0 C.
Specific Gravity	1.104 – 1.116

3.3 Methodology

3.3.1 Design of Mixes

In order to investigate fresh properties and engineering mechanical effects of fibers, SCC with two types of fibers (PVA and metallic "FibraFlex" of two different sizes) were used. FRSCC mixtures were developed based on a control SCC mixture. The control SCC mix used in this thesis was successfully used in Pearson International airport project in Toronto, Canada, in the year of 2000 [Lessard et al. 2002].

The control SCC mix was tested in the laboratory to optimize the superplasticizer (PS-1466) dosage to acquire required slump flow. For each of the trial mix, water mass is adjusted based on moisture content of the aggregates. In order to keep mix proportions of FRSCC mixtures similar to that of control SCC mixture, the mass of the added fibers was adjusted by reducing the mass of both fine and coarse aggregates (one third from fine aggregate and two third from coarse aggregate by mass). Table 3.6 shows mix design of 19 mixtures including the control SCC (Mix 1) with zero fiber.

Table 3.6 Mix design of concrete mixtures

Mix No.	Cement kg/m^3	Slag kg/m^3	Water kg/m^3	Aggregate kg/m^3		Fiber kg/m^3			SP PS1466 Kg/m^3
				Coarse	Fine	PVA	FF20L6	FF5E0	
PVA Concrete mixtures									
1	315	135	198.2	876.6	909.8	-	-	-	3.07
2	315	135	198.2	875.9	909.6	0.67	-	-	3.07
3	315	135	198.2	875.7	909.5	0.99	-	-	3.07
4	315	135	198.2	875.4	909.4	1.333	-	-	3.07
5	315	135	198.2	875.0	909.3	1.67	-	-	3.07
6	315	135	198.2	874.6	909.2	2.00	-	-	3.07
7	315	135	198.2	873.5	909.0	2.67	-	-	3.07
8	315	135	198.1	764.6	908.5	4.00	-	-	3.07
9	315	135	198.1	873.7	907.7	6.67	-	-	3.07
Metallic (FibraFlex) concrete mixtures									
10	315	135	203.9	872.0	903.2	-	7.2	-	3.07
11	315	135	203.9	874.5	902.3	-	14.4	-	3.07
12	315	135	203.9	872.8	901.5	-	21.6	-	3.07
13	315	135	203.9	871.0	903.2	-	-	7.2	3.07
14	315	135	203.9	874.5	902.3	-	-	14.4	3.07
15	315	135	203.9	871.0	901.5	-	-	21.6	3.07
Hybrid concrete mixtures									
16	315	135	204.0	874.5	902.6	0.43	2.4	2.4	3.07
17	315	135	203.9	872.8	901.2	0.87	4.8	4.8	3.07
18	315	135	203.9	873.2	901.4	0.54	2.4	7.2	3.07
19	315	135	204.0	874.6	902.5	0.20	1.2	4.8	3.07

Fresh properties of each of the concrete mixtures were recorded with the increase of fiber content while SP content was kept constant at 3.07 kg/m^3. With the increase of fiber dosages, workability of SCC decreased and hence, some mixes had gone out of SCC range in terms of fresh properties. The maximum range of fiber dosage for SCC was identified. In order to optimize Hybrid (using combination of fibers) FRSCC (Mixes 16 to 19), optimized dosages of fibers are combined to achieve the best flowable characteristics. Optimized Hybrid Mix 19 was designed

and produced with the highest percent of fibers to achieve excellent flow characteristics. This optimisation insured best flowability and best mechanical properties in the hardened state of the concrete.

3.3.2 Mix preparation

A STOW paddle mixer (Figure 3.9) consisting of a smooth steel drum with two paddles operated by and electrical 4.0hp motor was used. A programmed excel sheet for mix design was used to adjust and to calculate the amount of each of ingredients of the concrete mixtures for each batch. The water requirement of the mix was carefully adjusted by balancing the water absorption of both coarse and fine aggregates.

Before mixing all required materials were prepared and weighed as per batch requirements. A small electrical scale was used to measure super plasticizer and fiber amounts. All testing equipments to conduct slump flow, L-box, V funnel and rheology tests were prepared. The moulds for casting test specimens such as prisms, cylinders and beams were also made ready.

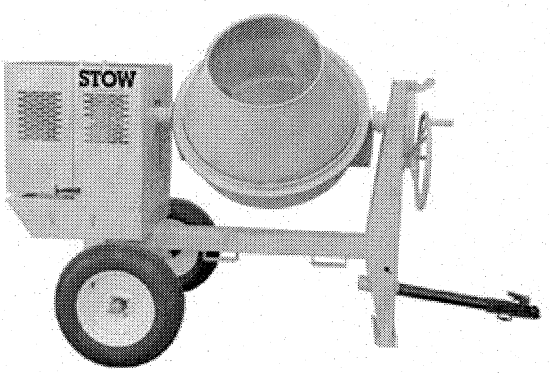

Figure 3.9 STOW concrete mixer

3.3.3 Mixing procedure

The mixing procedure involved the following steps:

1. After starting mixer, coarse and fine aggregate were added into drum and homogenized for 30 seconds.

2. Cement and slag were then added within 10 seconds of stopping period and then mixing continued for 30 seconds.
3. 60% of water was then distributed all over the mix and mixing continued for 30 seconds.
4. Remaining 40% of water mixed with super plasticizer was added and mixed for 60 seconds.
5. Stop and rest for 30 seconds.
6. Starting again the mixer and dispersing fibers by hand gradually over concrete mix within 60 seconds.
7. Mixing continued for additional 120 seconds and then stopped.

Total mixing time was 310 seconds.

3.3.4 Specimens

Immediately after concrete mixing, slump flow test followed by L-box, V funnel and segregation index were conducted. Another concrete quantity was poured into the viscometer container for rheological testing (plastic viscosity and shear yield tress). Cylinders (100 mm diameter x 200 mm height) and prisms (412 mm length x 102 mm width x 80 mm depth) were also cast without any compaction for strength and durability testing. Cylinders and prisms were covered by wetted burlap and later shifted into 95% humidity room with 24 ± 2 ^{o}C. Cylinders and prisms were released from moulds after 24 hours, investigated visually and then kept in a humidity room until the specified testing time.

3.4 Fresh Property Tests

Workability tests included the determination of slump flow diameter (spread), slump flow time (T_{500}), segregation index, L-box ratio and V-funnel flow time.

3.4.1 Slump Flow Diameter (spread) and Slump Flow Time (T_{500})

The slump flow test diameter represents concrete deformation against plate friction with flow time T_{500} to reach 500 mm diameter under its own weight without

compaction. Slump tests were conducted at three minutes after the stop of the concrete mixer which was 10 minutes from the first adding of water to the binder in the mixer drum.

An inverted mould cone, made of metal and clean with smooth interior was used (Figure 3.10) [PCI, TR-6-03, 2003]. The cone was placed at the centre of the slump steel plate and filled with concrete without compaction. While lifting up the cone, a stop watch was started recording the flow time. T_{500} is the time between the lifting of the slump cone and when concrete flow reached a spread diameter of 500 mm. The mean of two perpendicular diameters of the concrete sample spread were recorded to have the slump flow diameter/spread. Also for each batch, segregation was investigated at the border of the slump flow spread,

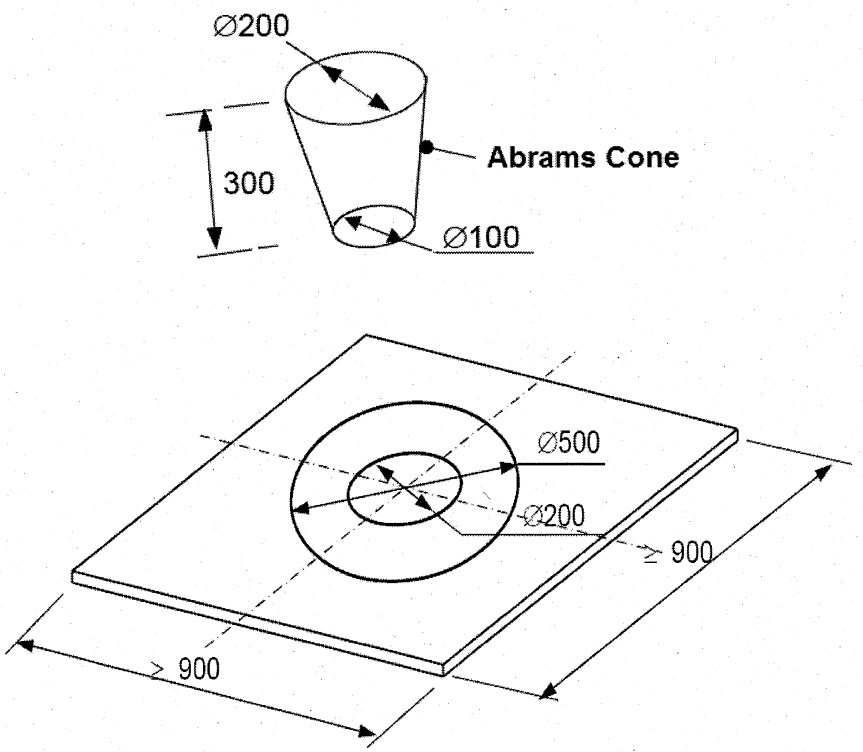

Figure 3.10 SCC slump cone and flow table plate

Viscosity can be assessed by T_{500} measured during the slump-flow test. T_{500} does not measure the viscosity of SCC but is related to it by describing the rate of flow [European SCC Guidelines, 2005].

3.4.2 L- box Test

The passing ability of FRSCC was investigated by L- box test apparatus [Figure 3.11) [PCI, TR-6-03, 2003]. Three bars of 12 mm diameter (with 41 mm gaps) were used at the passing gate. After closing vertical passing gate, concrete of less than 14 litres were poured in the vertical part of the L-box. The concrete was allowed to rest for one minute in order to display segregation and stability. The vertical gate was lifted gradually and the concrete was allowed to flow through the specified gaps between the steel bars into the horizontal part of the L-box. When the concrete stopped flowing, the distances "H1" and "H2" from Figure 3.11 were measured. The passing ability (L-box index/ratio), H2/H1, was calculated. Visually, if the concrete builds a plateau behind the reinforcement layer, the concrete has either blocked or segregated. Blocking usually displays itself by coarse aggregates gathered between the steel bars. If coarser aggregates are distributed on the concrete surface all the way to the end of the horizontal part of the L-box, the concrete can be regarded as stable.

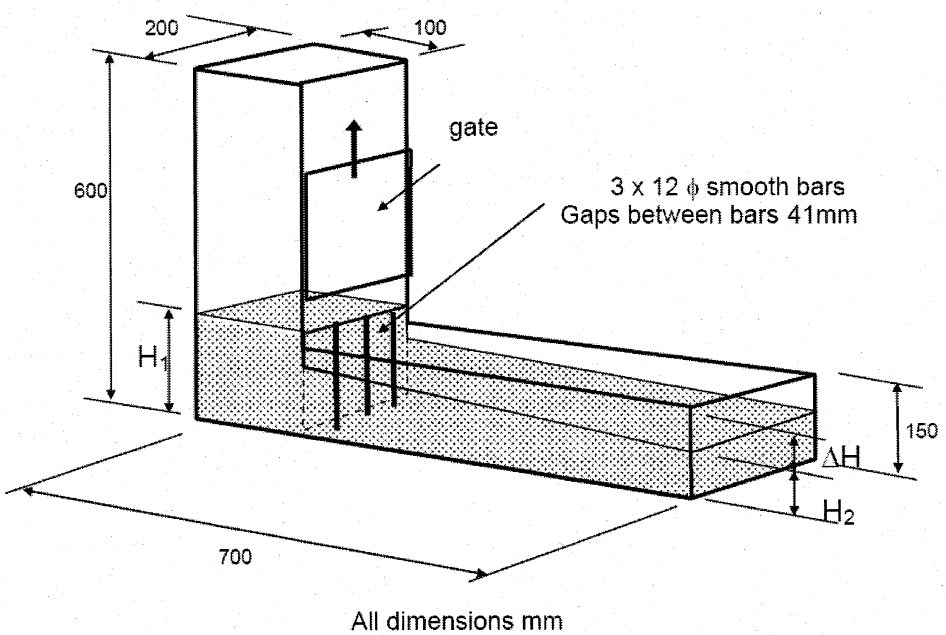

Figure 3.11 General assembly of L-box

3.4.3 V-funnel Test

The V-funnel flow time is the time required by a defined volume of SCC to pass through a narrow opening. It gives an indication of the filling ability of SCC provided that blocking and/or segregation do not take place [PCI, TR-6-03, 2003]. The test started with placing the cleaned V-funnel vertically (Fig. 3.12), wetting the interior of the funnel with a moist towel and removing the surplus water. It also involved the closing of the bottom gate and placing of a bucket under it in order to retain the concrete to be passed. The funnel was filled completely with a representative sample of SCC (14 litres) without compaction and then the gate was opened after a waiting period of 10 ± 2 seconds. A stopwatch was started at the same moment the gate opened and it was stopped at first light entered the funnel opening when clear space became visible.

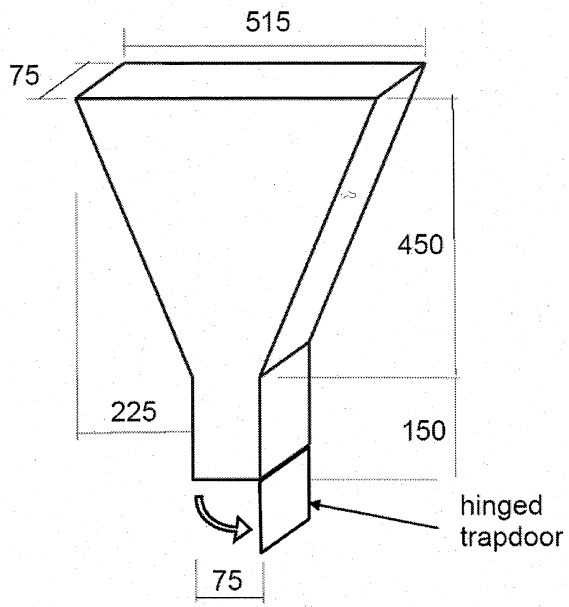

Figure 3.12 V-funnel made of steel (dimensions in mm)

3.4.4 Static Segregation of SCC

Static segregation of hardened SCC, due to gravity, is measured by hardened visual stability index (HVSI) which is rated from 0 to 3 in increments of 0.5, according to Illinois Test Procedure SCC- 6 [PCI, TR-6-03 2003].

0 (Stable)	1 (Stable)	2 (Unstable)	3 (Unstable)
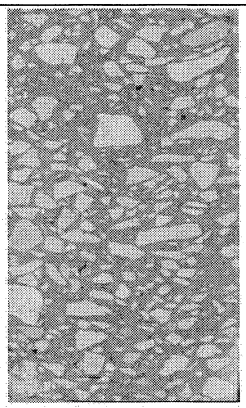	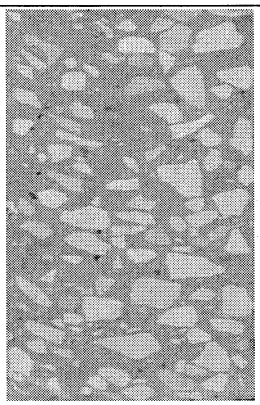	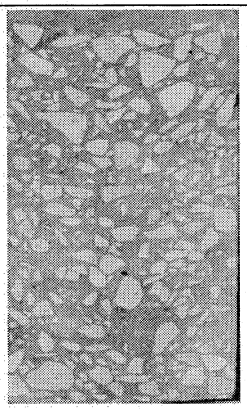	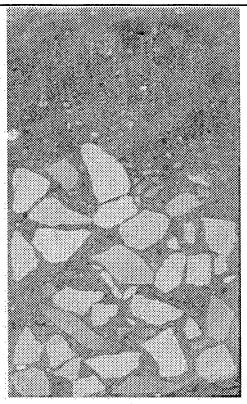

Figure 3.13 Static Segregation Rating for Hardened SCC Specimen with HVSI

The tested cylinder specimens were cut vertically to investigate visually variable layers (mortar or paste) at top of cylinders and to check apparent differences in the size and area of coarse aggregate throughout the depth, see Figure 3.13 and Table 3.7.

Table 3.7 Static segregation rating criteria for concrete cylinder specimens

Rating	Description
0 (Stable)	No mortar layer at the top of the cut plane and no variance in size and percent area of coarse aggregate distribution from top to bottom.
1 (Stable)	No mortar layer at the top of the cut plane but slight variance in size and percent area of coarse aggregate distribution from top to bottom.
2 (Unstable)	Slight mortar layer, less than 25 mm (1 in.) tall, at the top of the cut plane and distinct variance in size and percent area of coarse aggregate distribution from top to bottom.
3 (Unstable)	Clearly segregated as evidenced by a mortar layer greater than 25 mm (1 in.) tall and/or considerable variance in size and percent area of coarse aggregate distribution from top to bottom.

3.4.5 Dynamic Segregation Test Stability Index (VSI)

Dynamic segregation mainly depends on flow velocity during placement and aggregate properties. Dynamic segregation was characterized by visual stability

index (VSI) and was investigated visually according to the rating criteria presented in Table 3.8 [PCI, TR-6-03 2003].

Table 3.8 Dynamic segregation rating criteria using Visual Stability Index (VSI)

Rating	Description
0.0 (Stable)	No evidence of segregation in the slump flow patty, in the mixer drum, or in the sampling wheelbarrow.
0.5 (Stable)	No mortar halo or aggregate pile in the slump flow patty, but very slight evidence of bleed or air popping on the surface of the SCC in the mixer drum or sampling wheelbarrow.
1.0 (Stable)	Indicates no mortar halo or aggregate pile in the slump flow patty but some slight bleed or air popping on the surface of the SCC in the mixer drum or sampling wheelbarrow.
1.5 (Unstable)	Indicates just noticeable mortar halo and/or a just noticeable aggregate pile in the slump flow patty and noticeable bleeding in the mixer drum and sampling wheelbarrow.
2.0 (Unstable)	Indicates a slight mortar halo (<10 mm) (<0.4 inch) and/or aggregate pile in the slump flow patty and highly noticeable bleeding in the mixer drum and sampling wheelbarrow.
3.0 (Unstable)	Indicates clearly segregating by evidence of a large mortar halo (>10 mm) (>0.4 inch) and/or large aggregate pile in the center of the SCC patty and a thick layer of paste on the surface of the resting SCC in the mixer drum or sampling wheelbarrow.

3.5 Rheology Tests

Concrete mixes were investigated using ConTec BML 4 viscometer, for rheological properties (plastic viscosity and yield value) at time periods of 10 minutes, 40 minutes and 70 minutes from first adding of water to binder in the mixer drum. The values of yield shear stress and plastic viscosity with time at room temperature ($23 \pm 2\ ^{o}C$) were recorded.

3.5.1 Introduction

The ConTec BML 4 viscometer available at Ryerson University concrete laboratory (Figure 3.14) was designed and made in Iceland by ConTec Ltd, a company specialized in rheology of concrete. This instrument measures SCC yield shear stress and plastic viscosity [Wallevik 2003].

3.5.2 Basic Theory

Several equipments had been made to explore concrete workability and fresh deformation behaviour with time since Abrams in 1918 [Tattersall, 1973]. Later, new equipments were designed and developed based on Bingham behaviour of concrete [Ozyildirim and Lane 2003]. The Bingham behaviour of the concrete can be illustrated by Eq. 3.1:

$$\tau = \tau_o + \mu\gamma \qquad (3.1)$$

Where τ = Shear stress; μ= Viscosity; τ_o = Yield stress and γ = Shear rate

The new ConTec BML 4 viscometer has coaxial cylinders and is based on Bingham behaviour using a linear torque-speed (T-V) relationship as per Eq. 3.2.

$$T = g + hV \qquad (3.2)$$

By measuring the torque which produced on a stationary inner cylinder while the outer cylinder is rotating at various speed settings, the values of parameters g and h can be determined. These parameters define the workability of a particular concrete mix which as are as follows [Wallevik 2003]:

g : a measure of the force necessary to start a movement of the concrete (flow resistance).

h : a measure of the resistance of concrete against an increased speed of movement (viscosity factor).

3.5.3 Equipment Description

Viscometer (Figure 3.14) consists of a box with buttons (left) for electrical operation and emergency control as well as a laptop computer with control software and interface box with cables. In addition, it has a rotating bottom container with top cylinders to apply shear on fresh concrete samples. A controlled speed electrical motor is used to drive the container. In the top tower at right, there is an elevator cabin and jack with very sensitive plates to adjust top and bottom positions of top cylinder and ring.

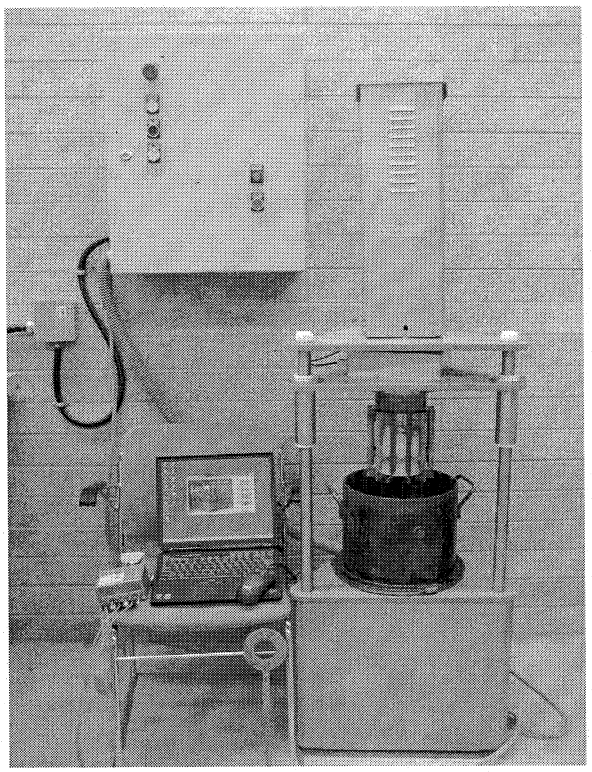

Figure 3.14 ConTek BML 4 Viscometer for SCC

The viscometer is fully-automated, user-friendly and is controlled by computer and a software called Fresh-Win connected to viscometer by instrument cable, PC cable and interface box. The interface box is connected to a PC card on the left side of the laptop computer.

A SCC standard measuring system C-200/1.3 was used for tests reported here, as per Table 3.9. The "C" stands for concrete and "200" is the diameter of the inner cylinder in millimetres while "1.3" presents the gap between outer and inner radius (Ro/Ri).

This coaxial cylinder measuring system consists of a top outer cylinder, the mix container, an inner cylinder unit with a pulp cylinder mounted at a top-ring, see Figure 3.15.

a- Top fixed ring

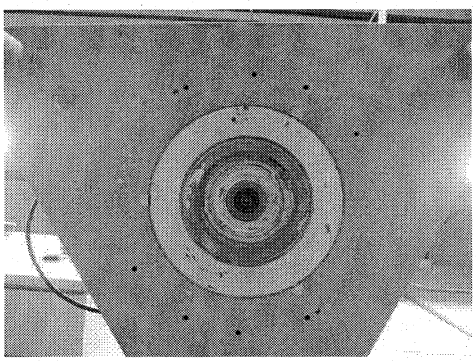

b- Top external ring

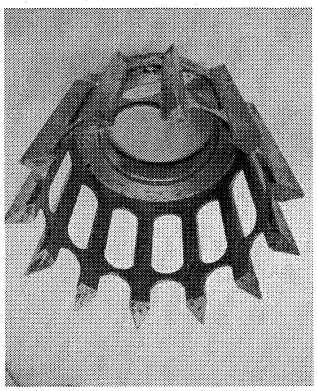

c- Top internal pulp cylinder

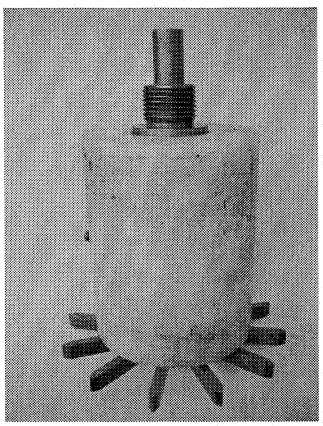

d- Bottom container

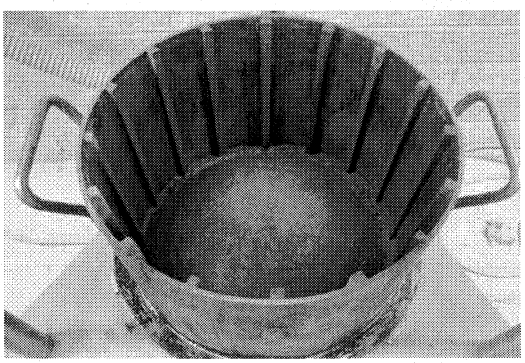

Figure 3.15 (a-b-c-d) SCC standard measuring system C-200/1.3

The outer cylinder is mounted on a rotating disk on the instrument where guide-ribs on the disk make sure that it is seated correctly [Wallevik 2003].

Table 3.9 SCC measuring system C-200/1.3

Measuring system	Inner radius (mm)	Outer radius (mm)	Effective height (mm)	Volume of testing material
C-200/1.3	100	131	150	~15 litres

The inner cylinder is constructed with a pulp cylinder component unit which registers the torsion-moment using a load cell while lowered into the outer cylinder by hydraulic system. Each test takes about 3 to 5 minutes from filling the bottom container by concrete sample until removing it [Wallevik 2003].

3.5.4 Testing Method for Rheology

Testing involves the following steps:

1- After the start of Freshwin program, it displays the main window screen, see Figure 3.16.

2- After 10 minutes from first adding of water to binder in mixer drum, 13 litres of concrete mix sample were filled into the bottom container, see Figure 3.17.

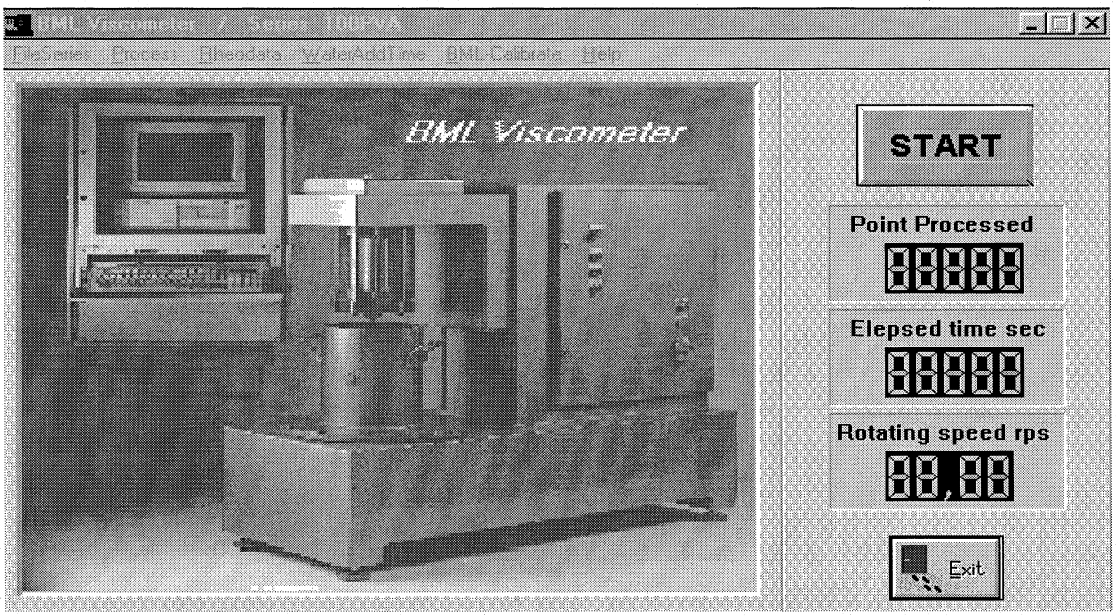

Figure 3.16 Computer Software FreshWin for ConTek VML 4 Viscometer

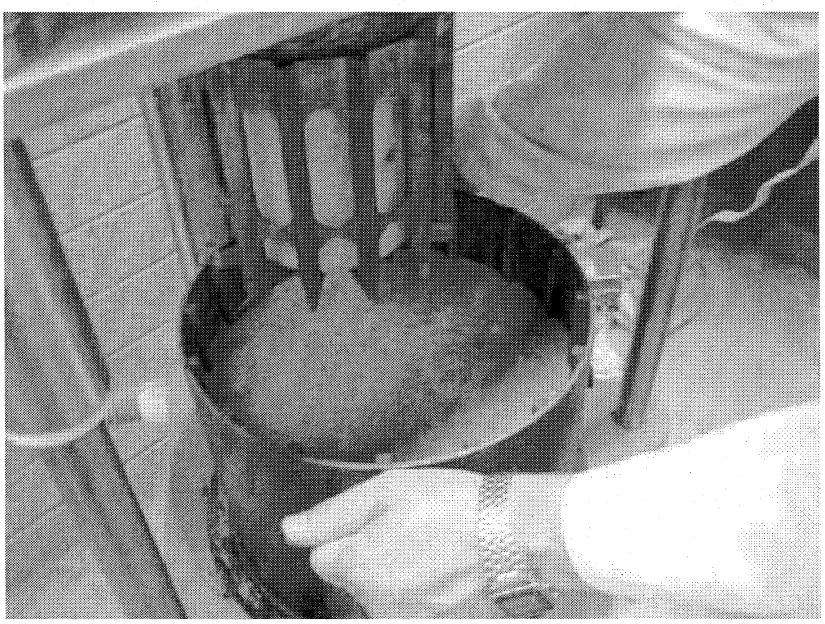

Figure 3.17 Measuring system and concrete sample for ConTek VML Viscometer

3- Select from Process menu option a parameter named concrete 1, see Figure 3.18, this is the standard set-up for concrete and then press OK.

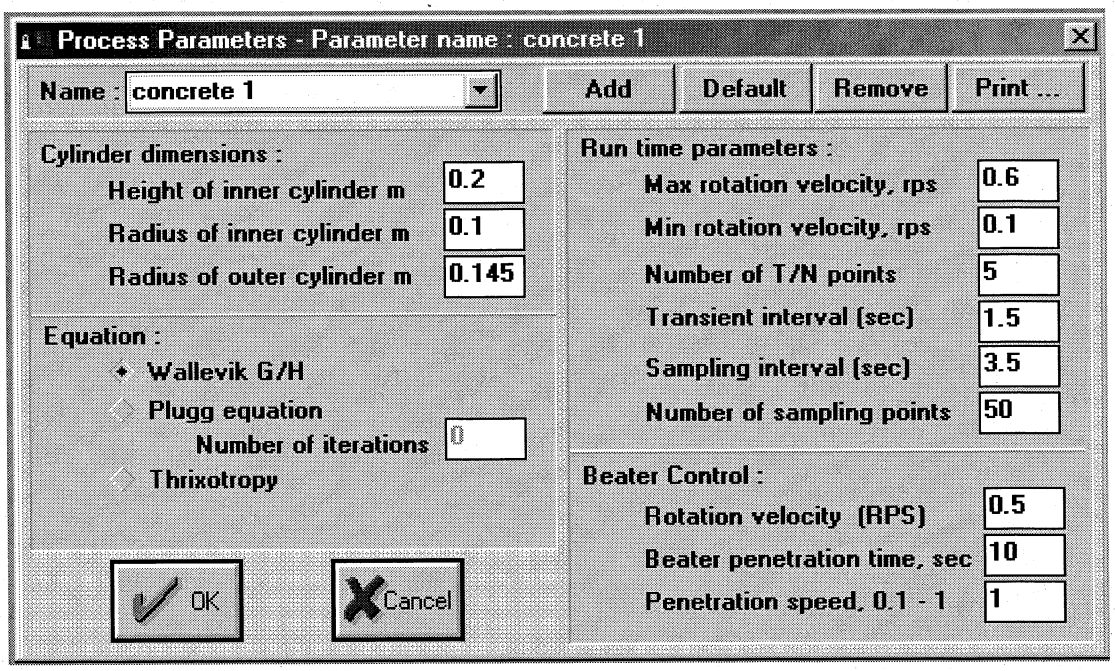

Figure 3.18 Standard set up for SCC

4- At each testing time, clicking on START button changed its color from cyan to red and the inner top cylinder which registers the torsion-moment was lowered into the bottom outer container by hydraulic system.

5- The fresh concrete sample was exposed to shear when bottom container started rotating from higher speed to lower speed according to the data given by the set-up parameter, see Figure 3.19.

6- The progress of the test while lower container rotating for around for one minute is displayed showing points processed, elapsed time, rotating speed and a diagram between resistance T [Nm] and velocity N [rps]. Finally, a diagram between resistance T [Nm] and velocity N [rps] was initiated, see Figure 3.20.

7- After bottom container stopped rotation, the inner top cylinder moved up from container and a list of rheology data and results were displayed on the screen, see Figure 3.21 and Table 3.10.

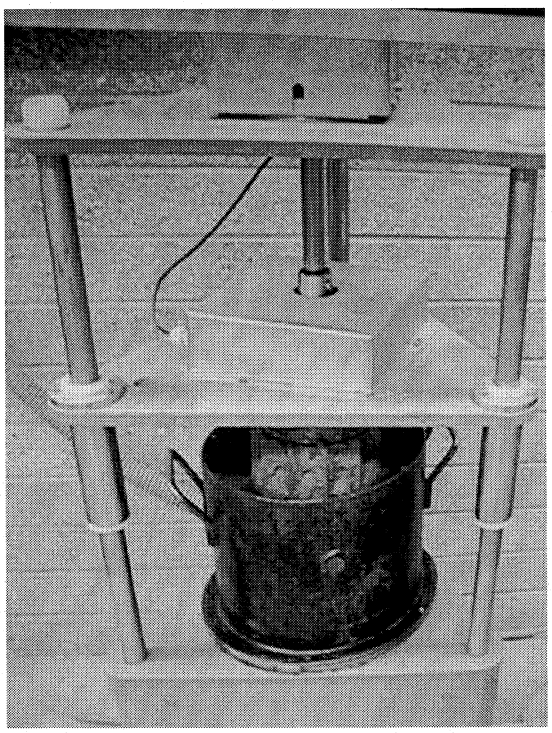

Figure 3.19 Top cylinders lowered into the bottom container

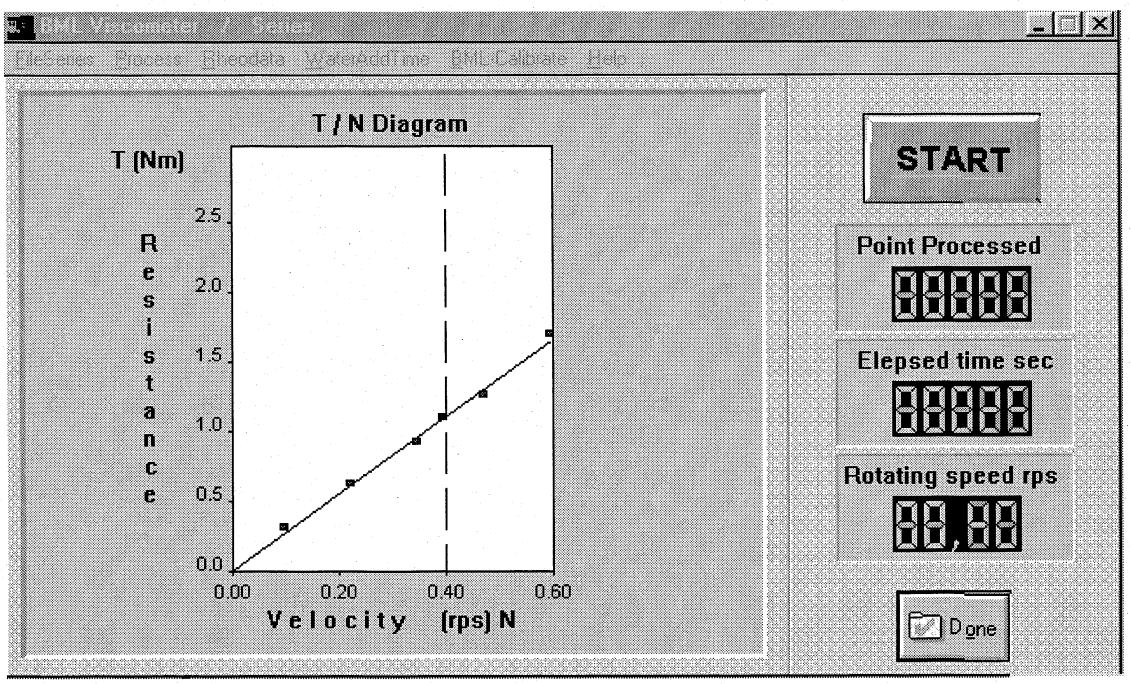

Figure 3.20 Test result appears in real time

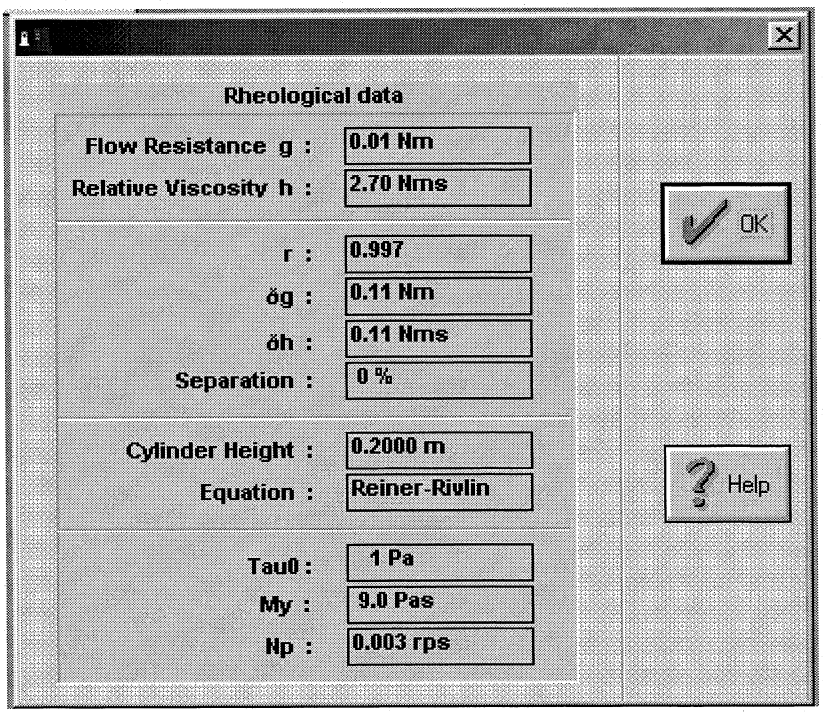

Figure 3.21 Rheological data and results

Table 3.10 Rheological properties and symbols

Properties	**symbol**	**Unit**
Flow Resistance	g	Nm
Relative Viscosity	h	Nms
Regression Coefficient	r	-
	delta g	Nm
	delta h	Nms
Segregation Coefficient	Sep.	%
Yield Value	Tau0	Pa
Plastic Viscosity	My	Pas
Plug Speed	Np	rps

8- Omit points from Figure 3.22 whose velocities are lower than the plug speed (shown in Figure 3.21 as Np), but at list three points are required in Figure 3.20.

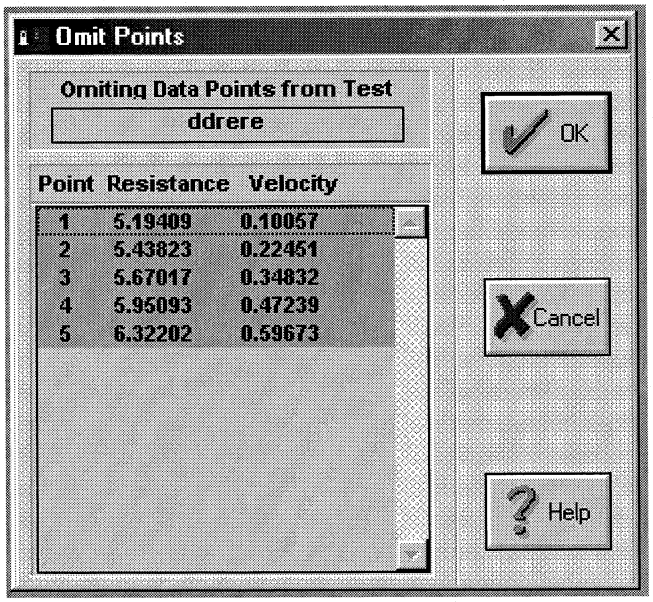

Figure 3.22 Omiting data points

3.6 Tests on Hardened Properties and Durability

It should be noted that the concrete specimens were cast without any mechanical vibration or compaction energy. At least two specimens were tested for each of the hardened properties at standard ages. Tests on cylinder compressive strength [ASTM C 39/ C 39M-01 2003], splitting tensile strength of cylindrical concrete [ASTM C 496-96 1996], beam flexural strength [ASTM C 78-0 1980], and three point load bending of notched beam for Fracture Energy [RILEM TC50-FMC 1985] were conducted to determine the hardened properties of the concrete mixtures. The density of the concrete was also measured. In addition, rapid chloride penetration (RCP) test was also conducted on concrete mixtures.

3.6.1 Rapid Chloride Penetration (RCP) Test

The purpose of this test was to determine the electrical conductance of concrete to provide a rapid indication of its resistance to the penetration of chloride ions as per ASTM C 1202 – 97 [1997]. Test set-up and classification of penetration resistance are presented in Figure 3.23 and Table 3.11, respectively. Water saturated concrete specimen, 100 mm diameter and 50 mm thick, was positioned in a cell

containing a fluid reservoir on both sides. One reservoir was filled with a sodium chloride (3% NaCl) solution and the other with a sodium hydroxide (0.3N NaOH) solution. A DC (60 V) voltage was applied over the cell with the negative terminal connected to the reservoir containing the (NaCl) solution and the positive to the (NaOH) solution, causing the negatively charged chloride ions to migrate towards the positive terminal.

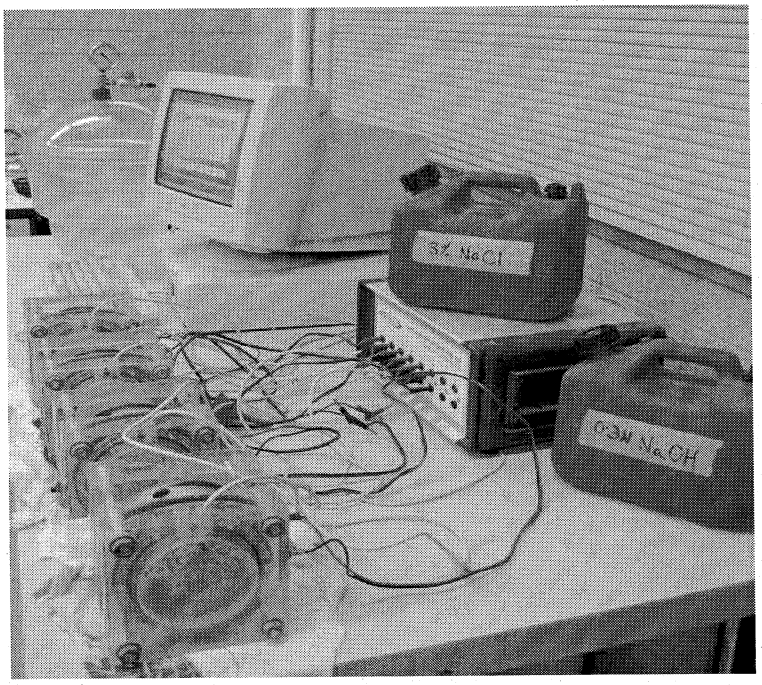

Figure 3.23 Test set-up showing voltage cells, vacuum desiccators & software

Table 3.11 Chloride Ion Penetrability with Coulombs

Charge Passed (Coulombs)	Chloride Ion Penetrability
>4000	High
2000 – 4000	Moderate
1000 – 2000	Low
100 – 1000	Very Low
<100	Negligible

According to ASTM C 1202 – 97, this test method can produce misleading results under some conditions. For calcium nitrite, admixed into a concrete, the results from this test on such concretes indicate higher coulomb values, that is, lower

resistance to chloride ion penetration, than from tests on identical concrete mixtures (controls) without calcium nitrite. However, long-term chloride pounding tests indicated that the concretes with calcium nitrite were at least as resistant to chloride ion penetration as the control mixtures. Since the test results are a function of the electrical resistance of the specimen, the presence of reinforcing steel or other embedded electrically conductive materials (such as steel fibers) may have a significant effect. The test is not valid for specimens containing reinforcing steel positioned longitudinally, providing a continuous electrical path between the two ends of the specimen [ASTM C 1202 – 97].

3.6.2 Compressive strength

Capped concrete cylinders (100 mm diameter with 200 mm height) made without compaction/vibration were crushed by compression machine at 14 and 28 days. The compression machine had a capacity of 400,000 lb. Medium failure load, range 3 (up to 80,000 lb) was used for all cylinders (Figure 3.24).

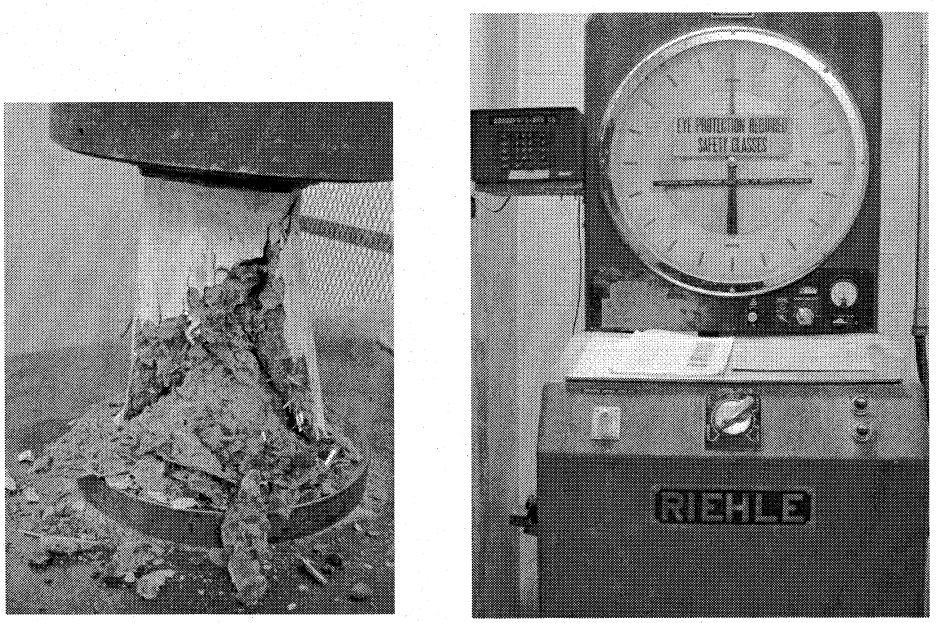

Figure 3.24 Cylinder under compression failure (Mix 12 0.3F20 with metal fiber)

3.6.3 Flexural strength

A universal testing machine (MTS) was used for testing flexural prisms. Loads were controlled and regulated by a computer (load rate <1MPa/min). Also, LVDT for displacements was connected to the computer with strain smart software for online display and recording. This test was done according to ASTM C78-80 which covers the determination of the flexural strength of concrete by the use of four point loading on non-notched beam. Beams were 412 mm length, 102 mm width and 80 mm depth (Figure 3.25).

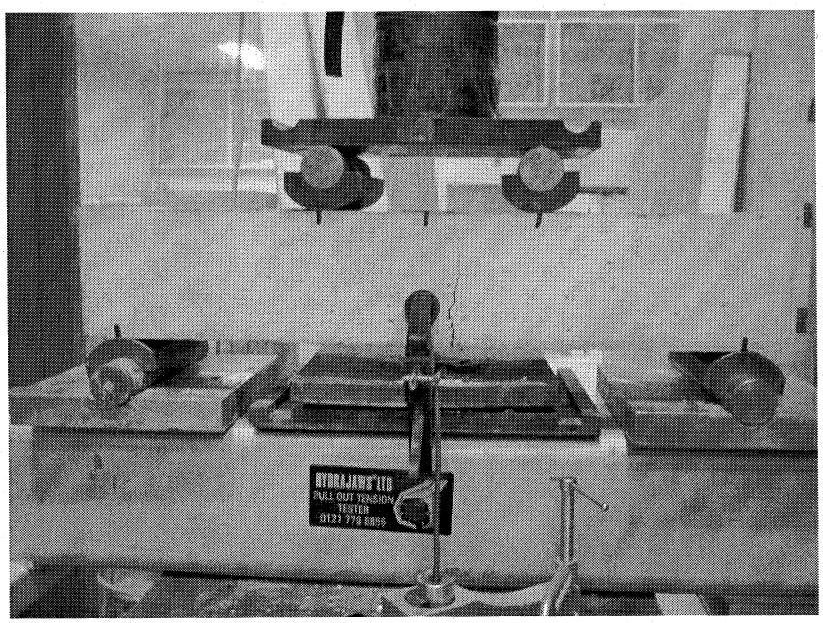

Figure 3.25 Test set-up and prism specimen under four point loading with LVDT

In testing, all cracks were initiated from the tension surface within the middle third of the span length. The modulus of rupture (flexural strength) is calculated by Eq. 3.3.

$$R = \frac{PL}{(bd)^2} \qquad (3.3)$$

Where R is the modulus of rupture in MPa, P is the maximum applied load indicated by the testing machine in N, L is the span length in mm, b is the width of the specimen in mm and d is the depth of the specimen in mm.

3.6.4 Fracture energy

According to RILEM TC50-FMC, the fracture energy is the area under the curve of three-point bend load on notched beam/prism with displacement. Fracture energy of concrete is defined based on the energy absorbed per unit crack area in widening the crack from zero to failure. Beams (412 mm in length, 102 mm in width and 80 mm in depth) were notched by electrical water-cooled diamond saw from the bottom at mid span. The notch was 4 mm wide and 25 mm in depth. A stiff universal testing machine was used for loading and loads were regulated by a computer. Also, linear variable differential transformer (LVDT) for displacement monitoring was connected to the computer with strain smart software for online display (Figure 3.26).

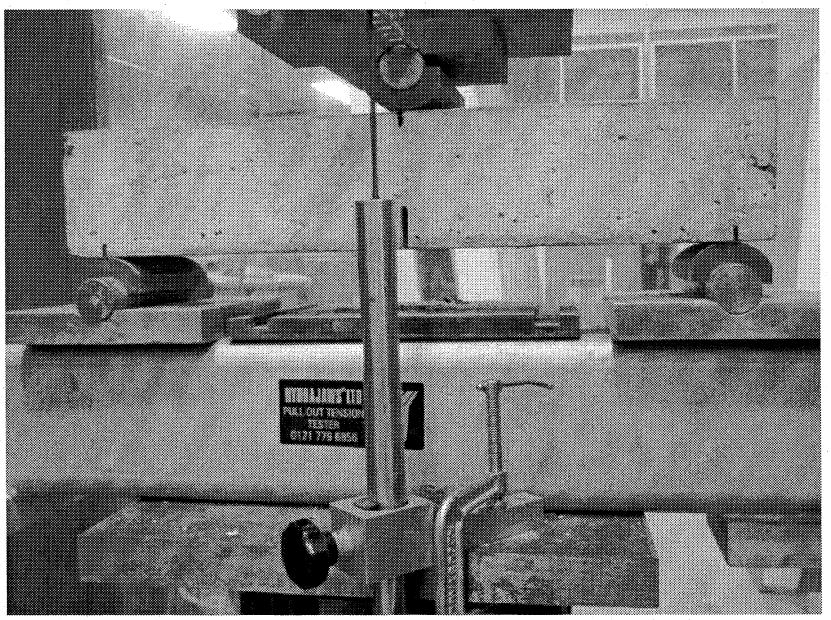

Figure 3.26 Test set-up and specimens under three-point loading for fracture

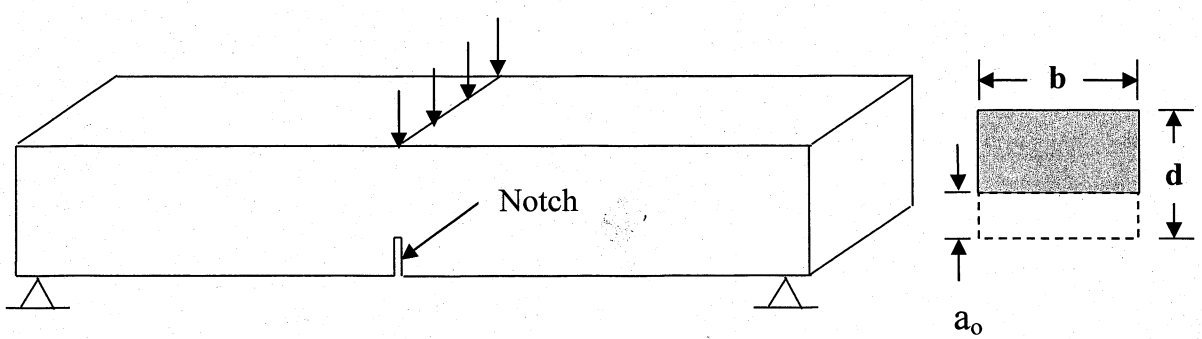

Figure 3.27 Fracture energy specimen details

The fracture energy (G_f) is calculated based on Eqs. 3.4 as per RILEM TC 50-FMC [1985]:

$$G_f = \frac{W_0 + mgd_0}{A_{lig}} \qquad (3.4)$$

where: G_f is the fracture energy (N/m), W_o is the area under load-deflection curve (Nm), m is the self weight (kg) of the beam between supports plus self weight of the loading arrangement which is not attached to the machine but follows the beam until failure, g is the gravity (9.81 m/sec^2), d_o is the last deformation at final failure of the beam (m), b is the width of the beam (m), d is the depth of the beam (m), a_o is the depth of the notch and A_{lig} (= b (d - a_o)) is the area of ligament (Figure 3.27).

3.6.5 Splitting tensile strength

In order to test indirect tension of concrete, cylinders of 100 mm dia and 200 mm length were tested at 28 days [according to ASTM C 496-96 1996] by a universal testing machine. Two LVDTs were fixed horizontally to measure the splitting lateral displacement (Figure 3.28). Loads and lateral displacement were recorded by a computer aided data acquisition system.

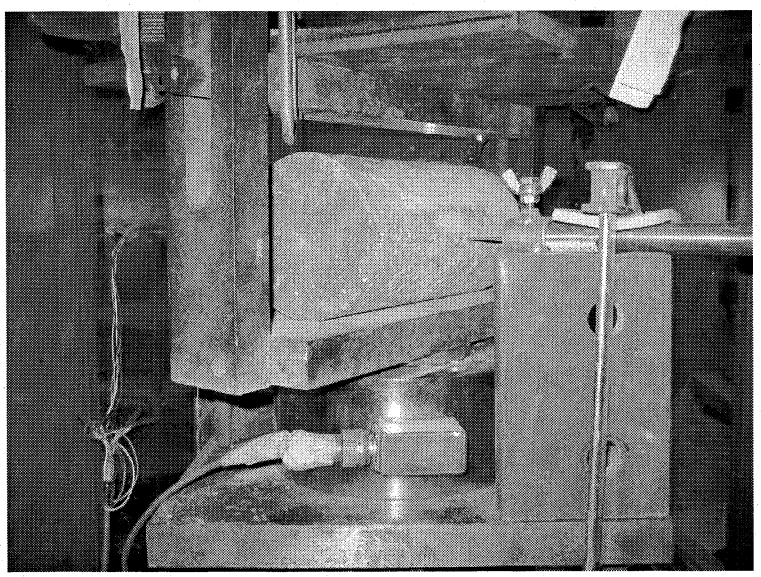

Figure 3.28 Splitting cylinder test set-up with LVDTs

The splitting tensile strength of the specimen is calculated by Eq. 3.5.

$$T = \frac{2P}{\pi lD} \qquad (3.5)$$

where:

T = splitting tensile strength (KPa),

P = maximum applied load indicated by the testing machine (KN),

l = length of the cylinder (m),

D = diameter of the cylinder (m).

4. Results and Discussions

4.1 Introduction

In this chapter, test results covering fresh (slump flow, flow time, segregation index and passing ability), rheological (yield stress and viscosity), mechanical (compression/flexural/splitting strength and fracture energy) and durability (in terms of chloride penetration resistance) characteristics of developed concrete mixtures with fibers will be described in addition to the control SCC mix.

Table 4.1 Mixtures and by volume

Mixture No.	Mixture Designation	Fiber Type and Volume (%)		
		PVA	FF20L6 (F20)	FF5E0 (F5)
1- Control SCC	0Fiber	0.0	0.0	0.0
2	0.05PVA	0.05	0.0	0.0
3	0.07PVA	0.07	0.0	0.0
4	0.1PVA	0.10	0.0	0.0
5	0.125PVA	0.125	0.0	0.0
6	0.15PVA	0.15	0.0	0.0
7	0.2PVA	0.20	0.0	0.0
8	0.3PVA	0.30	0.0	0.0
9	0.5PVA	0.50	0.0	0.0
10	0.1F20	0.0	0.1	0.0
11	0.2F20	0.0	0.2	0.0
12	0.3F20	0.0	0.3	0.0
13	0.1F5	0.0	0.0	0.10
14	0.2F5	0.0	0.0	0.20
15	0.3F5	0.0	0.0	0.30
16	Hybrid 1	0.033	0.033	0.033
17	Hybrid 2	0.067	0.067	0.067
18	Hybrid 3	0.042	0.033	0.100
19	Hybrid 4	0.015	0.017	0.067

A total of 18 concrete mixtures were developed by using two types and varying dosages of fibers based on the control SCC mixture (with 0% fiber). PVA and metallic FibraFlex (both long FF20L6 and short FF5E0) fibers were added to the control SCC mix to develop FRSCC mixtures. Table 4.1 shows concrete mixture

designations with types and dosages (in volume %) of fibers. Metallic fiber FF20L6 is designated as "F20" while FF5E0 is designated as "F5". Numerics at the beginning of the mix designation represent fiber percentage and letters/numeric together at the end represent fiber types. However, hybrid mixtures are designated differently. According to Table 4.1, fiber dosage varies from 0 to 0.5% by volume.

4.2 Fresh Properties

The results of workability tests such as slump flow (spread), slump flow time, segregation index, L-box ratio and V-funnel flow time are summarized in Table 4.2. Results were evaluated according to "The European Guidelines for Self Compacting Concrete" [European SCC Guidelines 2005].

Table 4.2 Workability properties

Mix No.	Mixture Designation	Spread (mm)	T_{500} (sec)	L-Box %	V-funnel Time (sec)	Static Segregation Index (HVSI)	Dynamic Segregation Index (VSI)
1	0Fiber	695	3.72	81	5.02	0.0	0.0
2	0.05PVA	651	2.53	n. p.	n. p.	0.0	0.0
3	0.07PVA	615	3.42	85	5.22	0.5	0.5
4	0.1PVA	595	3.80	82	5.66	0.5	0.5
5	0.125PVA	565	4.13	60	11.68	1.0	1.0
6	0.15PVA	520	n. p.	n. p.	n. p.	n. p.	n. p.
7	0.2PVA	476	n. p.	n. p.	n. p.	n. p.	n. p.
8	0.3PVA	410	n. p.	n. p.	n. p.	n. p.	n. p.
9	0.5PVA	380	n. p.	n. p.	n. p.	n. p.	n. p.
10	0.1F20	680	2.17	80	4.78	0.0	0.0
11	0.2F20	610	2.35	64	7.13	0.5	0.5
12	0.3F20	565	2.50	30	9.63	1.0	1.0
13	0.1F5	685	1.26	95	4.10	0.0	0.0
14	0.2F5	668	1.98	88	5.40	0.5	0.5
15	0.3F5	655	2.22	80	12.42	1.0	1.0
16	Hybrid 1	665	2.30	68	5.70	0.5	0.5
17	Hybrid 2	570	5.09	70	10.48	1.0	1.0
18	Hybrid 3	362	5.53	57	10.53	n. p.	n. p.
19	Hybrid 4	668	1.68	93	4.24	1.0	1.0

Note: (n. p.) i.e. (not performed)

4.2.1 Slump Flow Diameter (Spread) for Concrete Mixtures

Slump flow spread for a typical FRSCC mixture is shown in Figure 4.1. According to European SCC specifications, the minimum specified slump flow for SCC is 550 mm [European SCC Guidelines, 2005]. All concrete mixtures satisfied the criteria to be fiber reinforced SCC (FRSCC) except mixtures containing 0.15%, 0.2%, 0.3% and 0.5% PVA as well as Hybrid 3 (Table 4.2 and Figure 4.2). FRSCC can be achieved by using maximum of up to 0.125% of PVA and 0.3% of metallic FibraFlex fibers.

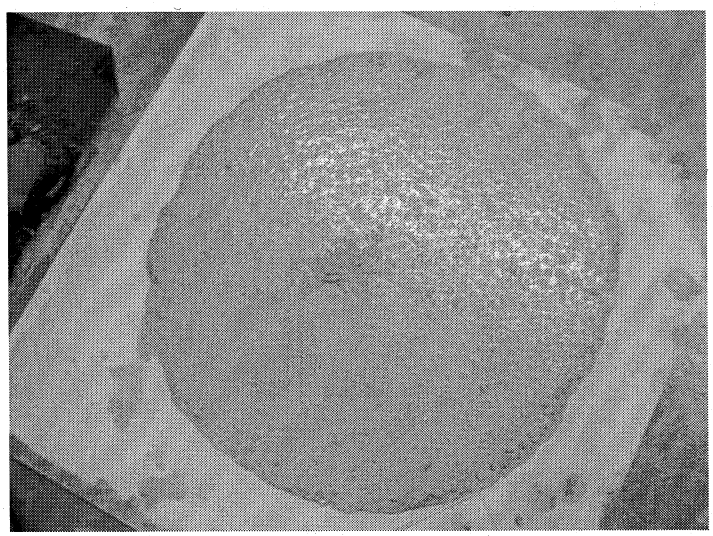

Figure 4.1 Slump flow diameter (Spread) for mix (2)

Based on slump-flow diameter, SCC is classified into three categories: SF1 (550 - 650 mm), SF2 (660 - 750) mm and SF3 (760 – 850) mm [European SCC Guidelines 2005]. Mix 2, Mix 3, Mix 4, Mix 5, Mix 11, Mix 12 and Hybrid 2 (Mix 17) fall into the category of SF1 – these mixtures can be suitable for un-reinforced or slightly reinforced concrete structures. Mix 10, Mix 13, Mix 14, Mix 15, Hybrid 1 (Mix 16) and Hybrid 4 (Mix 19) fall into the category of SF2 – these mixtures can be suitable for normal applications e.g. walls, columns.

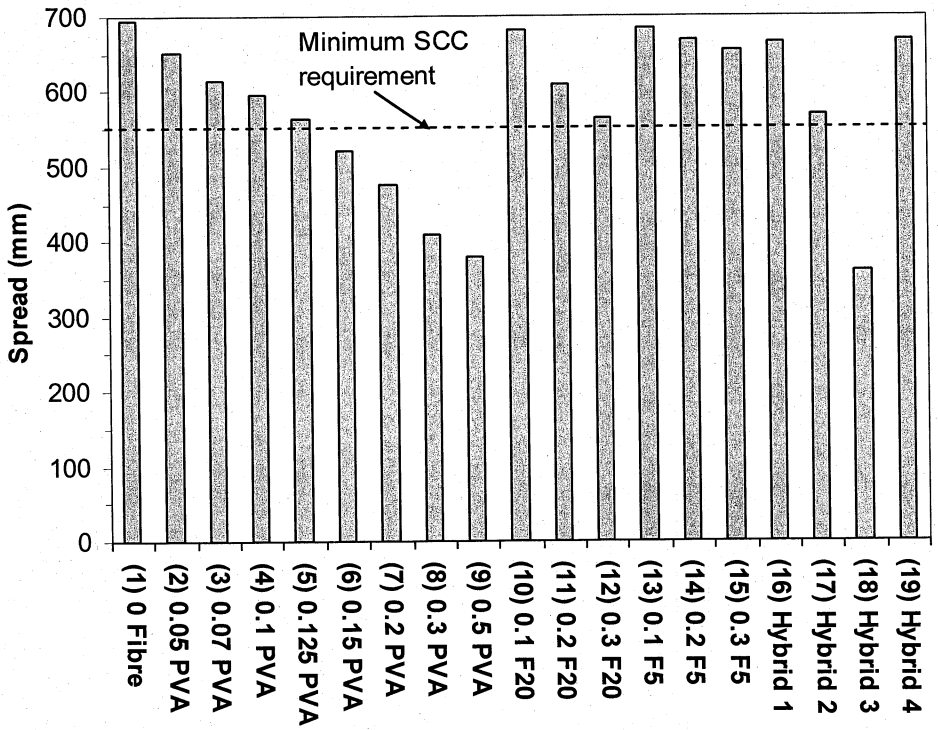

Figure 4.2 Slump flow (spread) of all concrete mixtures

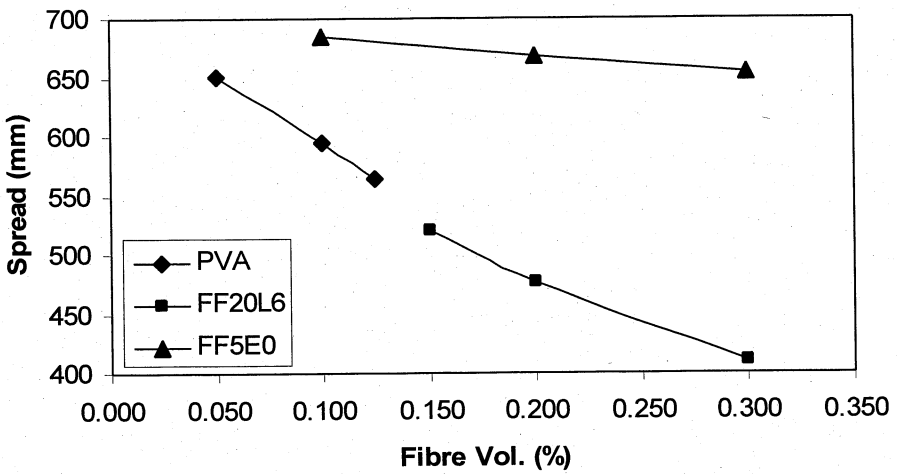

Figure 4.3 Effect of fiber volume on slump flow spread

Figures 4.2 and 4.3 show that an increase in fiber volume decreases the slump flow of all concrete mixtures containing PVA, metallic and hybrid compared control mix (0% fiber). This can be attributed to the fact that the incorporation fiber increases the internal resistance to flow. This is also confirmed from other research studies [Grünewald and Walraven 2001, Nehdi and Ladanchuk 2004].

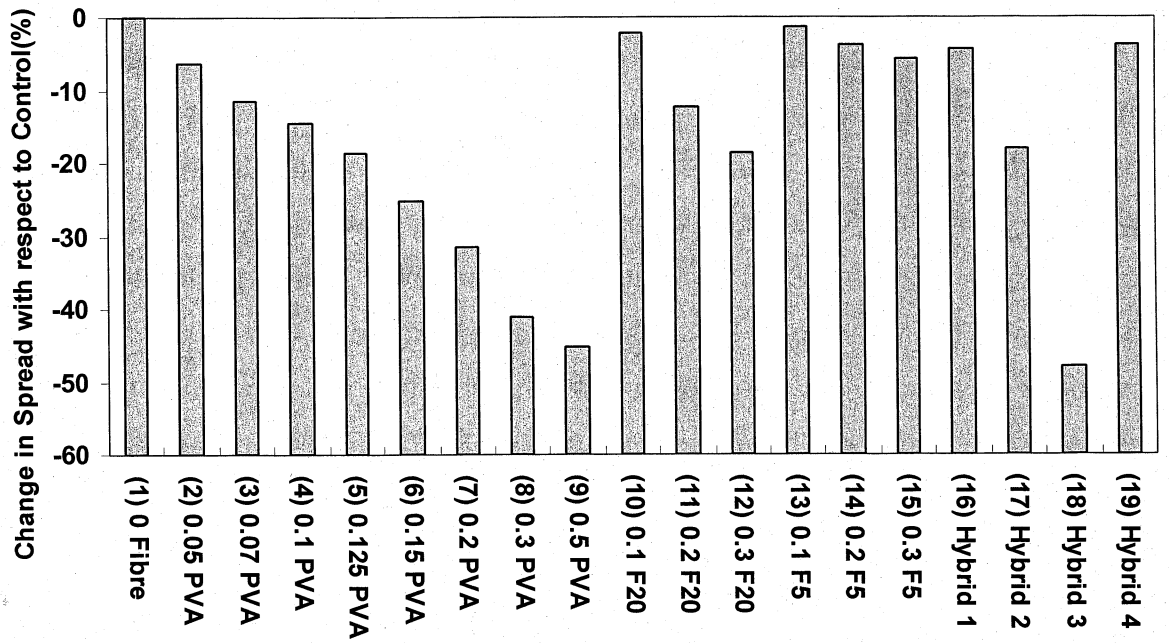

Figure 4.4 Slump spread reduction for concrete mixtures

An increase in PVA content from 0 to 0.5%, causes a slump spread reduction of about 45% (Figure 4.4). For metallic fiber, a reduction of 19% (for long fiber F20) and 6% (for short fiber F5) were observed when fiber volume is increased from 0 to 0.3%.

Figure 4.4 and Table 4.2 show that Hybrid 1 which contains equal (0.033%) volume percentages of PVA, FF20L6 and FF5E0 with a total fiber volume of 0.1% causes a spread reduction of 4% compared to control mix 1 (with 0% fiber). Hybrid 2 containing a total fiber volume of 0.2% shows a spread reduction of 18% while Hybrid 3 (with 0.175% total fiber volume) and Hybrid 4 (with 0.1% total fiber

volume) show a spread reduction of 48% and 4%, respectively. This shows that the spread reduction in a hybrid mix depends not only on the types and dosages of fiber but also on the interaction and synergic properties between different fiber types [Nehdi and Ladanchuk 2004].

At the same fiber volume content, the highest spread reduction was observed in concrete with PVA fiber. The use of short metal (F5) fiber showed lower reduction of slump flow than longer ones (F20). This can be attributed to the fact that the longer fiber can have more detrimental interference with the aggregates and can obstruct the flow more than short fibers. Combination of different types and configuration of fiber can (as in the case of Hybrid) eliminate fiber clustering and produce more workable SCC than using a single fiber. This is confirmed from the good flowability of Hybrid 4 FRSCC mixture developed in this study. In general, flowability is affected by the differences in the fiber stiffness, mechanical and geometric properties of fibers [Sahmaran et al. 2005]. These properties should be optimized to achieve a FRSCC with good flowability.

4.2.2 Slump Flow Time (T_{500})

T_{500} of all concrete mixtures are found to be lower than the control mix except Hybrid 2, Hybrid 3 as well as PVA mixes with more than 0.125% fiber volume (Figure 4.5). SCC can be classified as VS1 for $T_{500} \leq 2$ seconds or as VS2 for $T_{500} > 2$ seconds. Class VS1 has good filling ability while class VS2 is more likely to become fluid when shaken or stirred, and may be helpful in limiting the formwork pressure and improving segregation resistance [European SCC Guidelines, 2005].

Figure 4.5 indicates that the mixtures 13, 14 and 19 with a T_{500} of less than 2 seconds fall into the class VS1. These mixtures should have a good filling ability even with congested reinforcements and be capable of self-leveling to produce best surface finish.

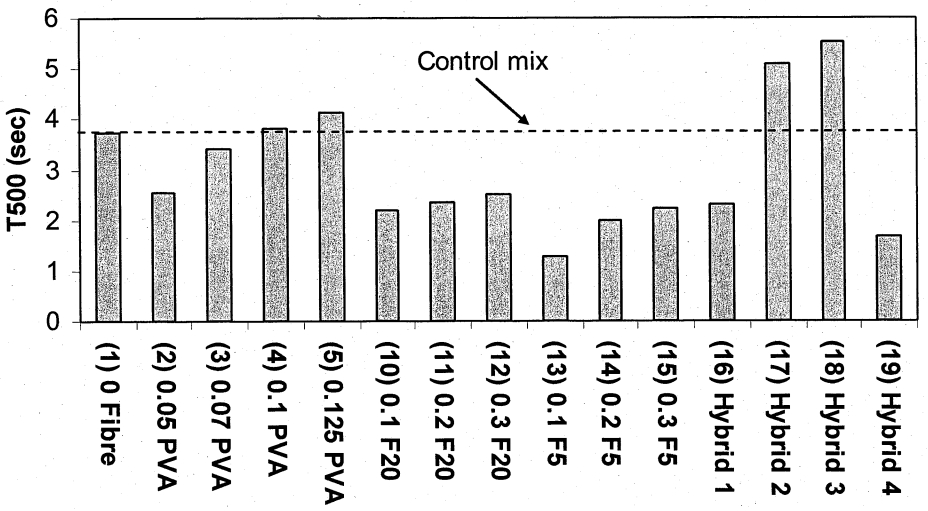

Figure 4.5 Slump flow time (T_{500}) of concrete mixtures

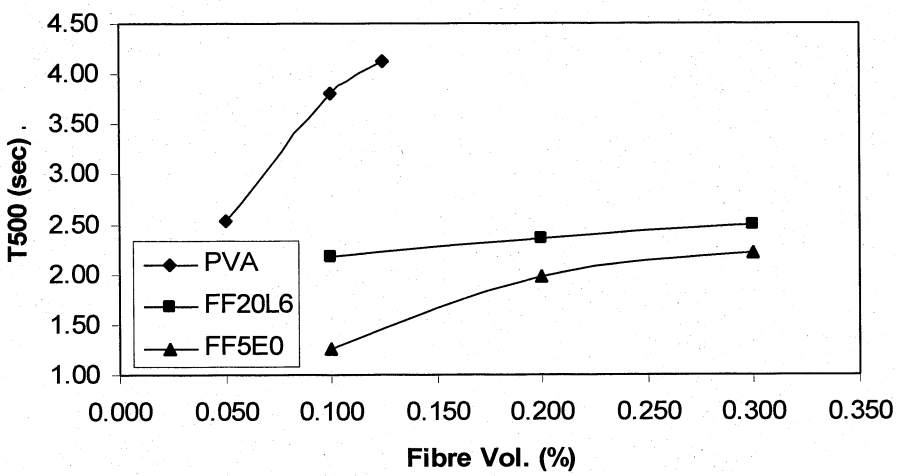

Figure 4.6 Variation of slump flow time (T_{500}) with volume of fiber

T_{500} increases with the increase of fiber dosages for mixes with either PVA or metallic fiber (Figure 4.6). However, short metal fiber (FF5) shows lower T_{500} than long metal fiber (FF20) for the same fiber dosages. The development of higher internal resistance to flow due to the incorporation of longer fiber compared to shorter ones is considered to be the reason.

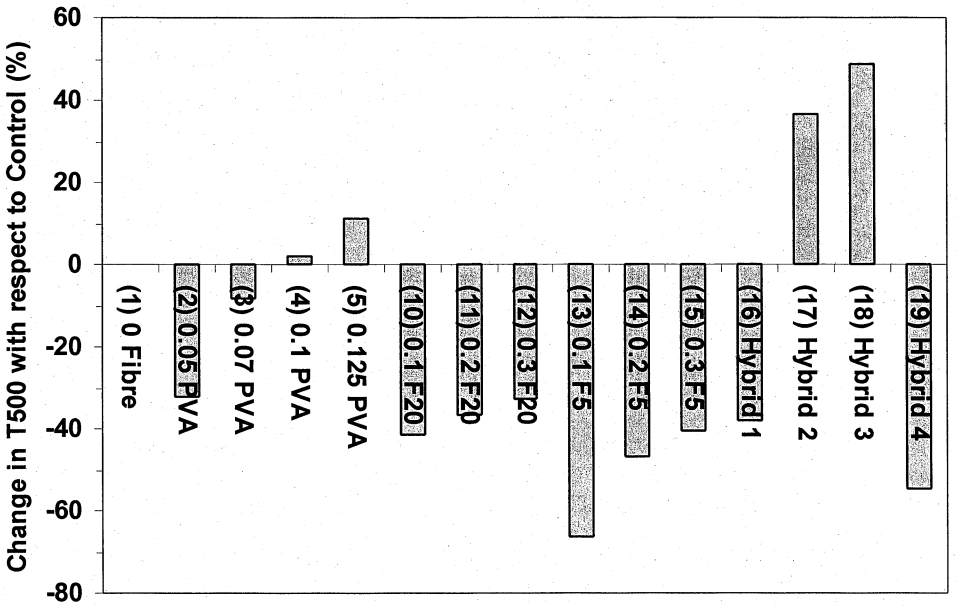

Figure 4.7 Change in T_{500} with respect to control

The reduction of T_{500} compared to control mix is prominent in mixes with metallic fiber (Figure 4.7). A reduction of about 65% is observed for Mix 13 (with 0.1% short FF5 fiber). It is also found that the optimized combination of fiber can produce lower T_{500} as observed in the case of Hybrid 4 where 55% reduction of T_{500} is achieved (Figure 4.7).

Increase of the dosage of PVA fiber beyond 0.1% increases T_{500} (Figures 4.5 and 4.7). This shows that the PVA fiber acts differently than metallic fiber in a concrete matrix. This may be due to the fact the PVAs are hydrophilic in nature and have very high surface area which may lead to the higher internal resistance to flow, particularly at higher dosage.

Figure 4.8 shows that a relation exists between spread and T_{500}. General trend indicates that the T_{500} decreases with the increase of slump spread, as expected.

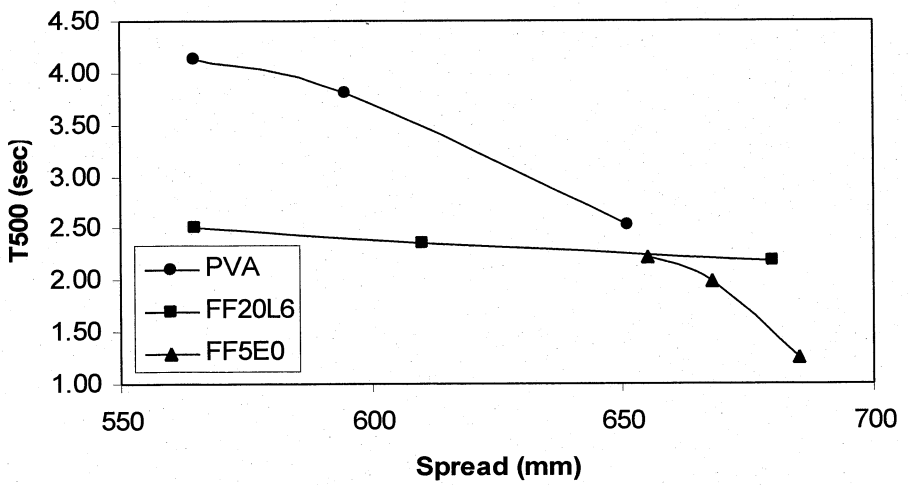

Figure 4.8 Relation between T_{500} and spread

4.2.3 L-Box Passing Ability

Aggregate blocking must be avoided as SCC flows through the reinforcement and the L-box test is an indicative of the passing ability. An L-box index of more than 80% represents a SCC with good passing ability [European SCC Guidelines, 2005].

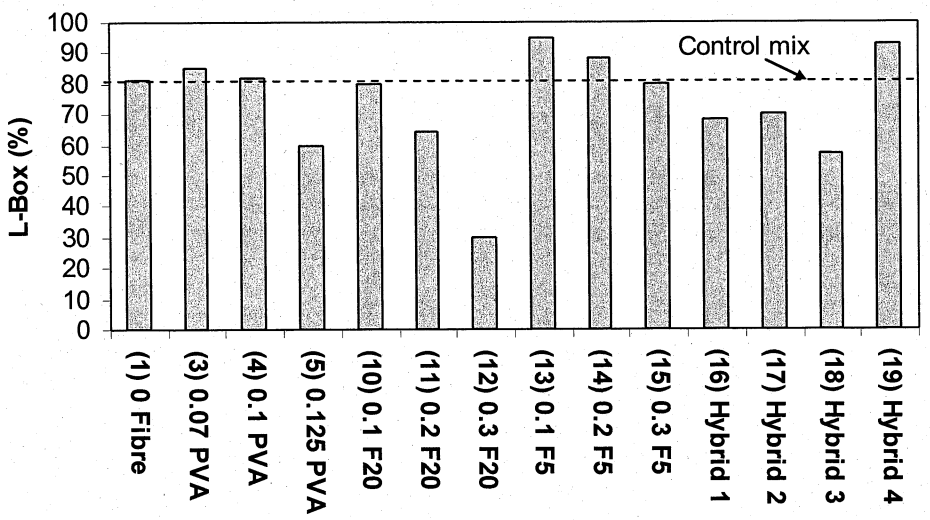

Figure 4.9 Passing ability of concrete mixtures: L-box index (%)

According to Figure 4.9, Mixtures 1, 3, 4, 10, 13, 14, 15, and 19 have good passing ability with an L-box index of more than 80%. These mixtures could be used for

structures with a rebar spacing of 60 mm to 80 mm [European SCC Guidelines, 2005].

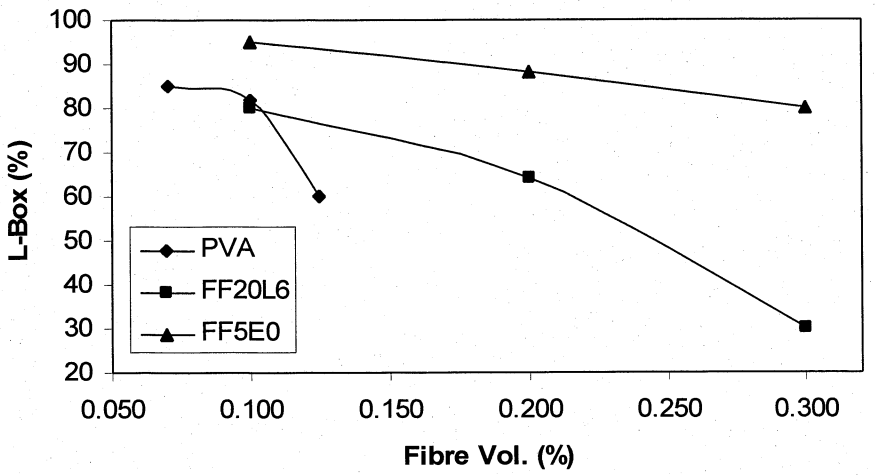

Figure 4.10 Variation of passing ability "L-Box index (%)" with fiber volume

Generally, passing ability "L-Box index (%)" decreases with the increase of fiber volume (Figure 4.10). Short metallic (FF5) fiber produced higher passing ability compared to long ones (FF20). The longer fiber with high surface area could clump and cluster in jammed orientations and can severely limit the flow of concrete and hence, can reduce passing ability between steel bars as observed in Mixes 11 and 12 with FF20.

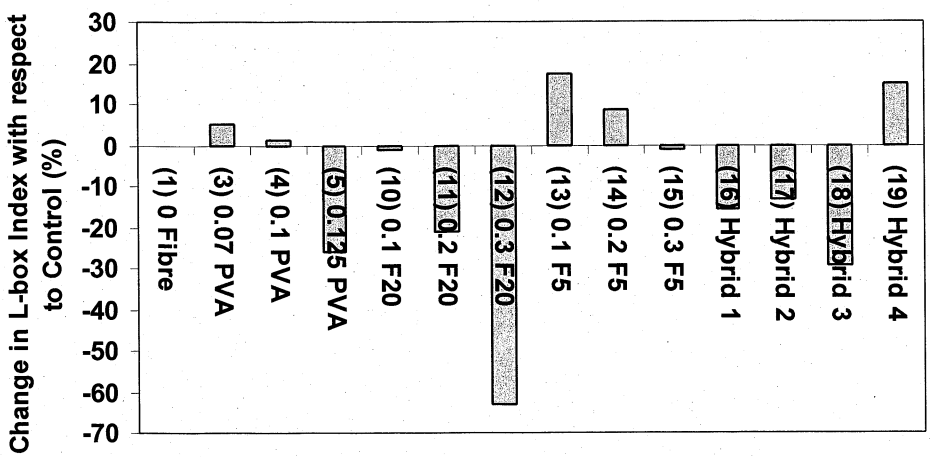

Figure 4.11 L-box of concrete mixtures with respect to control mix

Passing ability of concrete mixtures increased (maximum up to 19%) for mixtures (Mixes 3, 4, 13, 14, and 19) with low volumes of PVA and short metallic fiber (FF5) compared to control mix (Figure 4.11). However for other mixtures with higher dosages of fiber (mixes 5, 10, 11, 12, 16, 17 and 18), passing ability decreased (maximum of up to 61%).

Figure 4.11 illustrates that for a constant volume of fiber, short metallic fiber (FF5) achieved best results in terms of the lower reduction for passing ability while PVA achieved higher reduction. This could be due to the extremely high surface area (76.9 m^2/kg) of PVA fiber relative to the metallic ones (9.6 and 11.6 m^2/kg for FF20 and FF5, respectively).

Hybrid 4 (Mix 19) achieved higher L-box index of 93% and a 15% increase in passing ability compared to control mix (Figures 4.9 and 4.11). This shows that optimized combination of fiber dosages and types can produce better synergic effects and hence, increase the passing ability of a hybrid mixture.

4.2.4 Relation between Passing Ability L-Box (%) and Spread/T_{500}

Figure 4.12 shows that a relationship exists between L-box index (%) and slump flow, as expected. The general trend shows an increase in L-box (%) with the increase of slump flow spread for concrete mixtures with PVA or metallic fibers.

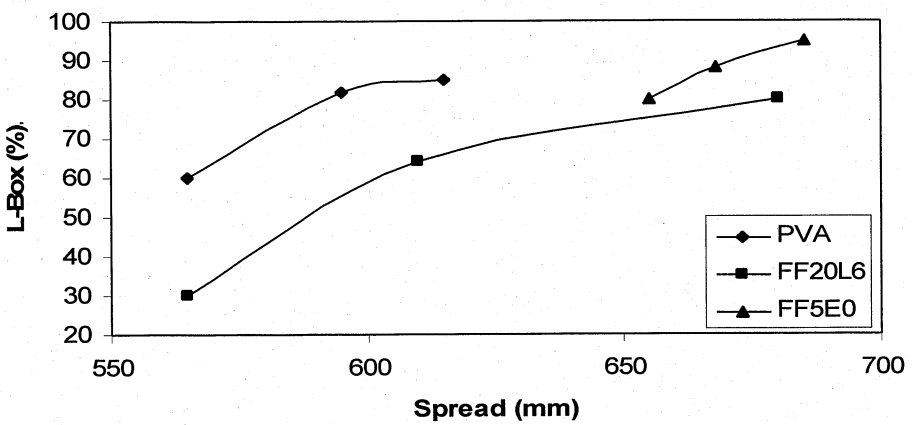

Figure 4.12 Relation between L-box passing ability and slump flow spread

Figure 4.13 also shows the relationship between L-box (%) and T_{500} with a general trend showing a decrease in L-box with the increase of T_{500} for concrete mixtures with PVA and metallic fibers. It is interesting to note that a dramatic reduction of L-box (%) occurs when T_{500} exceeds 2 seconds which is the maximum limit for achieving good flowability [European SCC Guidelines, 2005].

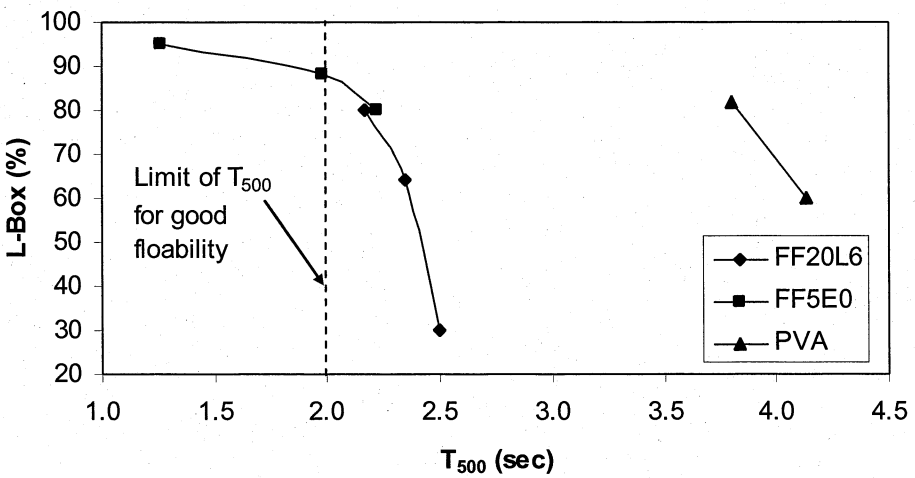

Figure 4.13 Relation between L-box passing ability and T_{500}

4.2.5 V-funnel (VF) Time of Concrete Mixtures

Concrete mixtures can be classified as VF1 if the V-funnel flow time is ≤ 8 seconds and VF2 if between 9 and 25 seconds. VF1 mixtures have good filling ability even with congested reinforcement and capable of self-leveling producing best surface finish. VF2 mixtures are more likely to exhibit thixotropic effects, which may be helpful in limiting the formwork pressure or improving segregation resistance. However negative effects may be experienced regarding surface finish (blow holes) and sensitivity to stoppages or delays between successive lifts during casting.

According to Figure 4.14, Mixes 1, 3, 4, 10, 11, 13, 14, 16, and 19 (Hybrid 4) with V-funnel time of less than 8 seconds fall into the category of VF1 and all other mixes fall into VF2.

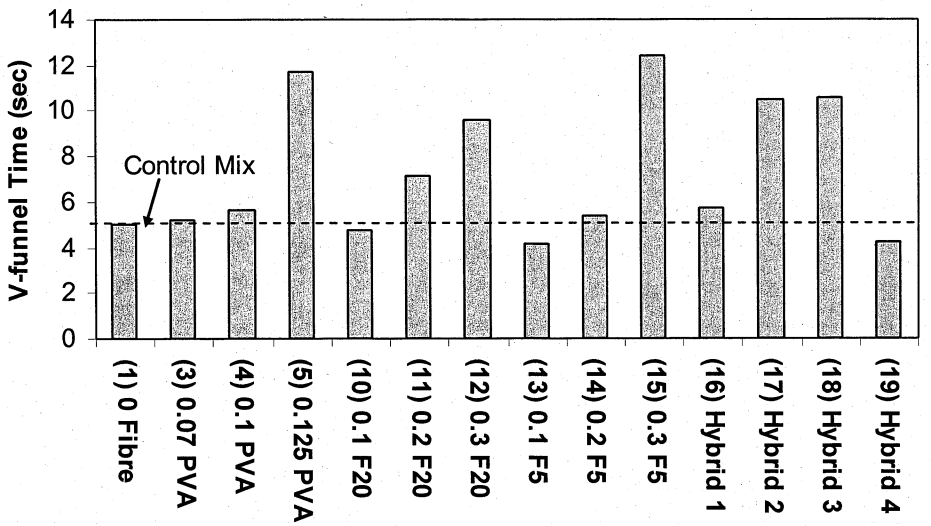

Figure 4.14 V-funnel time of mixtures

In general, V-funnel flow time increases with the increase of fiber content (Figures 4.14 and 4.15). Significant increase in V-funnel flow time was observed compared to control mix with the addition of fiber. Maximum V-funnel flow time increase of 132%, 92%, 147% and 110% were observed for PVA, long metallic (FF20), short metallic (F5) and Hybrid mixtures, respectively (Figure 4.16).

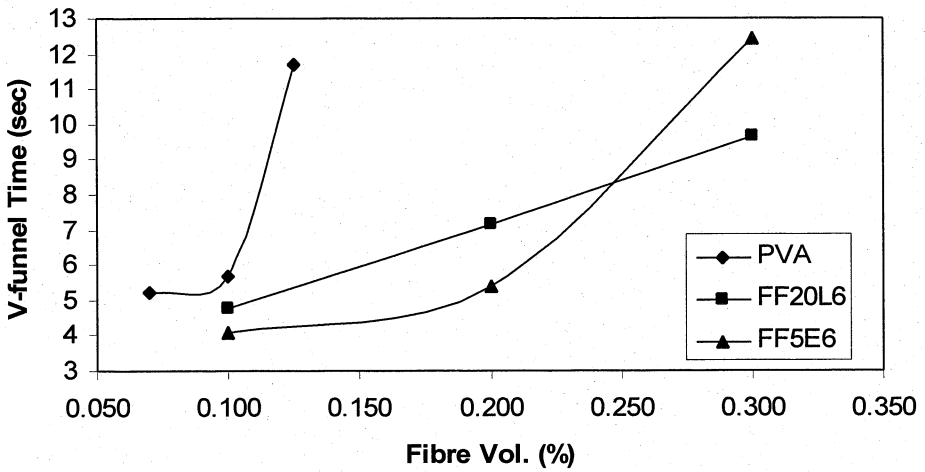

Figure 4.15 V-funnel time with fiber volume percentages

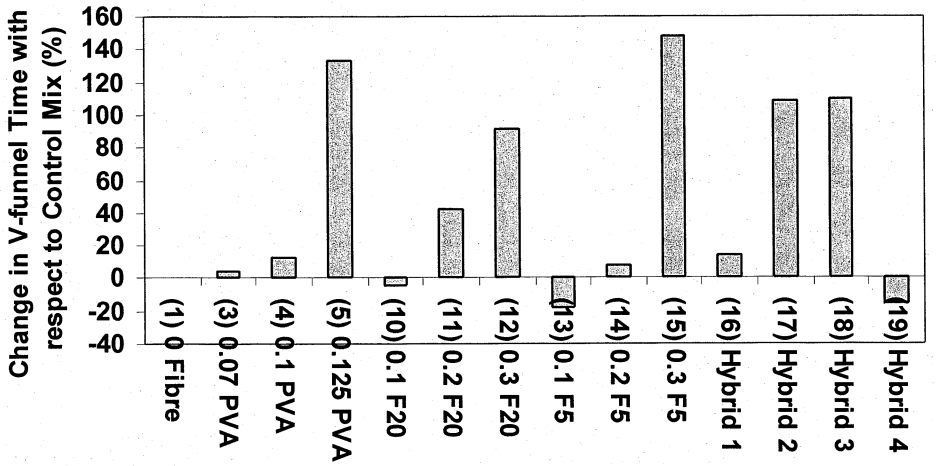

Figure 4.16: V-funnel flow time of concrete mixtures with respect to control mix

It is clear that PVA has distinguished higher influence on V-funnel flow time compared to metallic ones for the same fiber dosage. Higher surface area of PVA and its capacity to adsorb water around its surface in the early stage are the factors which reduce workability and hence, V-funnel flow time. This limits the dosage of PVA fiber to be low value (0.125% in the current study) compared with metallic fiber (0.3% in this study) to achieve a SCC mixture.

V-funnel time of lower than 8 seconds for Hybrid 4 (Mix 19) shows the possibility of producing concrete mixtures with good workability by optimizing combination of fiber dosages and types.

4.2.6 Relation between V-funnel Time, Spread, T_{500} and L-Box

Figure 4.17 shows that the V-funnel time decreases with the increase of slump flow spread. Both metallic and PVA fiber show similar trend of variation.

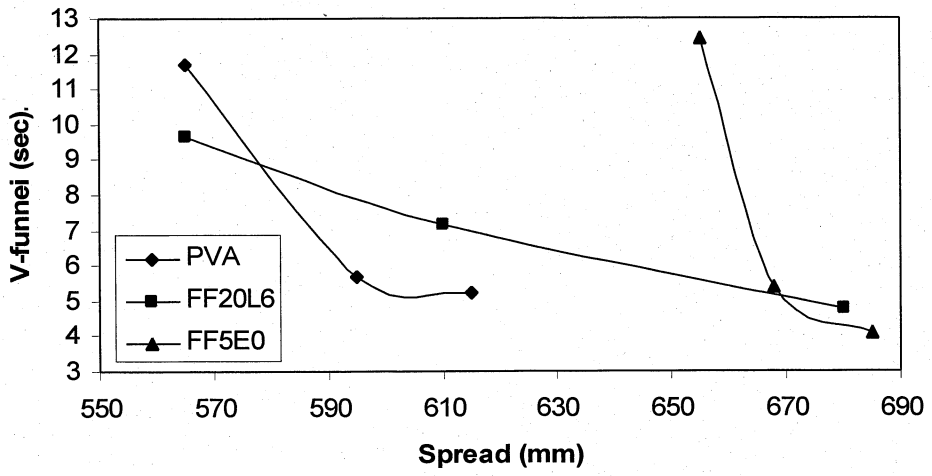

Figure 4.17 Relation between V-funnel time and spread

Figure 4.18 shows a decrease in V-funnel time with an increase in L-box for concrete mixtures with PVA and metallic fibers. It is interesting to note that the V-funnel flow time reduces significantly when L-box exceeds 80% (which is the minimum value for good passing ability). Of all the fibers, short metallic (FF5) showed a significant reduction in V-funnel time.

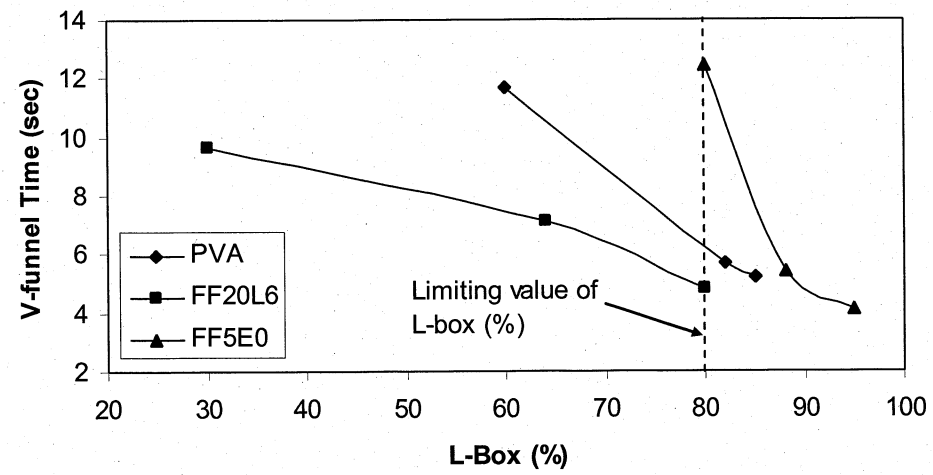

Figure 4.18 V-funnel time with L-Box

4.3 Rheology

Rheology by definition is the science of material flow. Yield value is the force that must be applied to a fluid layer to start flow, before any movement is produced. Plastic viscosity is the resistance to flow when the material has been subjected to a stress in excess of the yield value [Wallevik, 2003]. Rheological parameters (yield value and plastic viscosity) were measured for selected concrete mixtures using ConTec BML coaxial viscometer at time periods of 10, 40, and 70 minutes after adding water to the binder. Test results are presented in Table 4.3. The plastic viscosity and yield value of the developed mixtures satisfying SCC requirements (in terms of fresh properties) fall within the range (10 to 120 Pas for viscosity and 0 to 60 Pa for yield value) of typical SCC in developed countries [Nielsson and Wallevik 2003].

Table 4.3 Rheological parameters of mixtures

Mix No.	Mixture Designation	Yield Value (Pa)			Plastic Viscosity (Pas)		
		10 min	40min	70 min	10 min	40 min	70 min
1	0Fiber	1	2.5	5.5	9.0	12.4	15.1
2	0.05PVA	1	2	6	8.5	8.5	9.6
4	0.1PVA	4	7	9	4.1	5.2	6.5
5	0.125PVA	18	10.2	7.6	18.4	19.6	17.8
8	0.3PVA	80	52	48	17.3	17.8	18.5
9	0.5PVA	336	239	156	16.1	17.9	19.2
10	0.1F20	56.1	81	97	7.5	8.0	8.3
11	0.2F20	81	102	120	5.0	7.1	8.5
12	0.3F20	97	146	204	5.7	8.6	9.8
19	Hybrid 4	27	70	24	4.5	5.6	3.5

4.3.1 Yield Values for Concrete Mixtures

Generally, it is noticed that the yield value increases when fiber volume increases (Figure 4.19). Yield value for concrete mixtures also increases with time except for Mix 5 and Mix 19 where a decrease is noticed.

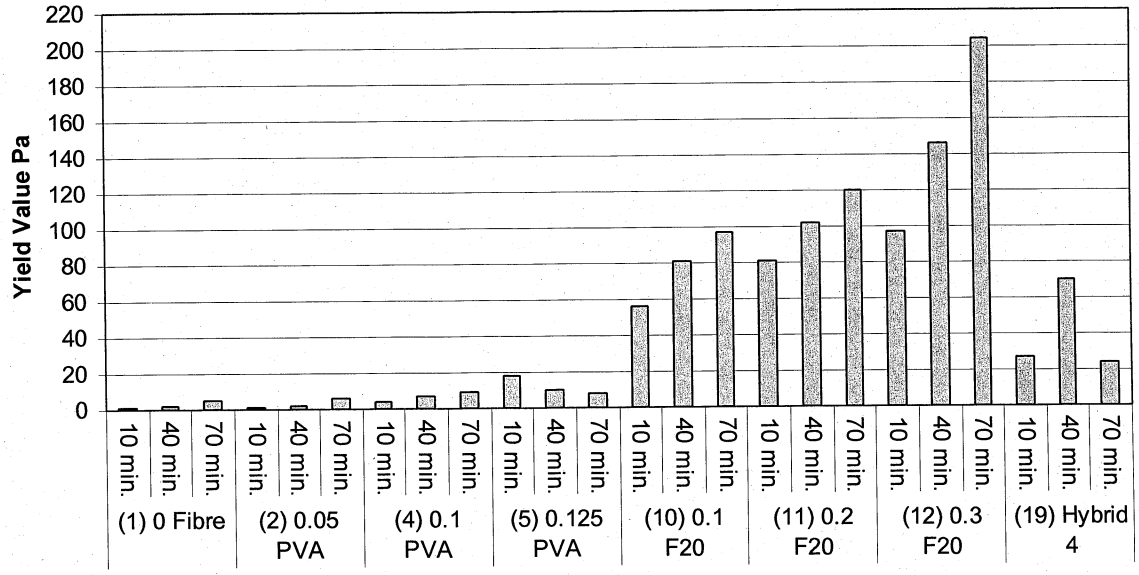

Figure 4.19 Yield value for concrete mixtures

Compared to control mix, yield value (at 10 minutes) of metallic fiber (FF20) mixes significantly increased (97 times) with the increase of fiber volume of up to 0.3% (Figure 4.20). For the similar dosages, the increase in yield value for metallic fiber is also significantly higher (14 times) compared to PVA. This can be attributed to the fact that the metallic fiber is more shear resistance to flow compared with PVA. Besides PVA is a polymer prepared by the polymerization of vinyl alcohol. Mixtures containing PVA may have significant effect on yield value due to interaction with polymer based superplasticizer (Polycarboxylate ether, as used in this study). Study of such interaction was outside the scope of this study.

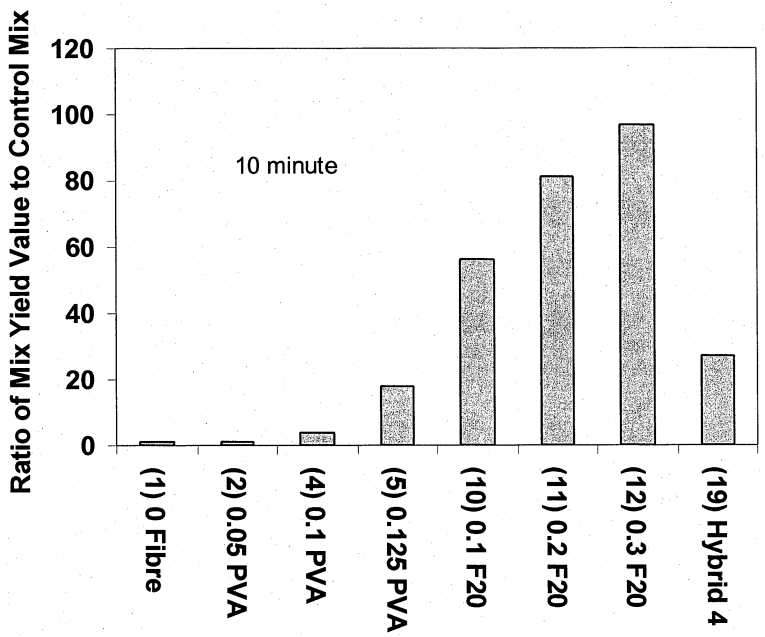

Figure 4.20 Development of yield value in concrete mixtures (at 10 minute)

Figure 4.21 also shows that at 0.1% fiber volume, metallic fiber (FF20) produced higher yield values compared to PVA at 10, 40 and 70 minutes (almost 6 times at 10 minutes, 8 times at 40 minutes and 10 times at 70 minutes).

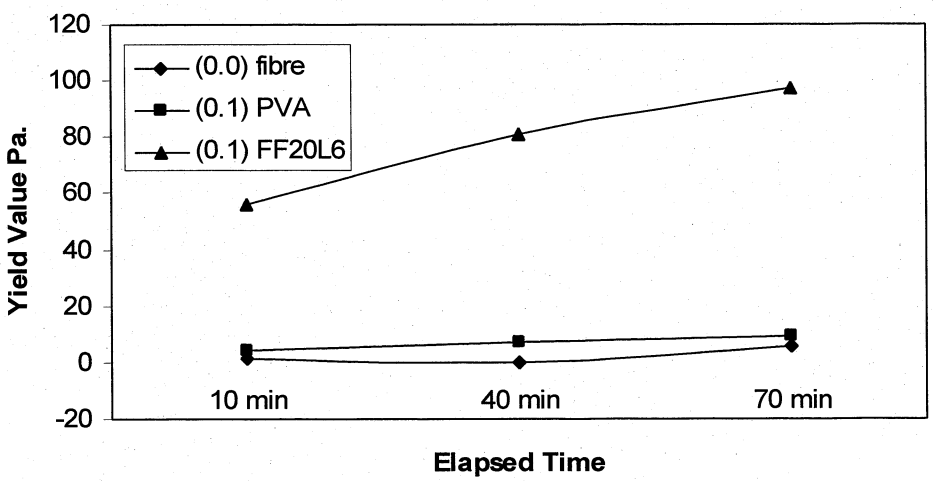

Figure 4.21 Comparison of yield value for concretes with PVA and metal

Figure 4.22 shows that the yield value remained less than 10 Pa up to 0.125 % of PVA dosage. Beyond 0.125%, yield value increases with the increase of fiber dosage and beyond 0.3%, it increases significantly. It is noticed that the yield value at 70 minutes was two times higher than that at 10 minutes for mix with 0.5%PVA.

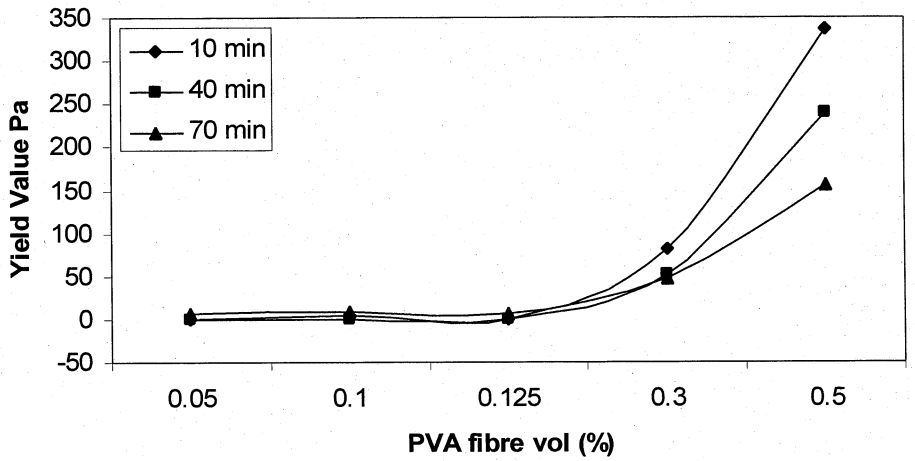

Figure 4.22 Yield value as a function of PVA fiber volume and time

Yield value also increases with the increase of the volume of metal fiber (FF20) from 0 to 0.3% and also with time (Figure 4.23). It is noticed that the yield value at 70 minutes was 2.5 times higher than that at 10 minutes for mix with 0.3% FF20.

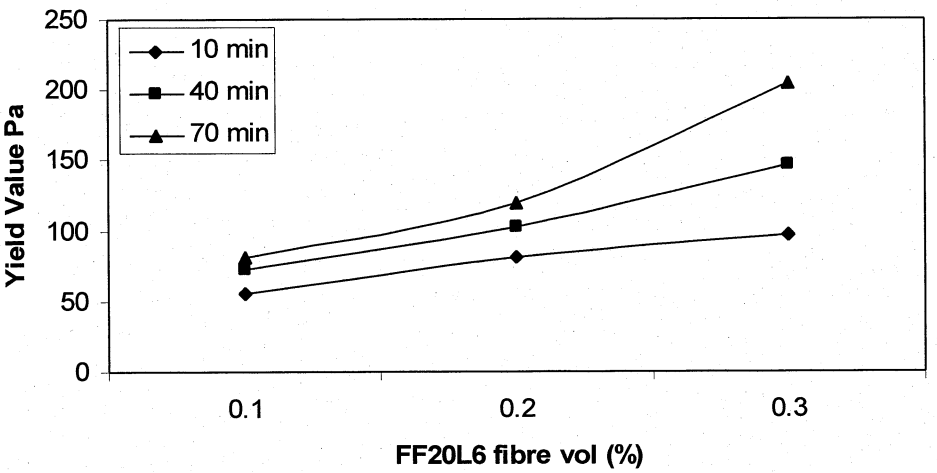

Figure 4.23 Yield value as a function of metallic (FF20) fiber volume and time

This increase in yield stress at 70 minutes can be useful for controlling the pressure on concrete formwork and time of its removal.

4.3.1.1 Relation between Yield Value and Fresh Properties

Figures 4.24 and 4.25 show the relationship between yield value and spread for concretes with PVA and metallic fiber, respectively. Both PVA and metallic fibers show similar trend of variation where yield value decreases with the increase of spread. In case of PVA, a significant drop in yield value was observed up to a slump spread of 450 mm - beyond 450 mm, the reduction in yield value was insignificant.

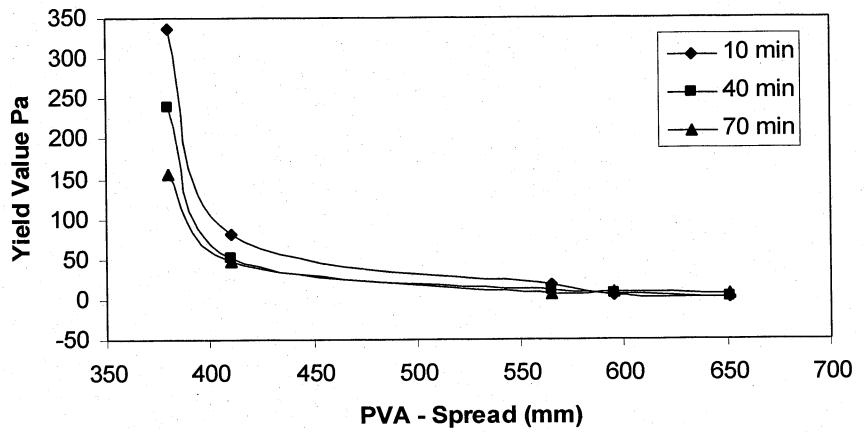

Figure 4.24 Relation between yield value and spread for PVA concrete

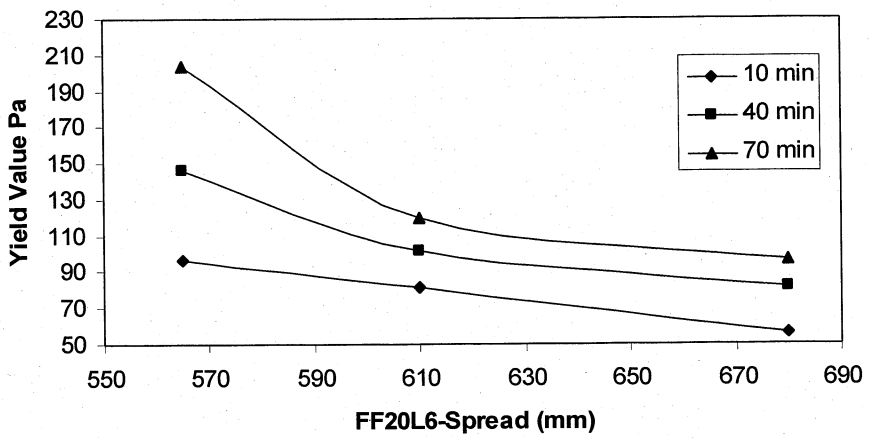

Figure 4.25 Relation between yield value and spread for metal fiber concrete

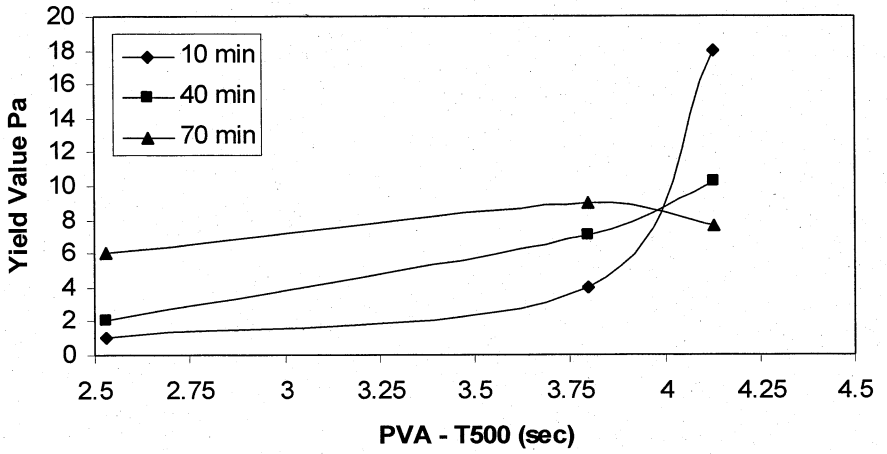

Figure 4.26 Relation between yield value and T_{500}

Figures 4.26 and 4.27 show that the yield value increases with the increase of T_{500} for both PVA and metallic (FF20) fibers. T_{500} is related to viscosity, and hence, yield value increases with the increase of viscosity (which is associated with higher T_{500}.

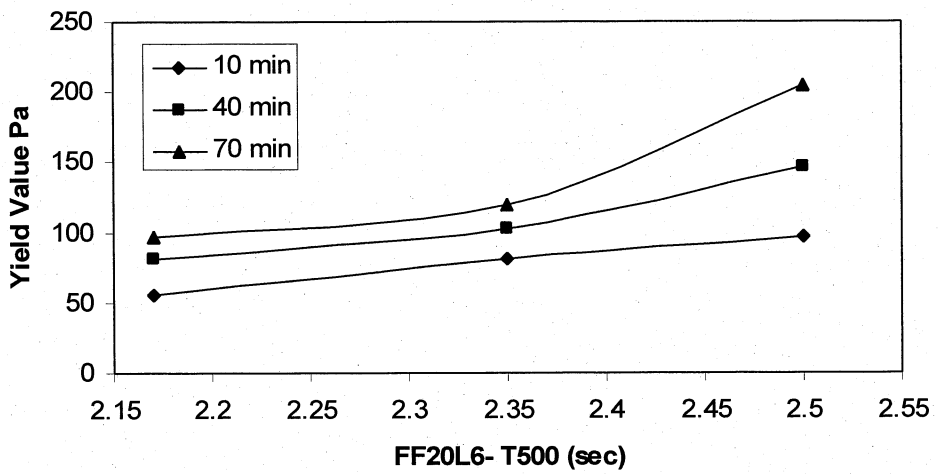

Figure 4.27 Relation between yield value and T_{500}

Figure 4.28 shows an increase of yield value with an increase of V-funnel time (associated with higher viscosity) for concretes with metallic fiber (FF20).

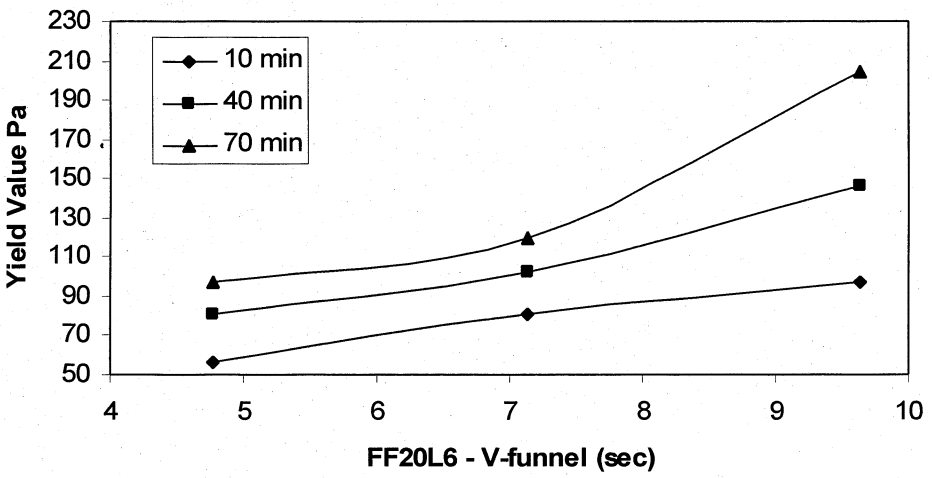

Figure 4.28 Relation between yield value and V-funnel time

In general, yield value decreases with the increase of L-box (%) for metallic (FF20) fibers (Figure 4.29).

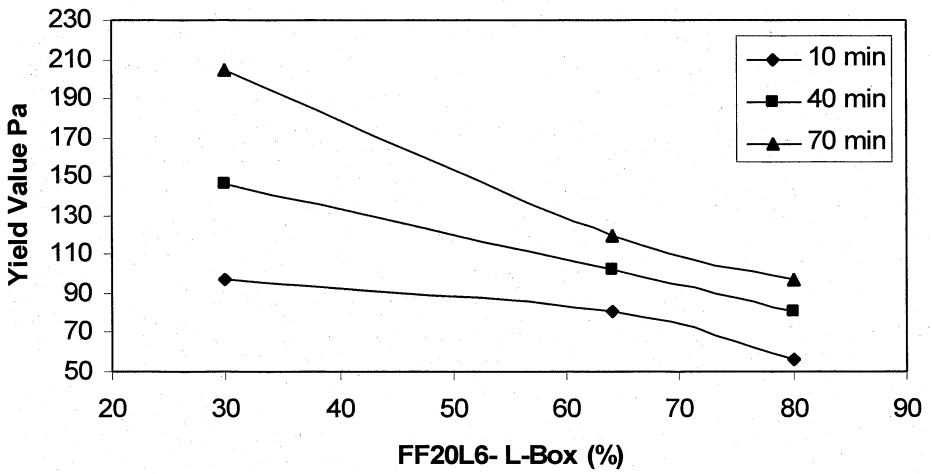

Figure 4.29 Yield value with FF20L6 L-Box (%)

4.3.2 Plastic Viscosity of Concrete Mixtures

Generally, plastic viscosity decreases with the increase of fiber volume in the concrete mixture and also increases with time (Figure 4.30). Plastic viscosity (at 10 minutes) for PVA mixes reduced (by 50%) with the increase of fiber volume from 0 to 0.1% (Figure 4.31). For metallic fiber, a reduction of 40% was observed when fiber content was increased from 0 to 0.3%. For the similar dosages, the

reduction in plastic viscosity for PVA fiber is higher compared to metallic fiber (FF20).

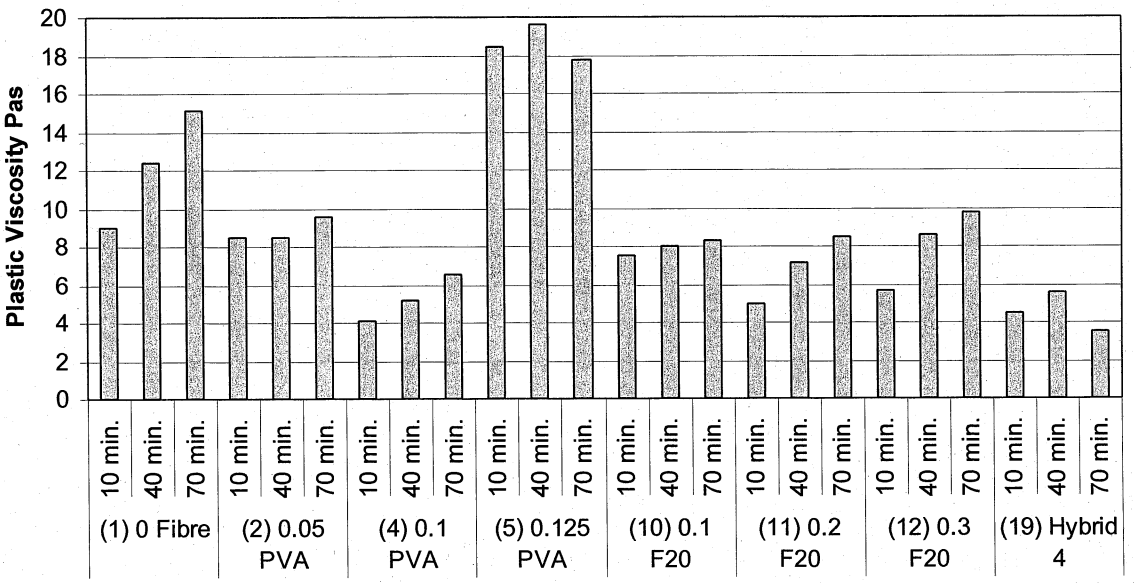

Figure 4.30 Plastic viscosities of concrete mixtures

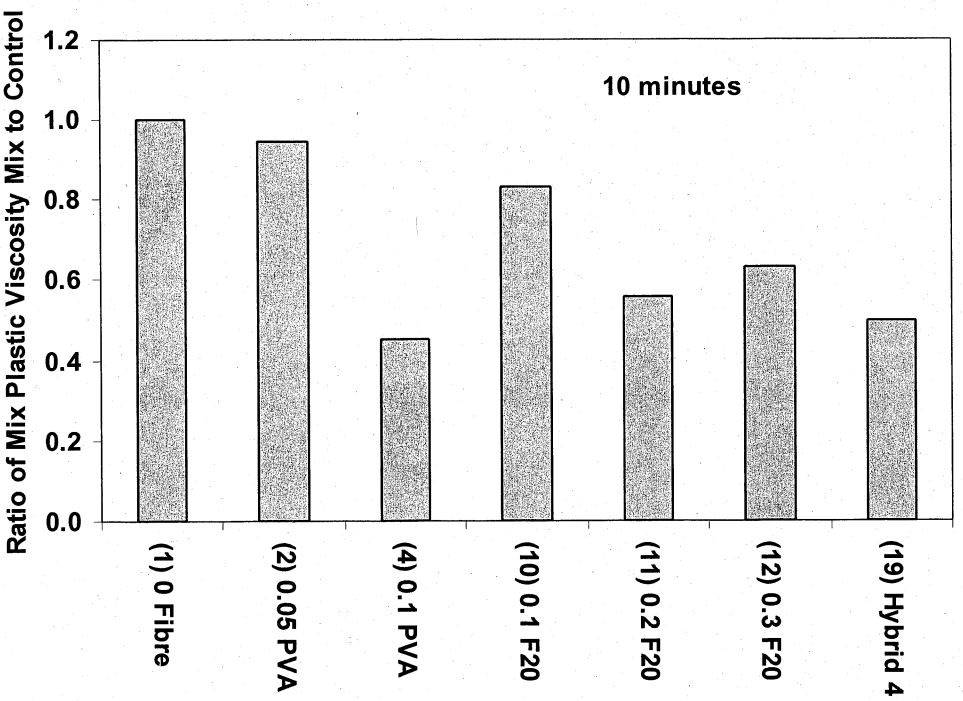

Figure 4.31 Development of plastic viscosity in concrete mixtures (at 10 minute)

Figure 4.32 also shows that at 0.1% fiber volume, both PVA and metallic fibers produced lower plastic viscosity compared to control mix (0 fiber). Metallic fiber produced higher plastic viscosity compared to PVA at 10, 40 and 70 minutes (almost 1.8 times at 10 minutes, 1.6 times at 40 minutes and 1.3 times at 70 minutes).

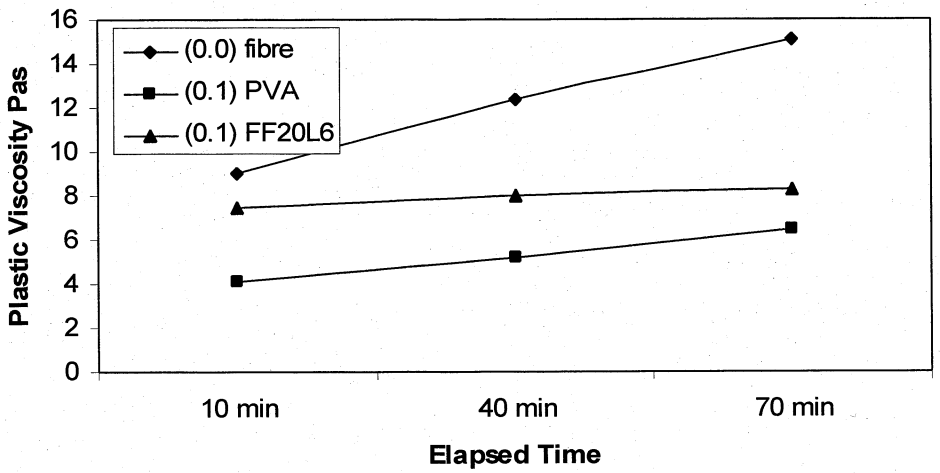

Figure 4.32 Comparative plastic viscosities with elapsed times

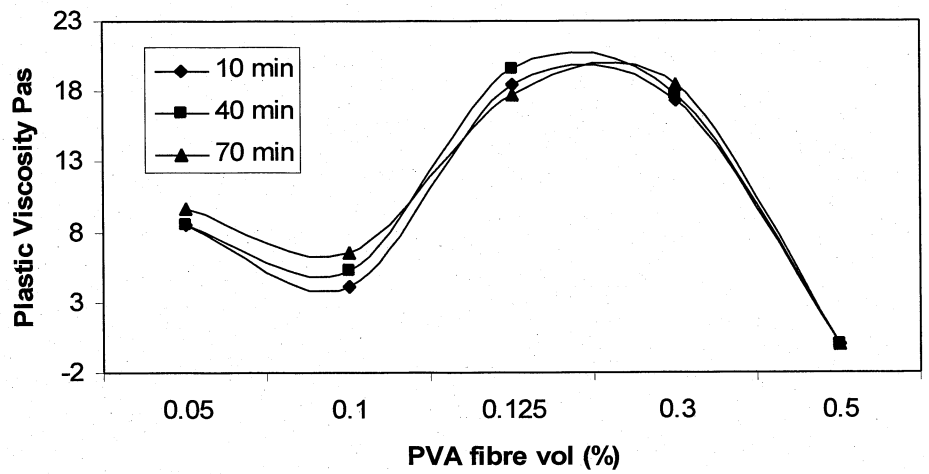

Figure 4.33 Plastic viscosities with PVA fiber volume and time

Figure 4.33 shows an increase in plastic viscosity with an increase of PVA fiber up to about 0.125%. Beyond 0.125% fiber content, plastic viscosity decreases with the increase of PVA fiber. Decease in plastic viscosity is also noticed at lower dosages of PVA (between 0.05 and 0.1%). This could be due to the interaction between

superplasticizer and PVA polymers, either physically for particles and/or chemically at microstructure level.

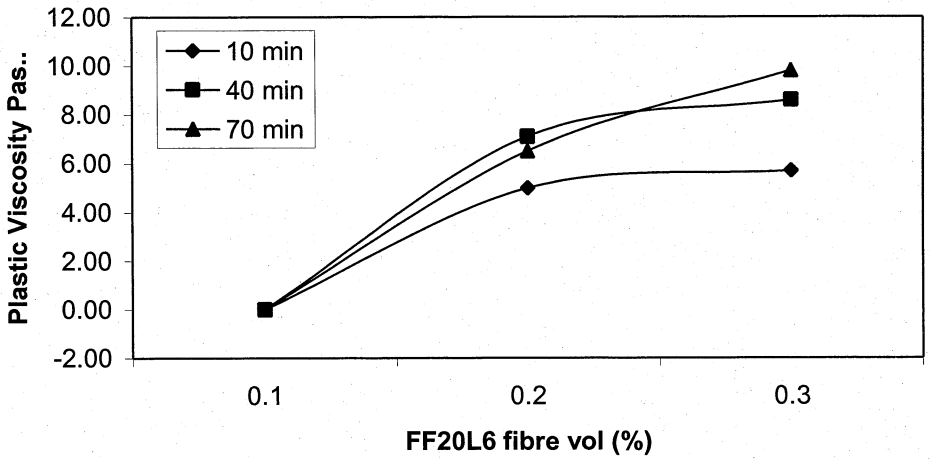

Figure 4.34 Plastic viscosities with metallic fiber volume and time

Figure 4.34 illustrates an increase in plastic viscosity of around eight times when metallic fiber (FF20) is increased three times in volume %. Plastic viscosity of such mixtures also increases with the increase of elapsed time.

4.3.2.1 Relation between Plastic Viscosity and Fresh Properties

Figures 4.35 and 4.36 show the relationship between plastic viscosity and spread for concretes with PVA and metallic fiber, respectively.

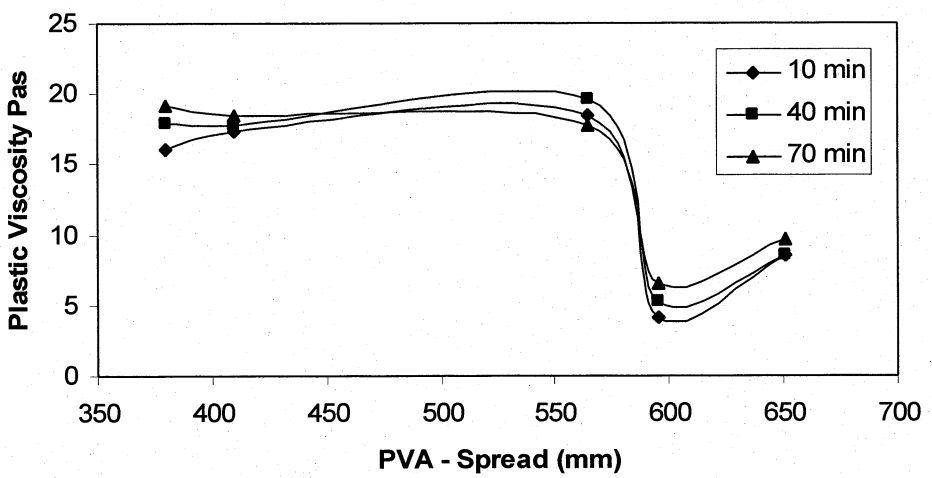

Figure 4.35 Relation between plastic viscosity and spread

Generally plastic viscosity decreases with the increase of spread. In case of PVA, a significant drop in plastic viscosity was observed at a slump spread of 550 mm (minimum value for SCC) - beyond 550 mm, the plastic viscosity is significantly lower.

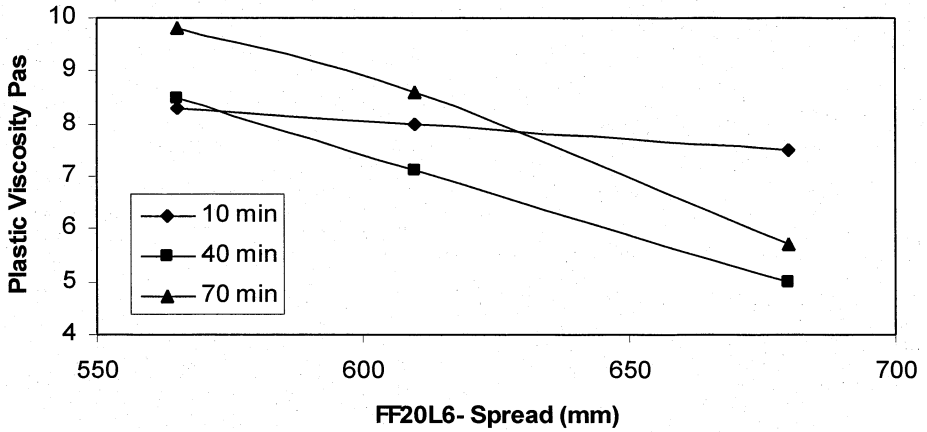

Figure 4.36 Relation between plastic viscosity and spread

Figures 4.37 shows that there is no definite correlation between plastic viscosity and T_{500} for PVA mixtures. However, there is a sharp increase in viscosity when T_{500} is about 4 seconds.

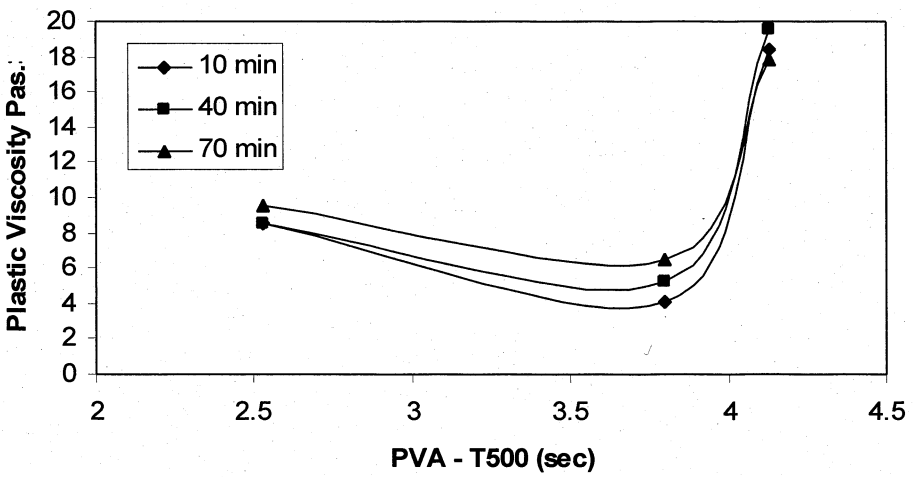

Figure 4.37 Relation between plastic viscosity and T_{500}

Figure 4.38 shows that plastic viscosities decrease with the increase of L-Box passing ability. The variation seems to be affected with time although patterns remain more or less similar. Figure 4.39 illustrates an increase of plastic viscosities with an increase of V-funnel times for the case of metallic fiber.

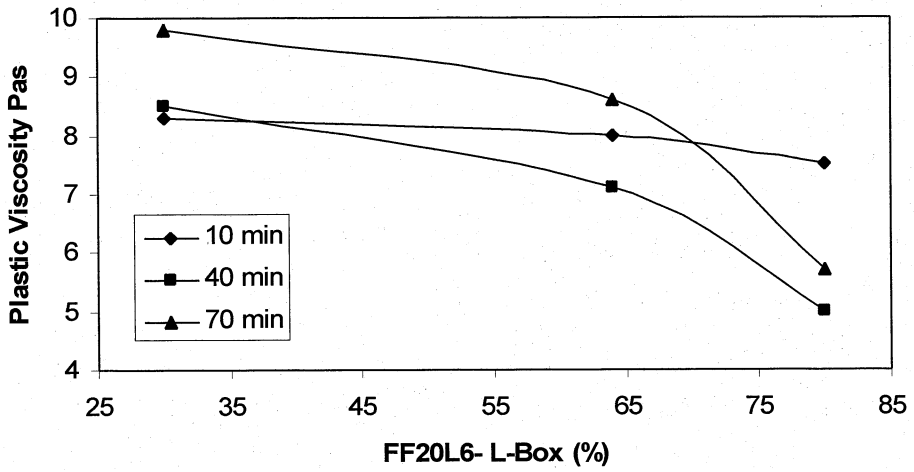

Figure 4.38 Relation between plastic viscosity and L-Box (%)

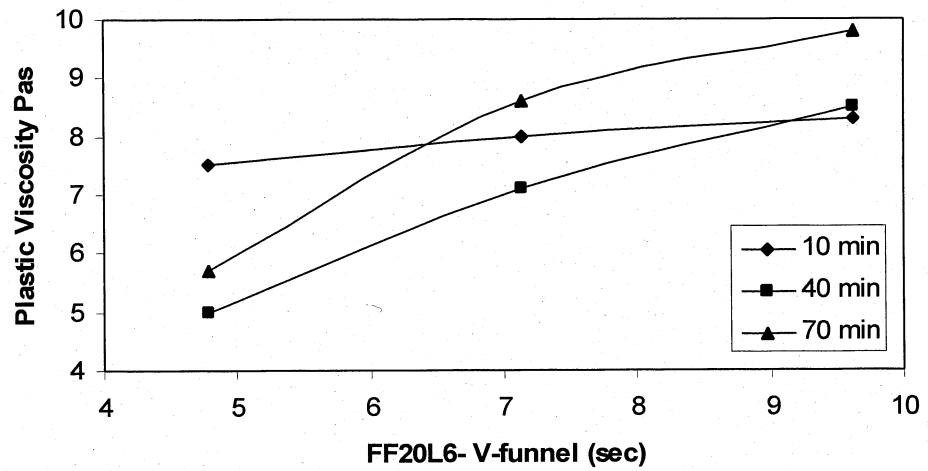

Figure 4.39 Relation between plastic viscosity and V-funnel time

4.4 Mechanical and Durability Properties

Mechanical properties such as compression/splitting/flexural strengths and fracture energy were investigated. Also for durability, electrical conductance test was

conducted to assess the concrete resistance against chloride ion penetration. Table 4.4 presents the mechanical and durability properties of all concrete mixtures including the control SCC mix without fiber. Density of concrete mixtures ranges between 2400 and 2600 kg/m^3.

Table 4.4 Mixtures Hardened Properties

Mix No.	Mixture Designation	Comp. Strength 14 day MPa	Comp. Strength 28 day MPa	Splitting Strength 28 day MPa	Flexural Strength MPa	Fracture Energy N/m	Rapid Chloride Pent. (RCP) Coulomb	Density kg/m^3
1	0Fiber	38	44	2.7	3.4	118	1537	2618
2	0.05PVA	35	38	3.0	n. a.	81	2184	2536
3	0.07PVA	n. p.	n. p.	n. p.	n. p.	n. p.	n. p.	n. p.
4	0.1PVA	n. p.	n. p.	n. p.	3.3	249	2312	2559
5	0.125PVA	32	38	n. p.	4.3	254	n. p.	2561
6	0.15PVA	35	42	n. p.	n. p.	n. p.	1238	2465
7	0.2PVA	n. p.	n. p.	n. p.	3.9	295	n. p.	n. p.
8	0.3PVA	36	40	n. p.	2.9	485	1815	2398
9	0.5PVA	37	46	n. p.	2.7	415	2164	2558
10	0.1F20	41	45	3.7	3.6	404	2408	2568
11	0.2F20	41	45	n. p.	4.9	576	2585	2570
12	0.3F20	42	48	3.5	5.3	719	3759	2590
13	0.1F5	40	42	3.6	7.6	275	n. p.	2558
14	0.2F5	42	44	n. p.	n. p.	n. p.	n. p.	2589
15	0.3F5	42	44	3.0	n. p.	n. p.	n. p.	2554
16	Hybrid 1	39	39	2.9	n. p.	n. p.	n. p.	2589
17	Hybrid 2	33	40	3.3	n. p.	n. p.	n. p.	2537
18	Hybrid 3	35	39	n. p.	n. p.	n. p.	n. p.	2569
19	Hybrid 4	36	44	2.9	4.0	267	1855	2582

Note: (n. p.) i.e. (not performed)

4.4.1 Compressive Strength

Figure 4.40 presents the compressive strength of concrete mixtures at 14 and 28 days. The 14 day and 28 day compressive strengths of control mix are 38 MPa and 44 MPa, respectively. The 14-day compressive strength ranges between 32 MPa and 37MPa for PVA mixtures, between 40 MPa and 42 MPa for metallic mixtures and between 33 MPa and 39 MPa for hybrid mixtures. The 28-day compressive

$\frac{\pi}{4} d^2 = 0.000785\ m^2$

strength ranges between 38 MPa and 46 MPa for PVA mixtures, between 42 MPa and 48 MPa for metallic mixtures and between 39 MPa and 44 MPa for hybrid mixtures.

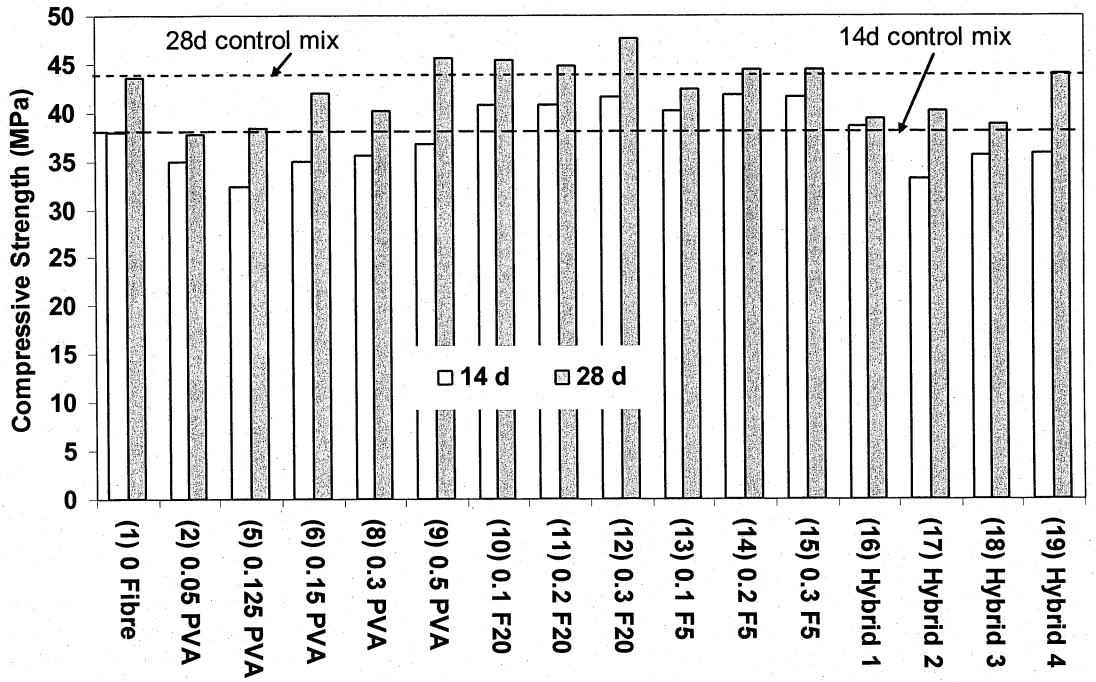

Figure 4.40 14 and 28-day compressive strength of concrete mixtures

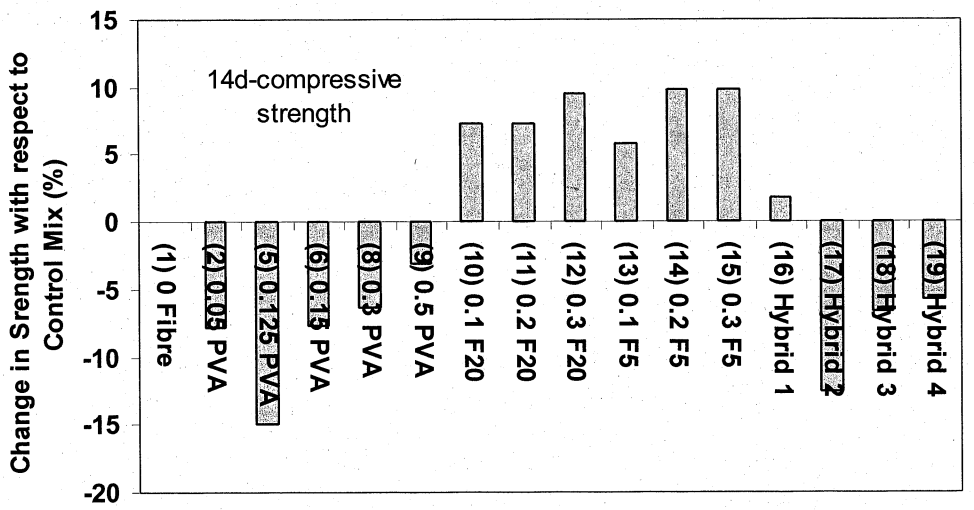

Figure 4.41 14-day compressive strength gain or reduction

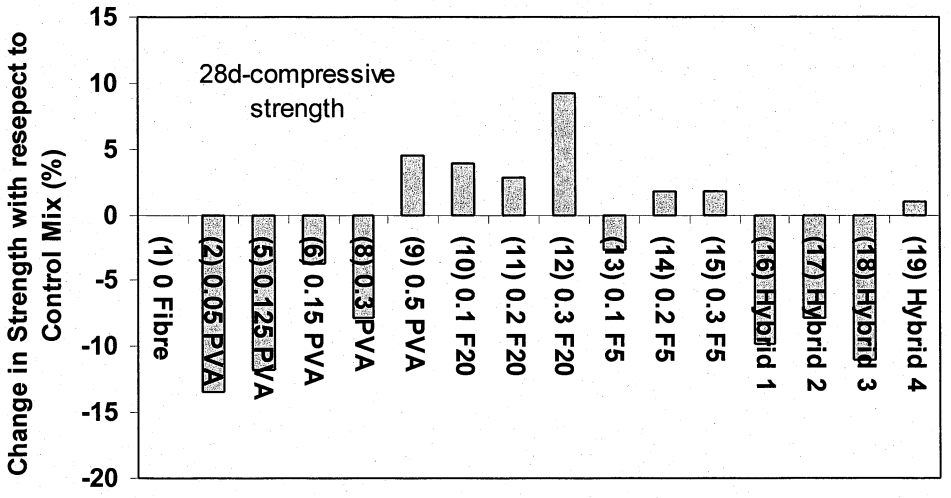

Figure 4.42 28-day compressive strength gain or reduction

Addition of PVA fiber did not improve the 14-day and 28-day compressive strength compared to control mix. A maximum strength reduction of about 15% is observed for PVA mixtures (Figures 4.41 and 4.42). The reduction of compressive strength with the addition of polymer fiber was reported in previous research studies [Grünewald and Walraven 2001, Yao et al. 2003, Soroushian and Mirza 1992]. However, addition of metallic fibers (both short FF5 and long FF20) improves the 14-day and 28-day compressive strength compared to control mix. A maximum strength increase of about 10% is observed for metallic mixtures (Figures 4.41 and 4.42) and in general, the increase of metallic fiber increases the strength of concrete mixtures. The increase of compressive strength with the addition of fiber is also supported from previous research studies [Nehdi and Ladanchuk 2004, Miao et al. 2003, Ding et al. 2008]. Hybrid mixtures also show a reduction in compressive strength (maximum of up to 12%) compared to control. A change in compressive strength of about 10 to 15% does not show a great influence of fiber addition on the compressive strength of concrete. This is found to be true from previous research studies [Nehdi and Ladanchuk 2004].

4.4.2 Splitting Tensile Strength

Figure 4.43 presents the 28-day splitting tensile strength of concrete mixtures. The 28-day splitting tensile strength of control mix is 2.7 MPa. The 28-day splitting tensile strength ranges between 3.0 MPa and 3.7MPa for PVA mixtures, between 3.0 MPa and 3.7 MPa for metallic mixtures and between 2.9 MPa and 3.3 MPa for hybrid mixtures.

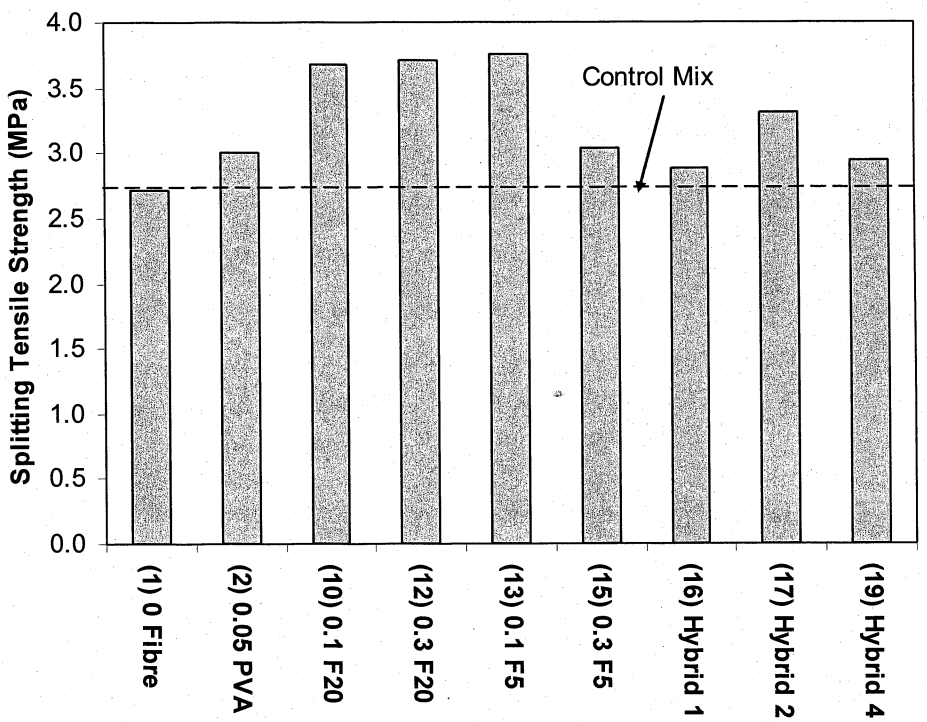

Figure 4.43 28-day splitting tensile strength of concrete mixtures

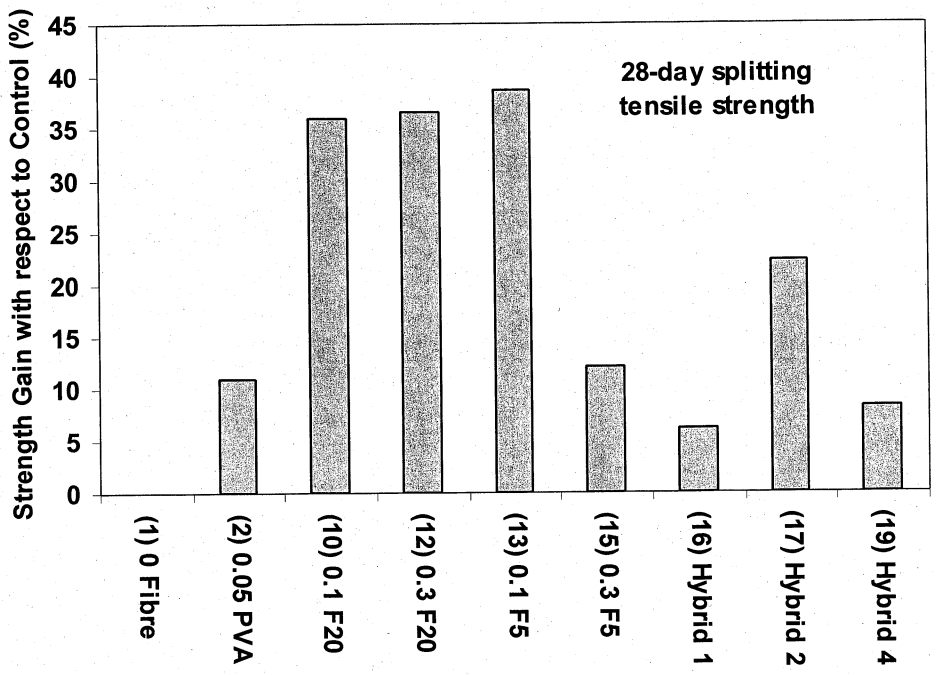

Figure 4.44 28-day splitting tensile strength gain

Addition of PVA fiber improves the 28-day spitting tensile strength compared to control mix. A strength gain of about 11% is observed for a mixture with 0.05% PVA (Figure 4.44). Addition of metallic fiber (both short FF5 and long FF20) significantly improves the 28-day splitting tensile strength compared to the control mix as observed in previous research studies by Nanni [1989]. A maximum strength increase of about 39% is observed for metallic mixtures (Figure 4.44). In general, the increase of both PVA and metallic fiber increases the splitting tensile strength of concrete mixtures. However, the strength gain due to metallic fiber compared to PVA is substantial. This can be attributed to the better interlocking characteristics of metal fiber in the concrete matrix. A splitting tensile strength gain of about 39% is substantial compared to 10% of compressive strength. This signifies that the use of FRSCC can reduce the amount of tensile reinforcement needed in reinforced concrete structures.

Load-lateral displacement responses of representative concrete mixtures from splitting tensile tests are presented in Figure 4.45. The load-displacement

response is significantly affected by the type and dosages of fiber in the concrete. The metallic fiber mixtures (also some of the hybrid mixtures) develop a second peak at a higher load after the formation of the first one before failure. The displacement at the second peak is much higher than that at the first peak which shows a considerable amount of ductility of such mixtures. This can be due to the ability of the steel fiber in arresting the crack development and crack propagation as well as capability to bridge on cracks in the concrete matrix. Control and PVA mixtures do not show any such 2nd peak and failed at much lower deformation showing a brittle failure without continuity for lateral displacement.

It should also be noted that the fiber performance in splitting tension depends on material strength, smoothness of fiber surface, microstructure bond and concrete granular skeleton. Optimization of above factors will ensure better concrete-fiber interaction to develop an efficient crack resisting mechanism up to failure.

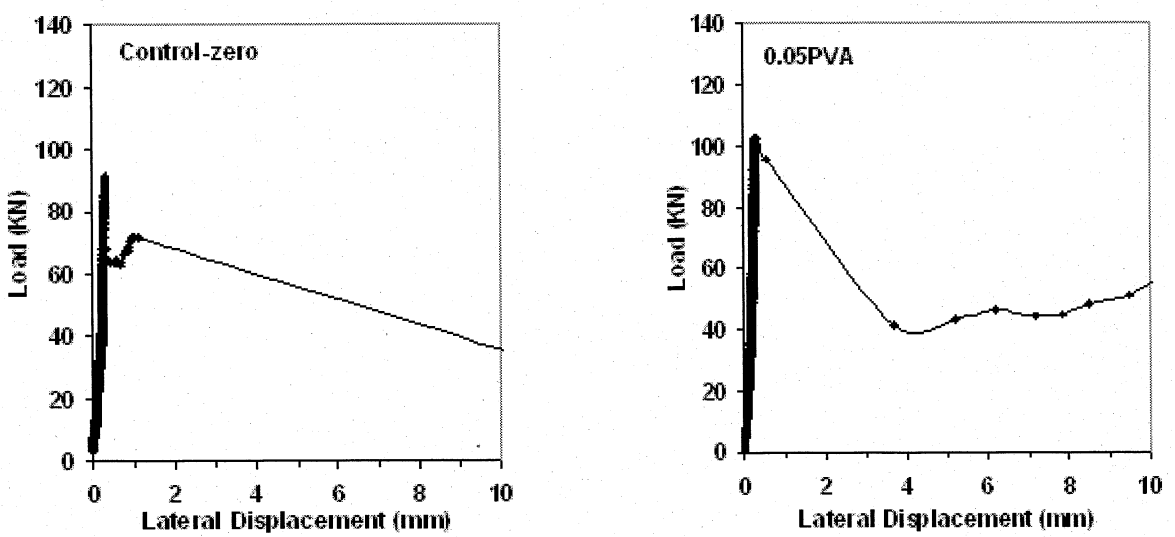

Figure 4.45 Load-lateral displacement responses under splitting tension, continue...

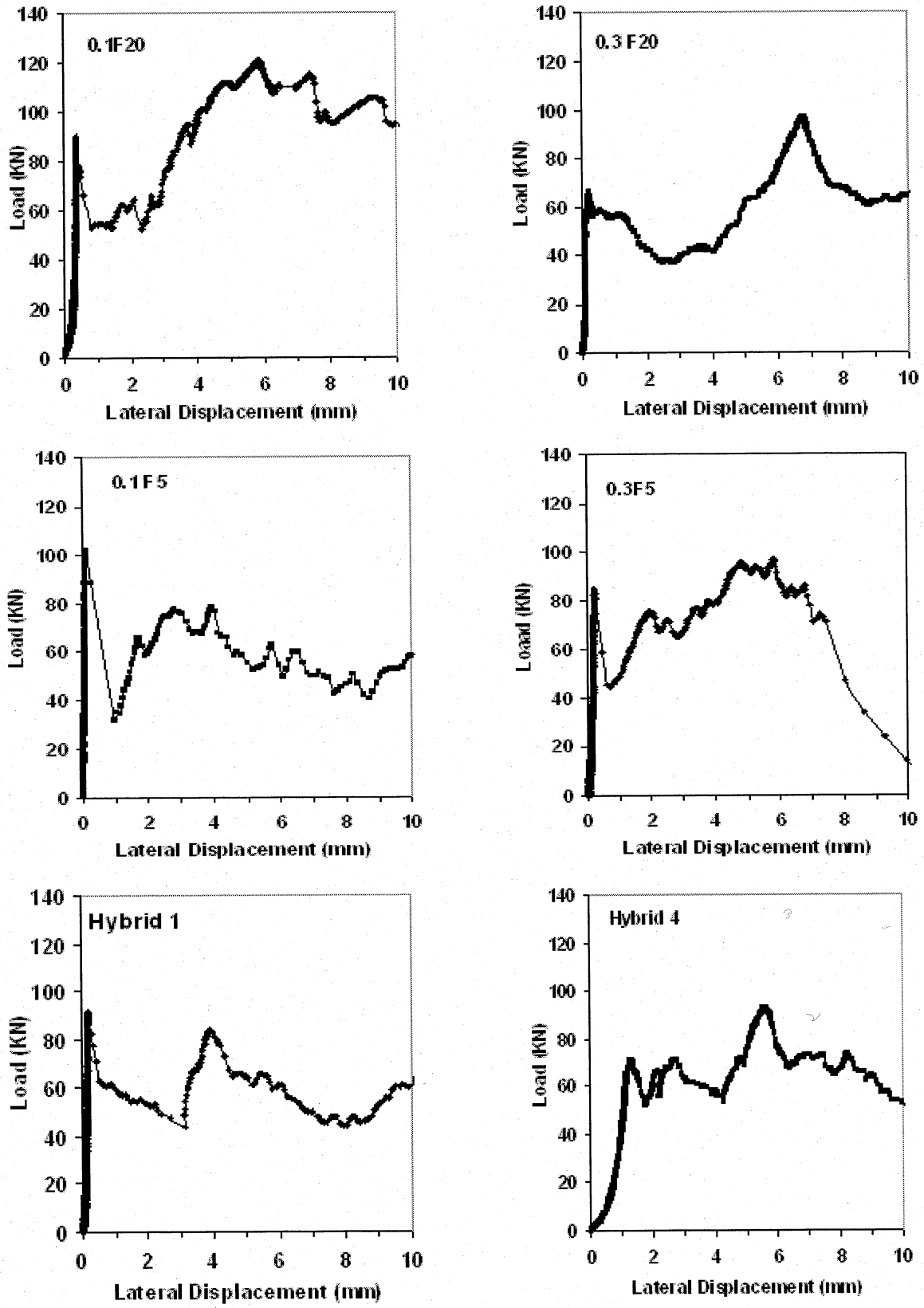

Figure 4.45 Load-lateral displacement responses under splitting tension

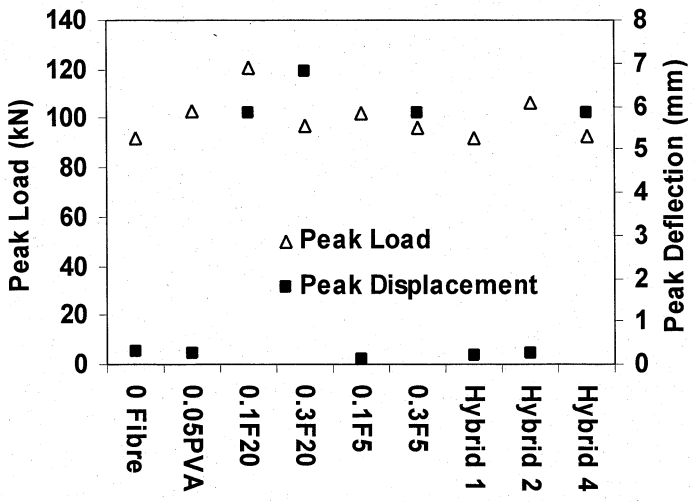

Figure 4.46 Peak load and peak displacement for concrete mixtures

Figure 4.46 shows a significant increase (about 22 times higher than control mix) of peak deflection in metallic fiber mixtures and also in a specified hybrid mixture (Hybrid 4). This could be very important in reinforced concrete structural design. The use of such metallic fiber based SCC mixtures can be very useful in providing ductility to the structure.

4.4.3 Flexural Strength

Figure 4.47 presents the 28-day flexural strength of concrete mixtures. The 28-day flexural strength ranges between 2.7 MPa and 4.3MPa for PVA mixtures, between 3.6 MPa and 7.6 MPa for metallic mixtures and 4.0 MPa for the hybrid mixture. The 28- day flexural strength of control mix is 3.4 MPa.

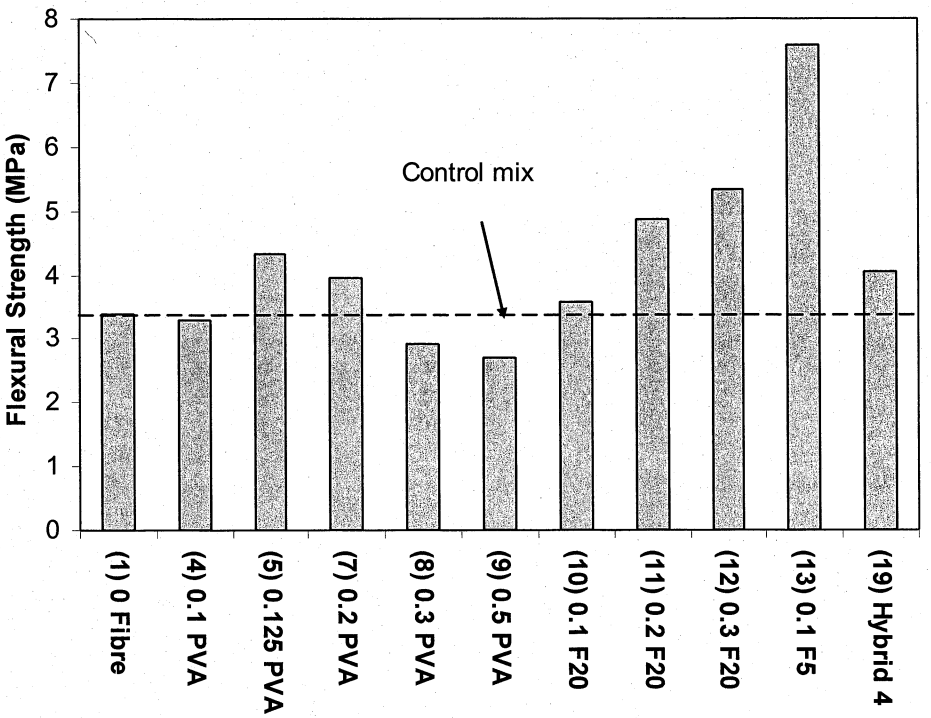

Figure 4.47 28-day flexural strength of concrete mixtures

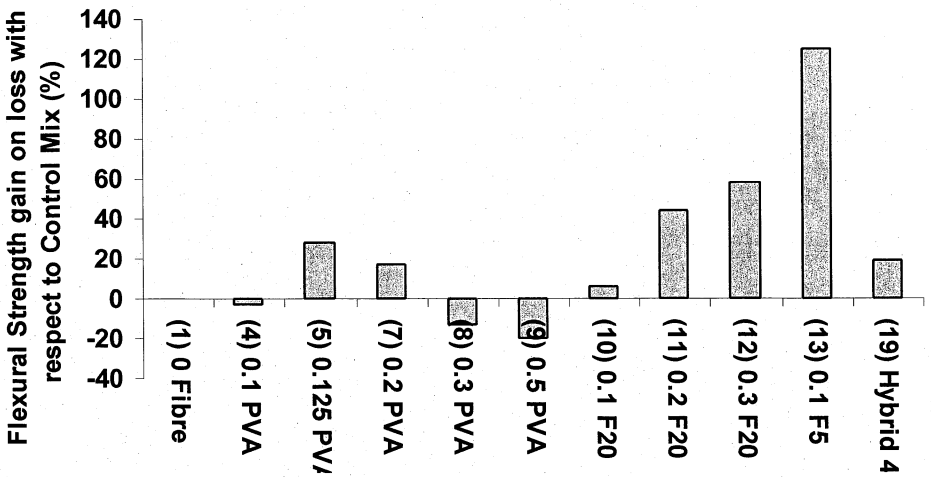

Figure 4.48 28-day flexural strength gain or loss

Addition of PVA fiber improves the 28-day flexural strength compared to control mix up to 0.125% PVA which is the maximum dosage to achieve SCC (Figure 4.48). A strength increase of 28% is obtained for this FRSCC mixture (Mix 5).

Beyond 0.125%, the concrete mixtures (Mixes 7, 8 and 9) do not fall into the category of SCC. For these concrete mixtures, strength decreases with the increase of PVA dosages possibly due to poor compaction and segregation (Figure 4.48). A slight increase in flexural strength with the addition of polymer fiber was reported in previous research studies [Mobasher and Li 1996].

Addition of metallic fibers (both short FF5 and long FF20) significantly improves the 28-day flexural strength compared to the control mix. A maximum strength increase of about 124% is observed for metallic mixtures (Figures 4.50). The increase in flexural strength with the addition of steel fiber is reported by other researchers, as well [Nehdi and Ladanchuk 2004, Qian and Stroven 2000, Ding et al. 2008, Deng 2005]. In general, the increase of both PVA and metallic fibers increases the flexural strength of concrete mixtures. However, the flexural strength gain due to metallic fiber compared to PVA is substantial as observed in the case of splitting tensile strength. A flexural strength gain of about 124% is substantial compared to 10% of compressive strength and 39% of splitting tensile strength (Figure 4.48). This indicates that the use fibers (especially the metallic ones) are more effective in increasing flexural strength of FRSCC than the compressive or splitting tensile strength.

Figure from 4.49 shows flexural load-deflection curves for concrete mixtures. Generally peak load increases with the increase of fiber volume (both PVA and metallic) as far as concrete remains SCC. Metallic fibers are more effective in increasing the peak load compared to those with PVA as can be seen from Figure 4.49.

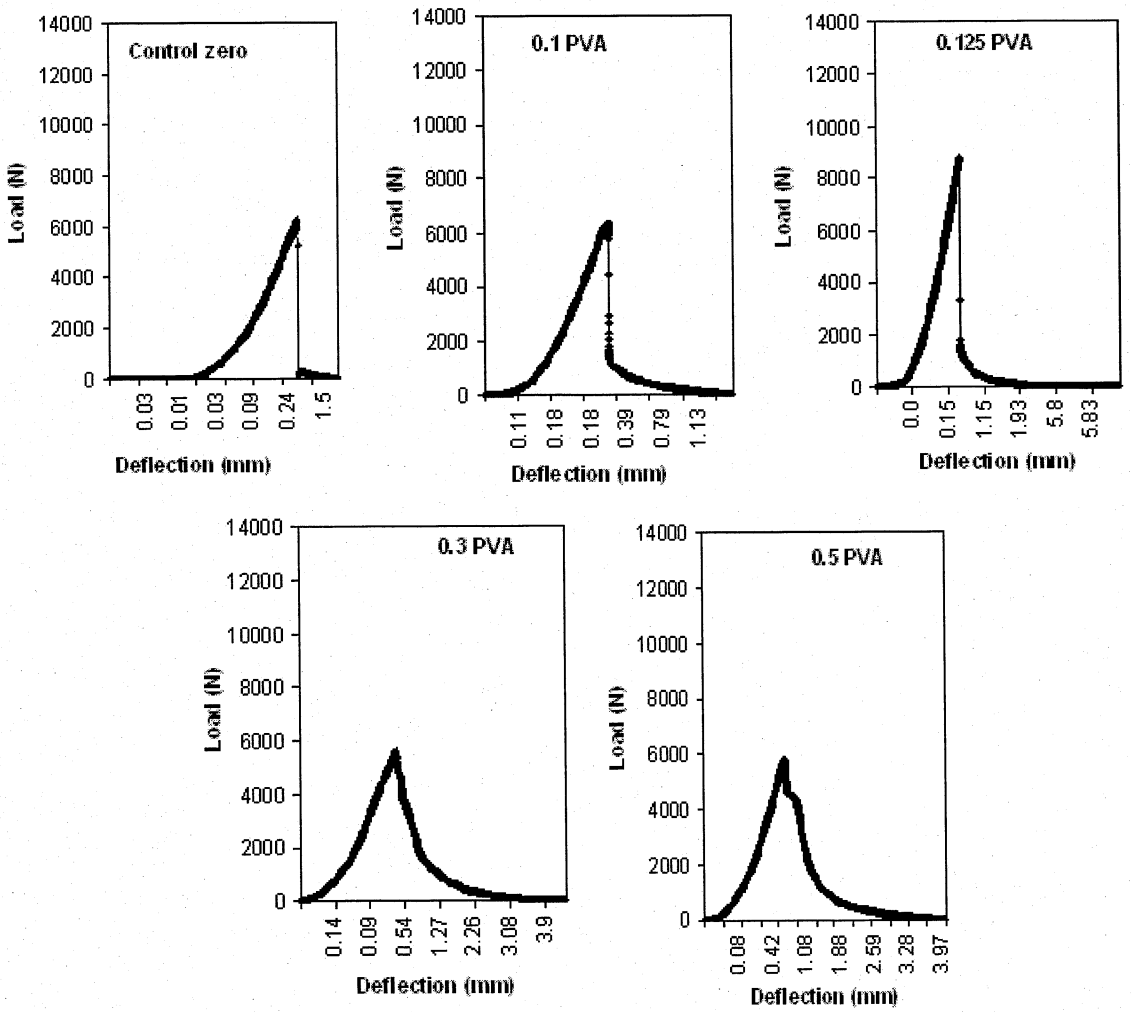

Figure 4.49 Load-deflection responses from flexural strength test, continue……

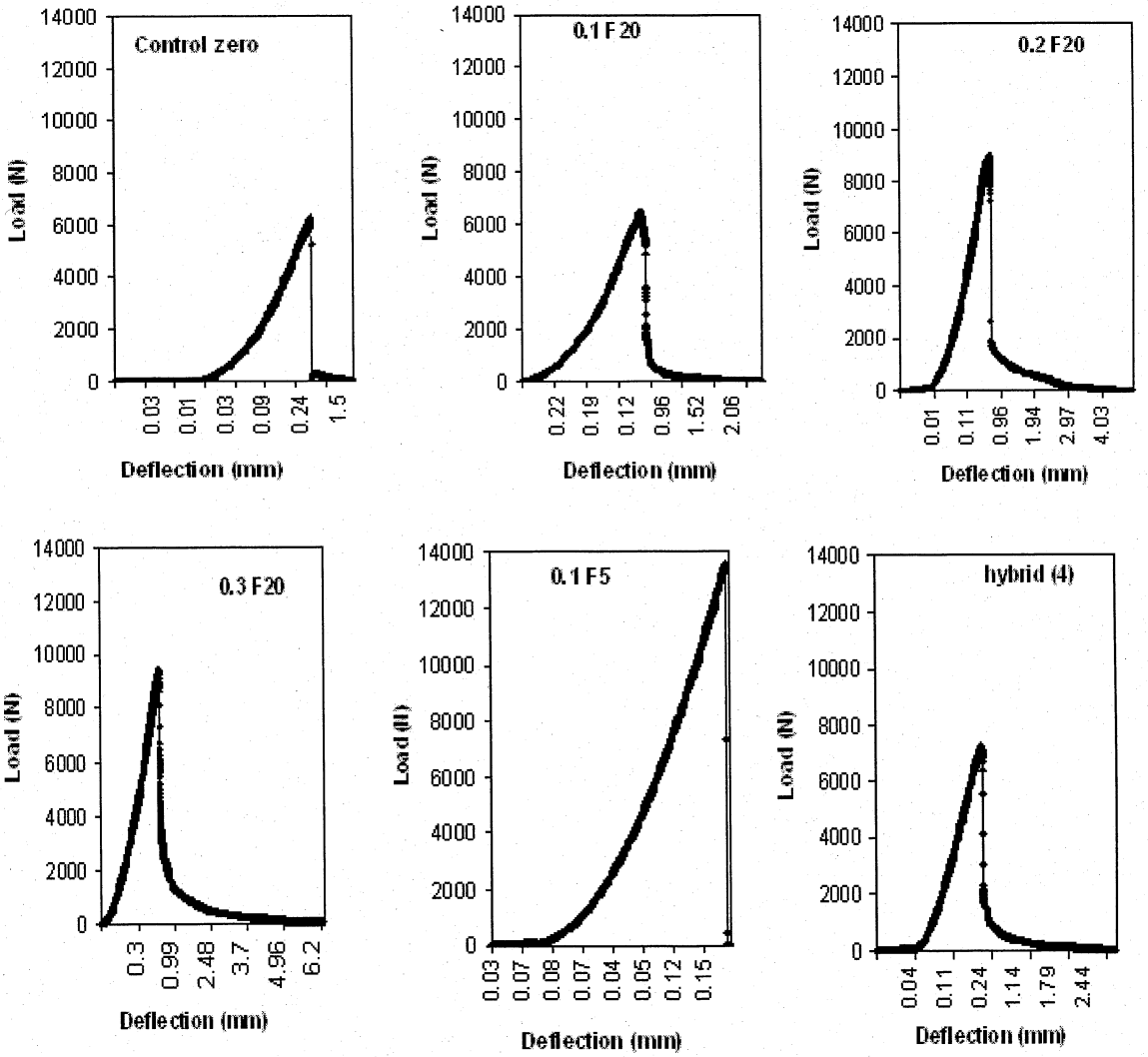

Figure 4.49 Load-deflection responses from flexural strength test

4.4.4 Fracture Energy

Figure 4.50 presents the 28-day fracture energy of concrete mixtures. The 28-day fracture energy ranges between 81 N/m and 485 N/m for PVA mixtures and, between 275 N/m and 719 N/m for metallic mixtures. The fracture energy of the hybrid mixture (Hybrid 4) and the control mix are 267 N/m and 118 N/m, respectively. Figure 4.50 indicates that the addition of fibers increases the fracture energy. Metallic long fiber (FF20) developed higher fracture energy than the other fibers at the same volume %.

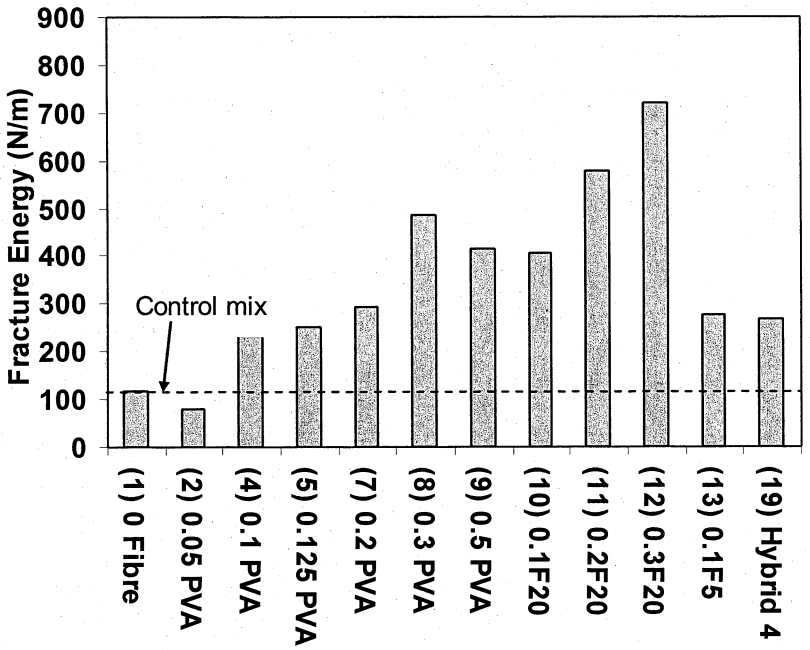

Figure 4.50 Fracture energies for concrete mixtures

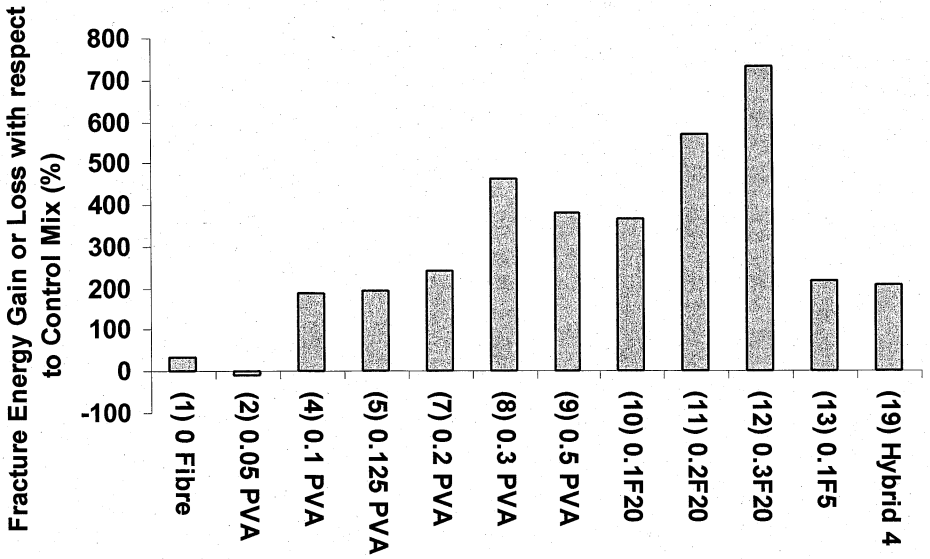

Figure 4.51 Fracture energy gain or loss

Addition of PVA fiber improves the fracture energy compared to control mix showing a maximum increase of about 380% (Figure 4.51). The increase in s strength and fracture energy is assumed to be due to the interaction of PVA with cement forming molecular bond [Singh and Sarita 2001]. The metallic (both short FF5 and long FF20) fibers significantly improve the fracture energy and a maximum increase of about 730% is observed compared to control SCC mix (0 % fiber). Previous research studies on steel fiber also confirmed significant improvement in fracture energy [Wang et al. 1996]. Long metal fiber (FF20) produces fracture energy which is about 1.5 times higher than the short metal fiber (FF5). Effectiveness of long steel fiber was also confirmed in previous research studies [Qian and Stroeven 2000].

It is also noted that the hybrid mixture (Hybrid 4) also produces 210% higher fracture energy compared with control SCC. This can be related to the existence of a positive synergy effect between metallic fibers and PVA in improving fracture characteristics. Previous research study also showed better toughness properties of SCC with the addition of fiber cocktail (a combination of steel fibers and PP fibers) [Ding et al. 2008].

In general, the increase of both PVA and metallic fiber increases the fracture energy of concrete mixtures. However, the fracture energy gain due to metallic fiber is substantial. A fracture energy gain of about 730% is substantial compared to 10% of compressive strength, 39% of splitting tensile strength and 124% of flexural strength (Figure 4.51). The use of fibers (especially metallic ones) is more effective in increasing the fracture energy of FRSCC than compressive/splitting tensile/flexural strength. This indicates that FRSCC can substantially increase the energy absorbing capacity concrete structures due to its high fracture energy characteristics.

Figure from 4.52 shows load-deflection curves from fracture energy tests for the concrete mixtures. Load-deflection curves are affected by the types and dosages of fibers. Generally, an increase in fiber volume increases the area under the load-deflection curve that signifies the higher fracture energy of the mixtures. The higher area under the load-deflection curve is associated with the development of higher peak load and larger ultimate deflection (Figure 4.52).

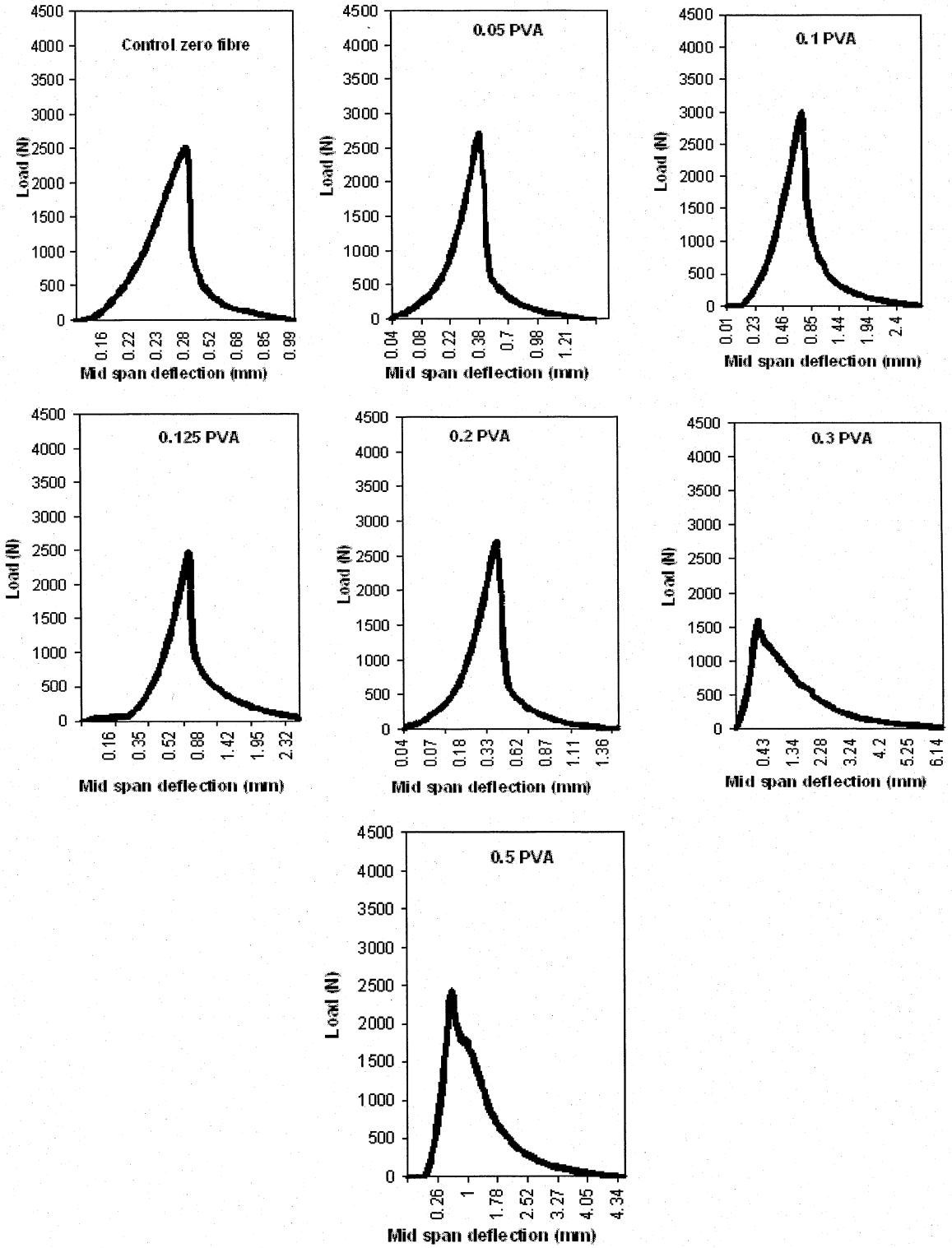

Figure 4.52 Load-deflection responses from fracture energy test, continue….

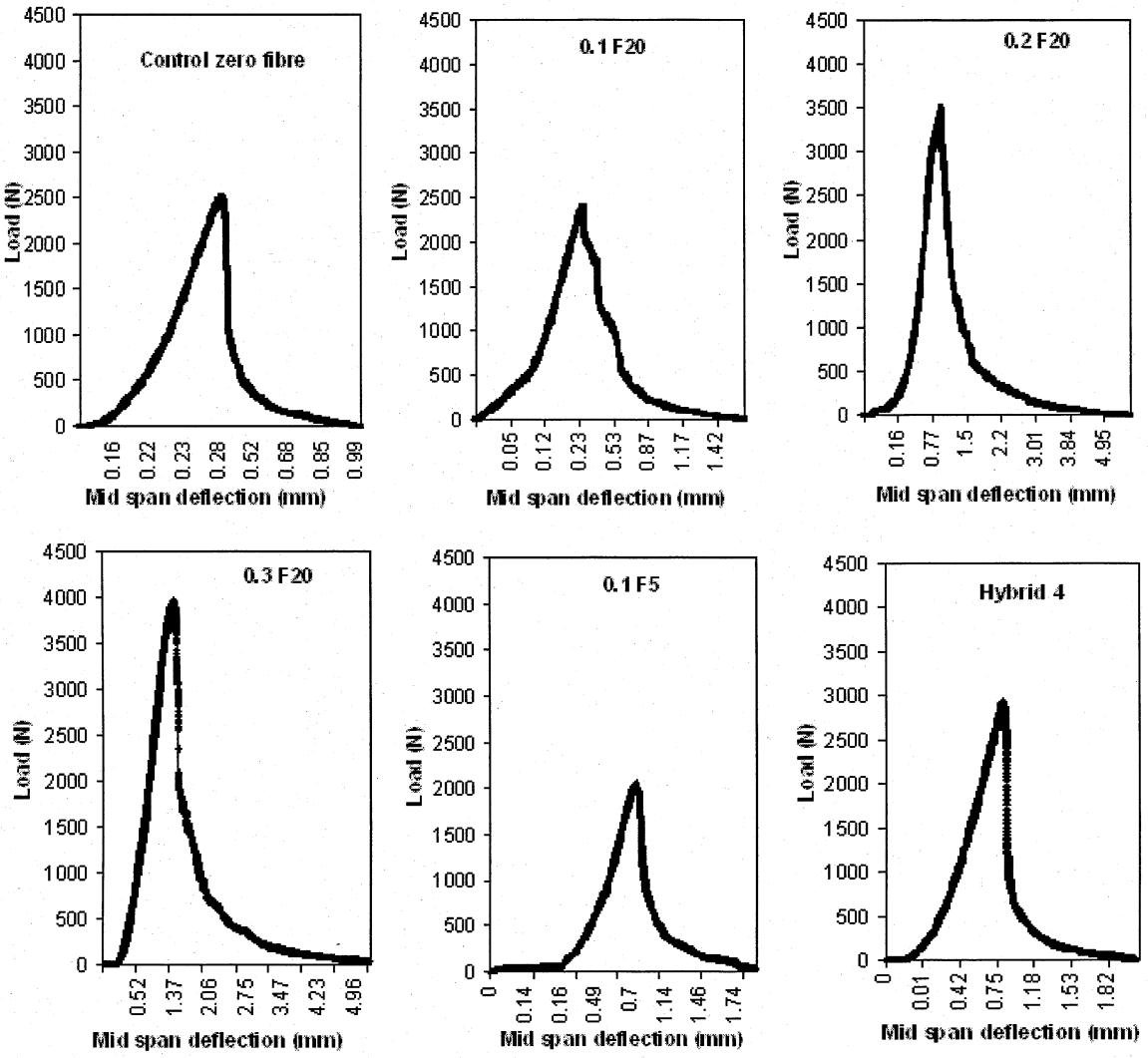

Figure 4.52 Load-deflection responses from fracture energy test

4.4.5 Rapid Chloride Penetration (RCP)

Figure 4.53 shows resistance against the penetration of chloride ions for concrete mixtures in Coulombs from RCP tests. In general, chloride penetration resistance decreases with the addition of fibers compared to control mix (with zero fiber). Concrete with PVA fiber shows higher chloride penetration resistance (lower Coulomb values) than those with metallic fibers. Mix 6 with 0.15% PVA, Mix 8 with 0.3% PVA, and mix 19 (hybrid 4) fall in the range between 1000 and 2000

coulombs and can be classified as "Low" as per ASTM C1202 [1997]. Other mixtures can be classified as "moderate" as the charge ranges between 2000 and 4000 Coulombs. The reaction of PVA fiber with cement at the early stages of hydration forms new compounds that fill the pores causing higher chloride penetration resistance of PVA mixtures [Singh and Rai 2001]. However, further research is needed in this direction.

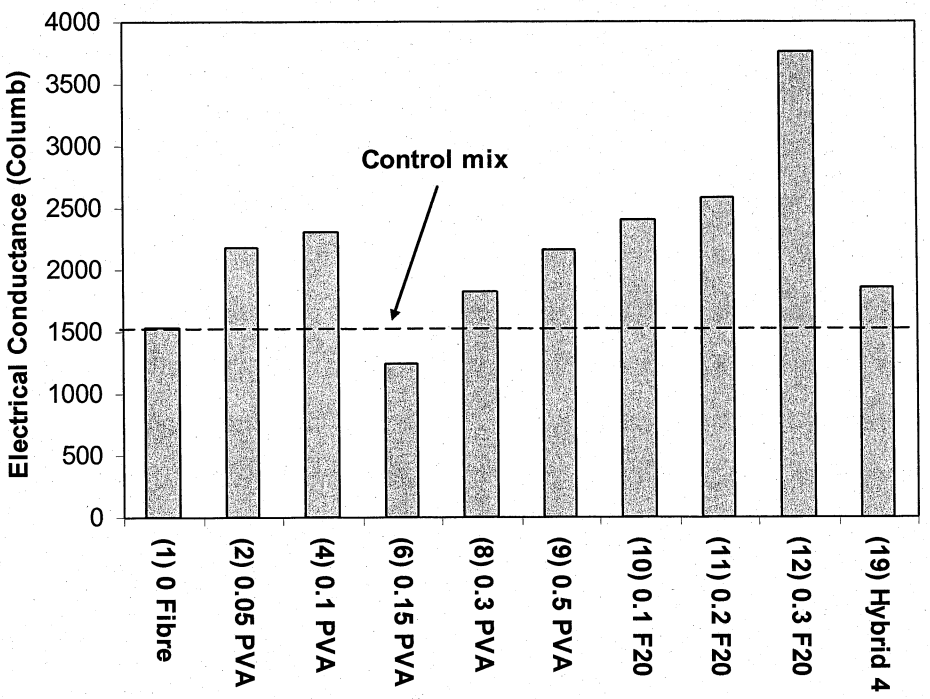

Figure 4.53 Chloride penetration resistance of concrete mixtures

It should also be noted that the RCP test as per ASTM C 1202 may not be suitable for concrete with fiber (especially steel or metallic) and can provide misleading results. Because, the test is based on electrical conductance and the presence of steel or metallic fiber can enhance the conductivity of the concrete depending on their continuity in the matrix. Therefore, the RCP values obtained for concrete with metallic fiber (in this study) should be interpreted accordingly.

5. Conclusions & Recommendations

5.1 Introduction

This research was intended to develop fiber reinforced self-consolidating concrete (FRSCC) by incorporating two different types of fibers and their combinations (hybrid). 18 concrete mixtures were developed based on a control self-consolidating concrete (SCC) mix (with zero fiber volume). Polymer polyvinyl alcohol (PVA) and metallic "FibraFlex" (of two different lengths classified as long and short) were used. Mixtures were produced with fiber volume ranging from 0 to 0.3%. Fresh, rheological, mechanical and durability properties of all 19 mixtures including the control SCC were evaluated. The fresh properties of the concrete mixtures were evaluated using empirical methods such as slump flow (spread), slump flow time (T_{500}), L-box passing ability, segregation resistance, and V-funnel flow time tests as per standard specifications. In addition, the rheological parameters such as plastic viscosity and yield stress of concrete mixtures were also evaluated using a viscometer. The mechanical properties including compressive/flexure/splitting tensile strength and fracture energy as well as durability in terms of chloride penetration resistance were also evaluated.

This chapter summarizes the conclusions and the recommendations for further research.

5.2 Conclusions

The following conclusions were drawn from the study:

1. In general, slump flow and L-box passing ability decreased and V-funnel time increased with the increase fiber volume in the developed concrete mixtures. PVA fiber showed distinguished higher influence on slump flow spread, V-funnel flow time and L-box passing ability (a measure of workability) compared to metallic ones for the same fiber dosage. With respect to control mix: (a) a maximum slump spread reduction of about 45% was observed with PVA

compared to 19% of metallic ones, (b) a maximum V-funnel flow time increase of 132% was observed with PVA compared to 92% of metallic ones and (c) a maximum reduction of up to 61% was observed for L-box passing ability due to the addition fiber.

2. PVAs higher surface area and its hydrophilic nature to adsorb/engage water around its surface as well as its reaction with cement in the early stage are considered to be the main contributing factors in producing higher workability reduction of concrete mixtures compared to metallic fibers. This limits the maximum dosage of PVA fiber to 0.125% compared with 0.3% of metallic fiber to achieve a FRSSCC mixture in this research study.
3. The use of short metal fiber improved workability of concrete mixtures compared to longer ones. This is attributed to the fact that the longer fiber can have more detrimental interference with the aggregates and can obstruct the flow more than short fibers.
4. It is also concluded that the workability of a hybrid mix depends not only on the types and dosages of fiber but also on the interaction and synergic properties between different fiber types. By optimizing the combination of fiber types/dosages (as confirmed from this study), it is possible to develop hybrid FRSCC mixtures with adequate fresh/workability characteristics.
5. Slump flow spread of FRSCC mixtures developed in this study ranged between 560 mm and 685 mm (fall within the range of SCC). FRSCC mixtures are classified into various groups [as per European SCC Guidelines 2005] for construction applications according to confinement conditions related to the geometry of structural element, type/location of reinforcement and concrete delivery/placing methods.
6. Relationship exists between fresh properties and the general trend shows an increase in L-box passing ability and a decrease in V-funnel time with the increase of slump flow spread. Both metallic and PVA fiber showed similar trend of variation.

7. The plastic viscosity and yield value of the FRSCC mixtures fall within the range (10 to 120 Pas for viscosity and 0 to 60 Pa for yield value) of typical SCC mixtures used in developed countries.
8. The yield value increases with the increase of fiber volume and time. For the similar dosages of fiber, the increase in yield value for metallic fiber was found to be significantly higher (about 14 times) compared to PVA. This can be useful for controlling the pressure on formwork and time of its removal.
9. Both PVA and metallic fibers showed similar trend of variation showing a decrease in yield value/plastic viscosity with an increase of slump flow spread, an increase in yield value/plastic viscosity with an increase of V-funnel time and an increase in L-box passing ability with a decrease in yield value/plastic viscosity.
10. The 28-day compressive strength of PVA, metallic and hybrid mixtures ranged between 38 MPa and 48 MPa. With respect to control mix, addition of PVA fiber reduced the compressive (maximum up to 15%) while the addition of metallic fibers improved the compressive strength (maximum up to 10%). Addition of PVA fiber did not improve 14-day and 28-day compressive strength compared to control mix. A change in compressive strength of about 10 to 15% does not show a great influence of fiber addition on the compressive strength of concrete.
11. Addition of PVA and metallic fiber improved the 28-day spitting tensile and flexural strength of FRSCC with metallic fiber showing the best performance. For PVA, a splitting tensile strength gain of about 11% was observed compared to about 39% of metallic mixtures. On the other hand, a 28-day flexural strength increase of up to 28% was observed in FRSCC mixtures with PVA compared to about 124% of metallic mixtures. The significant gain in splitting tensile/flexural strength due to metallic fiber compared to PVA can be attributed to the better interlocking characteristics of metal fibers in the concrete matrix. The 28-day splitting tensile strength of FRSCC mixture ranged between 2.9 MPa and 3.7MPa while flexural strength ranged between 2.7 MPa and 7.6 MPa.

12. The addition of both PVA and metallic fiber significantly improved the fracture energy of FRSCC mixtures with long metallic fiber showing the best performance. With respect to control mix, a maximum fracture energy increase of about 380% was observed for PVA compared to 730% of metallic fibers.
13. The fibers (especially metallic ones) are more effective in increasing the fracture energy of FRSCC than compressive/splitting tensile/flexural strength. A fracture energy gain of about 730% is substantial compared to 10% of compressive strength, 39% of splitting tensile strength and 124% of flexural strength.
14. The higher splitting tensile/flexural strength and fracture energy of FRSCC mixtures signifies that their use can significantly reduce the amount of tensile reinforcement in reinforced concrete structures as well can substantially increase the energy absorbing capacity of concrete structures.
15. Chloride penetration resistance decreased with the addition of fibers compared to control mix and FRSC with PVA fiber showed higher chloride penetration resistance compared to metallic fibers possibly due to the reaction of PVA with cement at the early stages of hydration forming new compounds that could fill up the pores.
16. Three best FRSCCs are identified from 18 concrete mixtures – a PVA mixture with 0.1% fiber volume, a metallic mixture with 0.2% fiber volume and a hybrid (PVA + metallic) mixture with a total fiber volume of 0.1%.

5.3 Recommendations for Further Research

Further researches are required to:

- Develop and optimize FRSCC by accommodating high volumes of fibers in wide range of mix proportions and enhancing mix granular skeleton in both solid and fluid phases.
- Evaluate the effect of the addition of fiber with different length/geometry/aspect ratio on rheology (with time) in order to characterize FRSCC mixtures by yield stress and plastic viscosity.

- Evaluate autogenous shrinkage, freezing and thawing characteristics, chloride/sulphate resistance, fire durability, and wear resistance of FRSCC mixtures.
- Evaluate FRSCC microstructure by Scanning Electron Microscopy (SEM) in order to develop models for predicting effect of different types/dosage/combinations of fibers and their working mechanism in an arbitrary mixture with respect to fiber distribution and fiber-matrix interface characteristics.
- Develop standard specifications for FRSCC by focusing on wide range of construction applications covering mix design, pump-ability, method of production and quality control.

6. Standards and References

6.1 Standards

ASTM C 128 (2003) "Standard Test Method for Density, Relative Density (Specific Gravity), and Absorption of Fine Aggregate," American Society for Testing and Materials, Philadelphia, PA.

ASTM C 136 (2005) "Standard Test Method for Sieve Analysis of Fine and Coarse Aggregates," American Society for Testing and Materials, Philadelphia, PA.

ASTM C 33 (2003) "Standard Specification for Concrete Aggregates," American Society for Testing and Materials, Philadelphia, PA.

ASTM C 78 (1980) "Test Method for Flexural Strength for Concrete," American Society for Testing and Materials, Philadelphia, PA.

ASTM C1202 (1997) "Standard Test Method for Electrical Indication of Concrete's Ability to Resist Chloride Ion Penetration," American Society for Testing and Materials, Philadelphia, PA.

ASTM C192 (2003) "Practice for Making and Curing Concrete Cylinders in the Laboratory," American Society for Testing and Materials, Philadelphia, PA.

ASTM C31 (2003) "Concrete Test Specimens, Making and Curing in the Field," American Society for Testing and Materials, Philadelphia, PA.

ASTM C39 (2003) "Compressive Strength of Cylindrical Concrete Specimens," American Society for Testing and Materials, Philadelphia, PA.

ASTM C496 (1996) "Standard Test Method for Splitting Tensile Strength of Cylindrical Concrete Specimens," American Society for Testing and Materials, Philadelphia, PA.

6.2 References

ACI Committee 544, (1984) "State-of-the-Art Report on Fiber Reinforced Concrete," International Symposium on Fiber Reinforced Concrete, ACI SP-81, pp.411-432.

ACI Committee 544, (1990) "State-of-the-art report on fiber reinforced concrete," ACI Manual of Concrete Practice, Part 5, 22 pp.

Al-Tayyib, A-H.J., and Al-Zahrani, M.M. (1990) "Corrosion of steel reinforcement in polypropylene fibre reinforced concrete structures," ACI Materials Journal, 87(2)108-113.

Aydin, A.C. (2007) "Self compactability of high volume hybrid fiber reinforced concrete," Construction and Building Materials, 21(6)1149-1154.

Bache, H.H. (1987) "Introduction to compact reinforced composite," CBL Reprint No. Aalborg Portland, 1987.

Banfill, P.F.G. (2003) "The rheology of fresh cement and concrete – a review," Proceedings of 11th International Congress on the Chemistry of Cement, Durban, South Africa, pp. 50–62.

Barluenga, G., and Hernández-Olivares, F. (2007) "Cracking control of concretes modified with short AR-glass fibers at early age. Experimental results on standard concrete and SCC," Cement and Concrete Research, 37(12)1624-1638.

Barragan, B., Gettu, R., De La Cruz, C., Bravo, M., and Zerbino, R. (2005) "Development and application of fiber-reinforced self-compacting concrete," Proceedings of the International Conference on Young Researchers' Forum, Thomas Telford Services Ltd., Jul 5-7, Dundee, Scotland, UK, p 165-172.

Beaudoin, J.J. (1982) "Fibre reinforced concrete," Canadian Building Digests CBD-223, originally published April 82 (http://irc.nrc-cnrc.gc.ca/pubs/cbd).

Beaudoin, J.J. (1990) "Handbook of fiber-reinforced concrete. Principles, properties, developments and applications," Noyes Publications, Park Ridge, NJ, xvii, 332 pp.

Bentur, A., and Cree, R. (1987) "Cement reinforced with steel wool," Int. J. Cem. Comp. & L Concr., Vol. 9, pp. 217-223.

Bentur, A., Mindess, S., and Skalny, J. (1989) "Reinforcement of normal and high strength concretes with fibrillated polypropylene fibers," Fibre Reinforced Cements and Concretes: Recent Developments, Papers presented at the International Conference held September 18-20, 1989 at the School of

Engineering, University of Wales College of Cardiff, UK; Ed. by R. N. Swamy and B. Barr; Elsevier Applied Science, London, pp 229-239.

Bui, V.K., Akkaya, Y., and Shah S.P. (2002) "Rheological model for self-consolidating concrete," ACI Materials Journal, 99(6), 549-559.

Chanvillard, G., and Aitcin, P-C. (1990) "Thin bonded overlays of fiber-reinforced concrete as a method of rehabilitation of concrete roads," Canadian Journal of Civil Engineering, 17(4) 521-527.

Corinaldesi, V., and Moriconi, G. (2004) "Durable fiber reinforced self-compacting concrete," Cement and Concrete Research 34, 249–254

Corinaldesi, V., and Moriconi, G. (2003) "Recycled aggregate concrete under cyclic loading," Role of Cement Science in Sustainable Development -Proceedings of the International Symposium – Celebrating Concrete: People and Practice, Sep 3-4, Dundee, United Kingdom, Thomas Telford Services Ltd, London, E14 4JD, UK, p 509-518.

De Larrard, F., Ferraris, C.F., and Sedran, T. (1998) "Fresh concrete: A Herschel-Bulkley material," Materials and Structures, 31(8/9), 494-498.

Deng, Z. (2005) "The fracture and fatigue performance in flexure of carbon fiber reinforced concrete," Cement and Concrete Composites, v (27), 1, January, p 131-140.

Ding, Y., Liu, S., Zhang, Y., and Thomas, A. (2008) "The investigation on the workability of fibre cocktail reinforced self-compacting high performance concrete," Construction and Building Materials, 22(7) 1462-1470.

Domone, P.L. (2006) "Self-compacting concrete: An analysis of 11 years of case studies," Cement & Concrete Composites 28, 197–208.

EFNARC (2006) "European federation for specialist construction chemicals and concrete systems, guidelines for viscosity modifying admixtures for concrete," (www.efnarc.org/publications.html).

Erdoğan, S.T. (2005) "Determination of aggregate shape properties using x-ray tomographic methods and the effect of shape on concrete rheology," Ph. Dissertation, the University of Texas at Austin, August, UMI Number: 3203531.

European SCC Guidelines (2005) "The european guidelines for self-compacting concrete, specification, production and use," (www.efca.info).

Fang, C., and Labi, S. (2007) "Image-processing technology to evaluate static segregation resistance of hardened self-consolidating concrete," Transportation Research Record, n 2020, Concrete Materials, 1-9.

Felekoğlu, B., Türkel, S., and Altuntaş Y. (2007) "Effect of steel fiber reinforcement on surface wear resistance of self-compacting repair mortars," Cement and Concrete Composites, 29(5) 391-396.

Ferrara, L., Park, Y.D., and Shah, S.P. (2007) "A method for mix-design of fiber-reinforced self-compacting concrete," Cement and Concrete Research, 37(6), 957-971.

Ferraris, C.F. (1999) "Measurement of rheological properties of High Performance Concrete: State of the art," report, Journal of Research of the National Institute of Standard and Technology. Vol. 104, September- October (1999) pp. 461 – 478.

Ferraris, C.F., De Larrard, F., and Martys, N.S. (2001) "Fresh Concrete Rheology: Recent Developments," Materials Science of Concrete VI, American Ceramic Society, S. Mindess and J. Skalny, eds., 215-241.

Fischer, G., and Li, V.C. (2002a) "Influence of Matrix Ductility on the Tension-Stiffening Behavior of Steel Reinforced Engineered Cementitious Composites (ECC)," ACI J. of Structures, 99(1) 104-111.

Fischer, G., and Li, V.C. (2002b) "Effect of Matrix Ductility on Deformation Behavior of Steel Reinforced ECC Flexural Members Under Reversed Cyclic Loading Conditions," ACI Structural Journal, 99(6) 781-790.

Goodier, C.I. (2003) "Development of self-compacting concrete," Proceedings of the Institution of Civil Engineers: Structures and Buildings, 156(4) 405-414, Publisher: Thomas Telford Services Ltd.

Grünewald, S., and Walraven, J. C. (2001) "Parameter-Study on the Influence of steel Fibers and Coarse Aggregate Content on the Fresh Properties of Self-Compacting concrete," Cement and Concrete Research, 31(12) 1793-1798.

Grünewald, S. (2004) "Performance-based design of self-compacting fibre reinforced," Delft University Press, P.O. Box 98, 2600 MG Delft, the Netherlands.

Guo, L.P., Sun, W., Zheng, K.R, Chen, H.J., and Liu, B. (2007) "Study on the flexural fatigue performance and fractal mechanism of concrete with high proportions of ground granulated blast-furnace slag," Cement and Concrete Research, 37(2) 242-250.

Hackman, L.E., Farrell, M.B., and Dunham, O.O. (1994) "Ultra high performance reinforced concrete in Fiber reinforced concrete, Development and Innovations," published by ACI, SP-142, pp. 235-248.

Hossain, K.M.A., and Lachemi, M. (2004) "Use of volcanic debris and industrial wastes in the development of self-consolidating concrete for sustainable construction," 5th Structural Specialty Conference of the Canadian Society for Civil Engineering, Saskatoon, Canada, June 2-5.

Hossain, K.M.A., and Lachemi, M. (2004) "Corrosion resistance and chloride diffusivity of volcanic ash blended cement mortar," Cement and Concrete Research, 34(4) 695-702.

Illinois Test Procedure SCC-6 (2005) "Standard Test Method for Static Segregation of Hardened Self-Consolidating Concrete Cylinders," August 2004, Illinois Dep. of Transportation, Peoria, IL.

Joe, N. (2003) "The ABCs of SCC," Concrete Construction, Addison, 48(3) 40-46, Copyright Hanley-Wood.

Khayat, K.H., Yahia A., and Sonebi M. (1999) "Applications of statistical models for proportioning underwater concrete," ACI Materials Journal, 96 (6) 634 – 640.

Khayat, K.H., and Roussel, Y. (2000) "Testing and performance of fibre-reinforced self consolidating concrete," Materials and Structures Journal, RILEM Publications SARL, 33(230) 391-397.

Khayat, K.H. (1998) "Viscosity-Enhancing Admixtures for Cement based materials - an overview," Cement and Concrete Composites, 20(2) 171-188.

Khayat, K.H., and Guizani, Z. (1997) "Use of viscosity-modifying admixture to enhance stability of fluid concrete," ACI Materials Journal, 94(4) 332-340.

Khayat, K.H., and Hwang, S.D. (2006) "Effect of high-range water-reducing admixture type on performance of self-consolidating concrete," SP239-13 ACI Special Publication, 239(13) 185-200.

Khayat, K.H., Assaad, J., and Daczko, J. (2004) "Comparison of field-oriented test methods to assess dynamic stability of self-consolidating concrete," ACI Materials Journal, 101(2) 168-176.

Khayat, K.H., Manai, K., and Trudel, A. (1997) "In situ mechanical properties of wall elements using self-consolidating concrete." ACI Materials Journal, Nov-Dec 1997. 94(6) 491-500.

Koehler, E.P. (2004) "Development of a portable rheometer for fresh Portland cement concrete", M.S. Thesis, the University of Texas at Austin, 2004.

Kong, H.J., Bike, S.G., and Li, V.C. (2003a) "Development of a self-consolidating engineered cementitious composite employing electrosteric dispersion / stabilization," Cement and Concrete Composites, 25(3) 301-309.

Kong, H.J., Stacy, G.B., and Li, V.C. (2003b) "Constitutive rheological control to develop a self-consolidating engineered cementitious composite reinforced with hydrophilic poly (vinyl alcohol) fibres," Cement & Concrete Composites press, 25(3) 333-341.

Kuraray America, Incorporation (2006) 600 Lexington Avenue, 26th Floor, New York, NY10022, and Tel: 212986-2230, Fax: 212 867-3543, (www.kuraray-am.com.)

Lachemi, M., Hossain, K.M.A., Lambros, V., and Bouzoubaä, N. (2003) "Development of cost-effective self-consolidating concrete incorporating fly ash, slag cement, or viscosity-modifying admixtures," ACI Materials Journal, 100(5) 419-425.

Lachemi, M., Hossain, K.M.A., Lambros, V., Nkinamubanzi, P. C., and Bouzoubaä, N. (2004) "Self-consolidating concrete incorporating new viscosity modifying admixtures," Cement and Concrete Research, 34(6) 917-926.

Lanier, M., Badman, C., Bareno, J., Baur, K., Boster, C., Calvert, C., Cunningham, R., Daczko, J., Hughes, D., Kaiser, J., Knight, G., Leaton, C., Logan, D., Mansky, E., Masek, O., Miller, R., Nadeau, F., Sprague, D., Vachon, M., Wade, M., Wamelink, J., and Yarbrough, D. (2003) "Interim guidelines for the use of self-consolidating concrete in PCI member plants," PCI Journal, 48(3) 14-18.

Lessard, M., Tabot, C., Phelan, S., and Baker, D. (2002) "Self-consolidating concrete solves challenging placement problems at the Pearson international airport in Toronto, Canada," Conference Proceedings: First North American Conference on the Design and Use of Self-Consolidating Concrete, Nov. 12-13, Center for Advanced Cement-Based Materials, p. 413-316.

Li, V.C. (1993) "From micromechanics to structural engineering – the design of cementitious composites for civil engineering application," Journal of Structural Mechanic and Earthquake Engineering, 10(2) 37-48.

Li, V.C. (2003) "On engineered cementitious composites (ECC), a review of the material and its applications," Journal of Advanced Concrete Technology, 1 (3) 215-230, Invited Paper, Japan Concrete Institute.

Li, V.C., and Kanda, T. (1998) "Engineered cementitious composites for structural applications," ASCE J. Materials in Civil Engineering, 10(2) 66-69.

Li, V.C., (1994) "Advances in strain-hardening cement based composites," Engineering Foundation Conference on Advances in Cement & Concrete, New Hampshire, Jul. 24-29.

Li, V.C., Kanda, T., and Lin, Z. (1997) "The influence of fibre/matrix interface properties on complementary energy and composite damage tolerance," Fracture and strength of solids : proceedings of the third International Conference on Fracture and Strength of Solids, Hong Kong, 8-10 December1997, Trans Tech Pub., Uetikon-Zuerich, Switzerland, 1998, Part 1, p. 465-472.

Li, V.C., Kong, H.J., and Chan, Y.W. (1998) "Development of self-compacting engineered cementitious composites," proceedings of the International Workshop on Self-Compacting Composites, Kochi, Japan, p. 46–59.

Liu, X., Ye, G., De Schutter, G., Yuan, Y., and Taerwe, L. (2008) "On the mechanism of polypropylene fibers in preventing fire spalling in self-compacting and high-performance cement paste," Cement and Concrete Research, 38(4) 487-499.

Malhotra, V.M., Garette, G.G., and Bilodeau, A. (1994) "Mechanical properties and durability of polypropylene fiber reinforced high-volume fly ash concrete for shotcrete applications," ACI Materials Journal, 91(5) 478-486.

Mehta, P.K., and Monteiro, J.M. (2006) "Concrete: microstructure, properties, and materials," 3rd Ed. New York: McGraw-Hill.

Mesbah, H.A., and Buyle-Bodin, F. (1999) "Efficiency of poly propylene and metallic fibres on control of shrinkage and cracking of recycled aggregate mortars," Construction and Building Materials, 13(8) 439-447.

Miao, B., Chern, J.C., and Yang, C.A. (2003) "Influences of fiber content on properties of self-compacting steel fiber reinforced concrete," Journal of the Chinese Institute of Engineers, Transactions of the Chinese Institute of Engineers, Series A/Chung-kuo Kung Ch'eng Hsuch K'an, 26(4) 523-530.

Mindess, S., Young, J.F., and Darwin, D. (2002) "Concrete," August 20, 2002, Published By Pearson Education.

Mobasher, B., and Li, C.Y. (1996) "Mechanical properties of hybrid cement-based composites" ACI Materials Journal, 93(3) p 284-292

Mufti, A.A., Jaeger, L.G., Bakht, B., and Wegner, L. D. (1993) "Experimental investigation of fibre-reinforced concrete deck slabs without internal steel reinforcement," Canadian Journal of Civil Engineering, 20(3) 398-406.

Naaman, A.E. (1991) "SIFCON: Tailored properties for structural performance, in High Performance Fiber Reinforced Cement Composites," Proceedings of the International Workshop held by RILEM, ACI and others, June 23-26, pp. 18-38.

Nagataki S., and Fujiwara, H. (1995) "Self-compacting property of highly flowable concrete," V.M. Malhotra edited, ACI, SP 154, pp. 301-314.

Nakagawa, H., Akihama, S., and Suenaga, T. (1989) "Mechanical properties of various types of fibre reinforced concretes," in Fibre Reinforced Cements and

Concretes: Recent Developments, Papers presented at the International Conference held September 18-20 at the School of Engineering, University of Wales College of Cardiff, UK; Ed. by R. N. Swamy and B. Barr; Elsevier Applied Science, London, pp 523-532.

Nanayakkara, A., Ozawa, K., and Maekawa, K. (1988) "Flow and segregation of fresh concrete in tapered pipes," Proceedings, 3rd International symposium on liquid – solid flows, ASME, FED- 75, pp. 139-144.

Nanni, A. (1988) "Splitting-tension test for fiber reinforced concrete," ACI Materials Journal (American Concrete Institute), 85(4) 229-233.

Nehdi, M., and Khan, A. (2001) "Cementitious composites containing recycled tire rubber: An overview of engineering properties and potential applications," Cement, Concrete and Aggregates, 23(1) 3-10.

Nehdi M., and Ladanchuk J.D. (2004) "Fiber synergy in fiber-reinforced self-consolidating concrete," ACI Materials Journal, 101(6) 508-517.

Newman, J., and Choo, B.S. (2003) "Advanced concrete technology, concrete properties," by Elsevier Science Publishers, Publisher: Butterworth-Heinemann and Elsevier ltd., pp.16/1.

Nielsson, I., and Wallevik, O.H. (2003) "Rheological evaluation of some empirical test methods, preliminary results," Third Int. Symposium of SCC, Reykjavik, Edited by Wallevik and Nielsson, RILEM publications PRO 33, Bagneux, pp. 59-68.

Niwa, J., and Tangtermsirikul, S. (1997) "Fracture properties of high strength and self compacting high performance concretes," Transactions of the Japan concrete institute, Vol. 19, pp. 73-80.

Okamura, H., and Ouchi, M. (2003) "Self-compacting concrete," Journal of Advanced Concrete Technology, Japan Concrete Institute, 1(1) 5-15.

Ouchi, M., Nakamura, S., Osterson, T., Hallberg, S., and Lwin, M. (2003) "Applications of self-compacting concrete in Japan, Europe and the United States," ISHPC, p 2-5.

Ozawa, K., Maekawa, K., Kunishima, H., Okamura, H. (1989) "Performance of concrete based on the durability design of concrete structures," Proce. the

second East-Asia-Pacific Conference on Structural Engineering and Construction, Volume 1, pp 445-456.

Ozawa, K., Sakata, N., and Okamura, H. (1995) "Evaluation of self-compactibility of fresh concrete using the funnel test," Proceeding of JSCE, 25, 59-75.

Ozyildirim, C., and Lane, D.S. (2003) "Final report, evaluation of self-consolidating concrete," Virginia Transportation Research Council, Charlottesville-Virginia, VTRC 03-R13.

Ozyurt, N., Mason, T.O., and Shah, S.P. (2007) "Correlation of fiber ispersion, rheology and mechanical performance of FRCs," Cement and Concrete Composites, 29(2) 70-79.

Patel, R., Hossain, K.M.A., Shehata, M., Bouzoubaä, N., and Lachemi, M. (2004) "Development of statistical models for mixture design of high-volume fly ash self-consolidating concrete," ACI Materials Journal, 101(4) 294-302.

PCI, TR-6-03, (2003) "Interim Guidelines for the Use of Self-Consolidating Concrete in Precast / Prestressed Concrete Institute Member Plants," Precast / Prestressed Concrete Institute, 209 West Jackson boulevard, Chicago, Illinois 60606-6938, (www: pci.org).

Pereira, E.N.B., Barros, J.A.O., Cunha, V., and Santos, S.P.F. (2005) "Compression and bending behavior of steel fiber reinforced self-compacting concrete," (www.scientificcommons.org/8414034).

Purdue University (2008) School of Civil Engineering, Transportation Engineering, (www.engineering.purdue.edu).

Qian, C., and Stroeven, P. (2000) "Fracture properties of concrete reinforced with steel–polypropylene hybrid fibers," Cement and Concrete Composites, 22(5) 343-351.

RILEM-Draft-Recommendation (RILEM TC50FMC) (1985) "Determination of the Fracture Energy of Mortar and Concrete by Means of Three Point Bend Test on Notched Beams", Materials and Structures, 18, pp. 285-290.

Rols, S., Ambroise, J., and Pera, J. (1999) "Effects of different viscosity agents on the properties of self-leveling concrete," Cement and Concrete Research, 29(2) 261-266.

Saak, A.W., Jennings, H.M., and Shah, S.P. (2002) "New methodology for designing self-compacting concrete," ACI Materials Journal, 99(5) 509-512.

Sahmaran, M., and Yaman, I.O. (2007) "Hybrid fiber reinforced self-compacting concrete with a high-volume coarse fly ash," Construction and Building Materials, 21(1)150-156.

Sahmaran, M., Yurtseven, A., and Ozgur, Y.I. (2005) "Workability of hybrid fibre reinforced self-compacting concrete," Building and Environment, 40(12) 672–1677, Elsevier Ltd.

Saint-Gobain (2008) "FibraFlex Activity," SEVA, SAINT-GOBAIN SEVA - Département FIBRAFLEX - 43 Rue du Pont de Fer - BP 176 - 71105 CHALON-sur-SAÔNE CEDEX, (www.fibraflex.com).

Shah, S.P., and Skarendahl, A. (1986) "Steel Fiber Concrete," Elsevier Applied Science Publishers, London.

Singh, N., and Sarita, R. (2001) "Effect of polyvinyl alcohol on the hydration of cement with rice husk ash," Cement and Concrete Research, 31(2) 239-243, Elsevier Science Ltd.

Tang, C., Yen, T., Chang, C., and Chen, K. (2001) "Optimizing Mixture Proportions for Flowable High-Performance Concrete via Rheology Tests," ACI Materials Journal, 98(6) 493-502.

Tattersall, G.H. (1973) "Rationale of a two-point workability test," Magazine of Concrete Research, 25(84) 169-172.

Tlemat, H., Pilakoutas, K., and Neocleous, K. (2003) "Pullout Behaviour of Steel Fibers Recycled from Used Tyres." In Role of Concrete in Sustainable Development, Proceedings of International Symposia on Celebrating Concrete: People and Practice, Thomas Telford Ltd, Dundee, 3-4 September, pp 175 – 184.

Torrijos, M.C, Barragán, B.E., and Zerbino, R.L. (2007) "Physical–mechanical properties, and mesostructure of plain and fibre reinforced self-compacting concrete," Construction and Building Materials, In Press, Available online 12 July.

Vondran, G.L. (1991) "Applications of Steel Fiber Reinforced Concrete," ACI Concrete International, 13, 44-49.

Wallevik, O. (2003) "The BML ConTec Viscometer Manual," version 2003, ConTec Ltd, Laugarasvegur 7, 104 Reykjavik, Iceland, Laugarasvegur 7 - 104 Reykjavik - Iceland - Tel: +354 896 9674 - Fax: +354 588 2880 - E-mail: contec@contec.is, (www.contec.is).

Walraven, J. (2003) "Structural applications of self compacting concrete," Proceedings of 3rd RILEM International Symposium on Self Compacting, Reykjavik, Iceland, ed. Wallevik O. and Nielsson I, RILEM Publication PRO 33, Bagneux, France, August, pp 15-22.

Wang, N., Mindess, S., and Ko, K. (1996) "Fibre reinforced concrete beams under impact loading," Cement and Concrete Research, 26(3) 363-376.

Wang, K., Shah, S.P., White, D.J., Gray, J., Voigt, T., Gang, L., Hu, J., Halverson, C., and Pekmezci, B.Y. (2005) "Self-consolidating concrete, applications for slip-form paving: Phase I (Feasibility Study)," Center for Portland Cement Concrete Pavement Technology, Iowa State University, 2901 South Loop Drive, Suite 3100 Ames, IA 50010-8634.

Wang, S., and Li, V.C. (2006) "High-Early-Strength Engineered Cementitious Composites," ACI Materials Journal, 103(2) 97-105.

Williamson, G. R. (1965) "The Use of Fibrous Reinforced Concrete in Structures Exposed to Explosive Hazards," Miscellaneous paper No. 5-5, U.S. Army Ohio River Division Laboratory.

Xie, Y., Liu, B., and Zhou, S. (2002) "Optimum mix parameters of high-strength self-compacting concrete with ultra pulverized fly ash," Cement and Concrete Research (32) 477-480.

Ye, G., Liu, X., De Schutter, G., Taerwe, L., and Vandevelde, P. (2007) "Phase distribution and microstructural changes of self-compacting cement paste at elevated temperature," Cement and Concrete Research, 37(6) 978-987.

Zhong, S.Y., Bao, M.X., and Xue, M. (2006) "Rheologic parameters of self-compacted concrete with poly carboxylate superplasticizer," Jianzhu Cailiao Xuebao/Journal of Building Materials, 9(5) 521-526.